STRUCTURE AND REACTIVITY OF SELECTED ORGANIC INCLUSION COMPOUNDS

by

AYESHA JACOBS
B.Sc.(HONS) UNIVERSITY OF CAPE TOWN

Thesis presented to the

UNIVERSITY OF CAPE TOWN

for the degree of

DOCTOR OF PHILOSOPHY

Department of Chemistry
University of Cape Town
Rondebosch
7701
South Africa

February 2002

University of Cape Town

The copyright of this thesis vests in the author. No quotation from it or information derived from it is to be published without full acknowledgement of the source. The thesis is to be used for private study or non-commercial research purposes only.

Published by the University of Cape Town (UCT) in terms of the non-exclusive license granted to UCT by the author.

University of Cape Town

In loving memory

Of my

Grandfather

Ishmail Jacobs

University of Cape Town

ACKOWLEDGEMENTS

I would like to extend a word of thanks to:

My supervisors, Professor L.R. Nassimbeni and Professor M.R. Caira for their brilliant guidance and keen interest.

Dr John Bacsa for data collections.

Vincent Smith for all the help and conversations.

Mr Klaus Achleitner for technical help.

All the members of the crystallography group for their friendship.

My mother, grandmother and brother, Anwar, for their support and encouragement.

University of Cape Town

PUBLICATIONS AND CONFERENCES

Parts of this thesis have been published:

Complexation with diol host compounds. Part 33. Inclusion and separation of pyridines by a diol host compound, J. Bacsa, M.R. Caira, A. Jacobs, L.R. Nassimbeni, F. Toda, *Cryst. Eng.*, 3, 251, 2000.

Parts of this thesis have been presented at the following conference:

XVIII International Union of Crystallography Congress in Glasgow, Scotland, 4-13 August 1999, M.R. Caira, A. Jacobs, L. R. Nassimbeni, Inclusion Compounds of an Acetylenic Host.

University of Cape Town

ABSTRACT

The inclusion behaviour of the two host compounds 1,1,6,6-tetraphenylhexa-2,4-diyne-1,6-diol and cyclotriveratrylene (2,3,7,8,12,13-hexamethoxy-5,10-dihydro-15*H*-tribenzo[a,d,g]cyclononene) was studied. Small organic guests were complexed with these hosts and their crystal structures determined.

The stability and reactivity of these inclusion compounds were investigated. Kinetics of desolvation were determined for some of the inclusion compounds using both isothermal and non-isothermal methods. Rate laws were proposed and activation energies established. The selectivity of the host 1,1,6,6-tetraphenylhexa-2,4-diyne-1,6-diol for certain guests was determined by competition experiments. Lattice energies were calculated in some cases. Solid state reactions were performed with the host 1,1,6,6-tetraphenylhexa-2,4-diyne-1,6-diol and selected solid guests. The resultant complexes were analysed using X-ray powder diffraction. Guest exchange reactions were also performed and the reactions were monitored either by differential scanning calorimetry or thermogravimetry. The structures of the inclusion compounds were reconciled with their physico-chemical properties.

University of Cape Town

ABBREVIATIONS AND SYMBOLS

α	extent of reaction
	angle between b and c unit cell axes
β	angle between a and c unit cell axes
γ	angle between a and b unit cell axes
b.p.	boiling point
CSD	Cambridge Structural Database
DMF	N,N-dimethylformamide
DMSO	dimethyl sulfoxide
DSC	differential scanning calorimetry
E	normalised structure factor
Endo	endothermic
F	structure factor
G	guest
H	host
k	rate constant
LE	lattice energy
m.p.	melting point
M_r	molecular mass
o-na	o-nitroaniline
m-na	m-nitroaniline
p-na	p-nitroaniline
NMR	nuclear magnetic resonance
T	temperature
TG	thermogravimetric analysis
T_{on}	onset temperature
T_b	boiling point
τ	torsion angle
V	cell volume
Z	number of formula units in the unit cell

University of Cape Town

University of Cape Town

TABLE OF CONTENTS

University of Cape Town

University of Cape Town

University of Cape Town

University of Cape Town

University of Cape Town

CHAPTER 1

University of Cape Town

CHAPTER 1 INTRODUCTION

Alfred Nobel stated that a prize be given to those who "shall have conferred the greatest benefit on mankind" and that a portion be reserved for those who "shall have made the most important chemical discovery or improvement." Below are listed Nobel prize winners who have contributed and continue to contribute to the field of supramolecular chemistry[1].

Year	Nobel Prize winners	Field	Research
1914	M.T.F. von Laue	physics	discovery of the diffraction of x-rays by crystals.
1915	W.H. Bragg and W.L. Bragg	physics	application of x-ray diffraction to structure determination.
1954	L. Pauling	chemistry	the nature of the chemical bond and its application to structure determination of complex substances.
1958	F. Sanger	chemistry	structure determination of proteins, especially insulin.
1962	M.F. Perutz and J.C. Kendrew	chemistry	structure determination of haemoglobin and myoglobin.
1964	Dorothy Crowfoot Hodgkin	chemistry	structure determination of penicillin and vitamin B_{12}
1982	A. Klug	chemistry	development of crystallographic electron microscopy and the structure determination of nucleic acid-protein complexes.
1985	H.A. Hauptman and J. Karle	chemistry	development of direct methods for the determination of crystal structures.
1987	D.J. Cram, J-M. Lehn and C.J. Pedersen	chemistry	synthesis of molecules that can "recognise" each other.
1988	J. Deisenhofer, R. Hyber and H. Michel	chemistry	determination of the 3D structure of a photosynthetic reaction centre.
1996	R.F. Curl, H.W. Kroto and R.E. Smalley	chemistry	discovery of fullerenes.
2000	A.J. Heager, A.G. MacDiarmid and H. Shirakawa	chemistry	discovery and development of conductive polymers.

University of Cape Town

SUPRAMOLECULAR CHEMISTRY

Supramolecular chemistry was defined in 1978 by Jean-Marie Lehn[2] (who later won the Nobel prize in 1987), as "chemistry of molecular assemblies and of the intermolecular bond". It is also referred to as the "chemistry of the non-covalent bond".

In recent years the field of supramolecular chemistry has grown extremely rapidly and has crossed disciplines such as biology, physics, chemistry, biochemistry and materials science. This has often led to a broadening of the definition to include systems which are held together by both covalent and non-covalent bonds[3]. An example of this would be organic components that are held together by metal-donor bonds. This study however, is concerned with one of the traditional and basic concepts of supramolecular chemistry, which is host-guest chemistry.

University of Cape Town

The roots of supramolecular chemistry can be traced back to 1811 when Davy[4] discovered the chlorine clathrate hydrate. Then in 1841 and 1849 graphite intercalates[5] and β-quinol H_2S clathrate[6] respectively were prepared. Progress continued throughout the early 20th century. In 1948 Powell[7] proposed structures for the β-quinol inclusion compounds and introduced the term '**clathrate**', whereby the guest is entirely encapsulated within a cavity created by the host lattice.

Numerous articles have been written concerning the nomenclature to be used when describing host-guest compounds. A brief summary of a few of the views held will be

discussed. In an article by Davies et al.[8] a distinction was drawn between three broad types of host-guest compounds:

- A clathrate as described by Powell[7] eg. host-guest compounds formed by Dianin's compound[9].
- An intercalate refers to a guest situated in spaces between the layers of the host framework eg. graphite has a layered structure which can accommodate atoms or molecules between the layers[5].
- An inclusion compound arises when the guest occupies voids in the host structure which differ from the ones previously mentioned eg. Werner-type inclusion compounds such as $Ni(4\text{-}Mepy)_4\ (NCS)_2$ [10].

Weber and Josel[11] have preferred a more detailed system whereby a host-guest compound has to fulfil numerous criteria before classification. No attempt will be made to describe the intricacies of this system. In the first stage the authors distinguish between a clathrate and a complex. Thereafter the topology of the host-guest compound and the interaction between the host and the guest is taken into account. Finally the number of molecular or ionic components is considered.

In general, inclusion compounds can be classified into two different groups. A schematic diagram is shown in Figure 1.1.

- **Molecular inclusion**: a single host molecule contains a cavity or void, which can encapsulate another molecule. The most studied and commercially attractive examples are the cyclodextrins. Other examples include the crown ethers and the cryptands.
- **Lattice inclusion**: the host molecules form solid state lattices that contain voids and are capable of including guest molecules. Most inclusion compounds fall into this category.

University of Cape Town

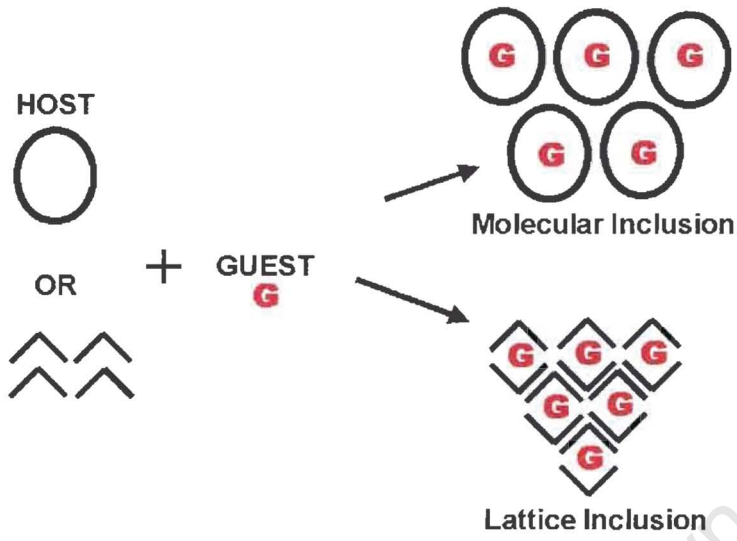

Figure 1.1 Schematic diagram illustrating the two basic types of inclusion.

University of Cape Town

The nature of the voids created by the host framework varies from closed cage-like structures to channels and layered arrangements. The most common types are shown in Figure 1.2.

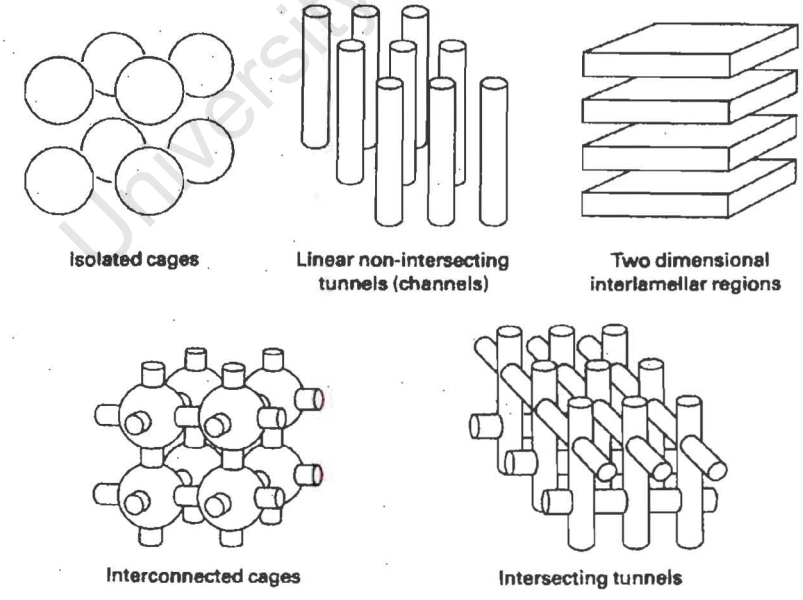

Figure 1.2 Common topologies of voids created by the host framework in solid state host-guest compounds[12].

NON–COVALENT INTERACTIONS

For inclusion compounds in the solid state, self-organization is primarily determined by non-covalent or intermolecular interactions. In particular, organic host-guest compounds are held together by dipole-dipole interactions, hydrogen bonding, van der Waals interactions, π–π stacking and C–H•••π interactions.

HYDROGEN BONDING

The hydrogen bond plays a major role in the formation of supramolecular structures. The strength of the hydrogen bond in organic inclusion compounds can vary from 4 kJmol^{-1} for the weakest interaction to 120 kJmol^{-1} for the strongest interaction[13,14]. In general, hydrogen bonds take the form, A—H•••B and can be defined by the following geometric parameters: the distances A—H and H•••B and the hydrogen bond angle A—H•••B (θ). This type of interaction is highly directional with the strongest hydrogen bonds nearly linear ($\theta \approx 150\text{-}180^{\circ}$)[15]. Strong hydrogen bonds are formed when both A and B are electronegative. eg. O—H•••O or N—H•••O. A typical O•••O distance would be 2.50-2.80Å. Weaker hydrogen bonds would be of the type C—H•••O or C—H•••N. In 1982 Taylor and Kennard[16] studied 113 structures on the CSD determined by neutron diffraction and found that C—H•••O contacts frequently have distances less than 2.4Å. This distance is less than the van der Waals sum of 2.6Å. However some researchers[17] believe this criterion to be too limiting and regard C•••O distances of 2.8 and even >3Å as acceptable weak hydrogen bond distances.

University of Cape Town

VAN der WAALS FORCES

The term van der Waals interactions is used to describe dispersion and repulsion forces[13]. Dispersion forces are attractive in nature and result from the interactions of fluctuating multipoles in adjacent molecules. The repulsive forces balance the dispersion forces and define molecular shape and conformation. These forces are non-directional, are less than 5kJmol^{-1} in strength and are most important in compounds where small organic guests are included in crystal lattices or molecular cavities.

π — π STACKING

This type of interaction occurs between aromatic rings and is referred to as a face-to-face interaction. Stacking of aromatic rings is especially favoured when some of the rings are electron-deficient and others are electron-rich. Face-to-face interactions are normally staggered, as direct overlap would be repulsive. The strength of this interaction varies from 0-50 kJmol^{-1}. π– π stacking plays an important role in the structure of DNA-intercalates and porphyrins[18].

C—H•••π INTERACTIONS

Edge-to-face interaction of aromatic rings also fall into this category. In 1997 Malone[19] et al. published a CSD analysis of X—H•••π interactions and found large variations in the geometry of this type of interaction. In 1998 studies done by Braga[20] on organometallic crystals found average distances from the centroid of the aromatic ring to the oxygen or carbon atom in (C)O—H•••π to be 3.41(3) and 3.69(2)Å respectively.

University of Cape Town

OTHER INTERACTIONS

Short nonbonded contacts of halogens Cl, Br and I have a stabilizing effect on crystal structures[21]. These halogens also form directional interactions with oxygen atoms[22]. Some are of the view that these short contacts are due to elliptically shaped atoms[23] while others believe that specific attractive forces occur between halogen atoms[24]. Sulphur also forms short contacts[25] of the form; S•••S, S•••N and S•••Cl.

HOST DESIGN

In general, rigid bulky molecules are designed as hosts. Irregular hosts are preferred as they pack inefficiently and require guest molecules to occupy voids created by the host lattice. Host molecules can be classified according to their shape and functionality. A few examples of these are given below:

- **Wheel and axle hosts**[26]: long linear axis terminated by rigid, bulky substituents. The bulky terminal groups prevent close-packing around the linear spacer. These can either be in the form of a molecule or a supramolecular equivalent[27] where the wheel and axle shape is created in situ as illustrated in Figure 1.3.
- **Molecular tweezer type hosts**[28] consist of two aromatic chromophores linked by a spacer. The host binds a guest by squeezing with its arms. Planar aromatic guests can be held by the tweezer-type conformation of the host where charge-transfer type face-to-face interactions and C—H•••π type edge-to-face interactions are responsible for the binding.

University of Cape Town

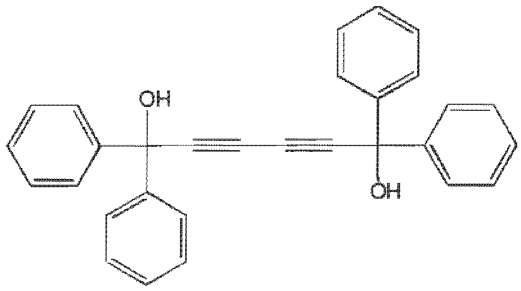

1

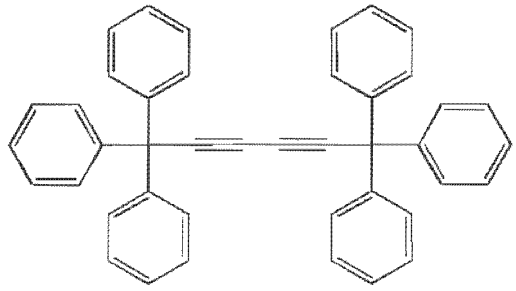

2

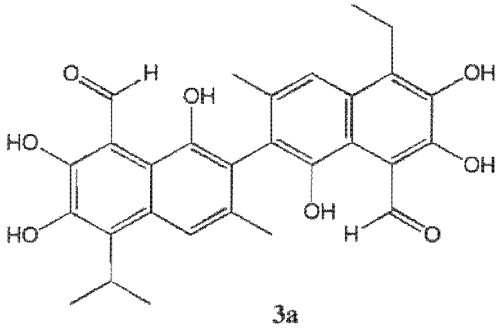

3a

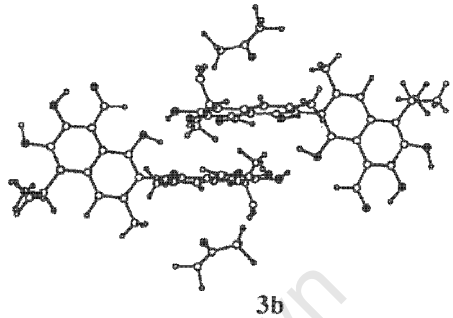

3b

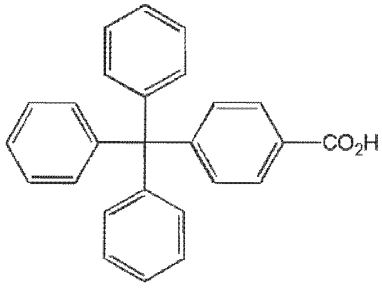

4a

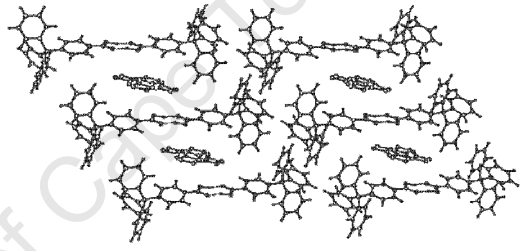

4b

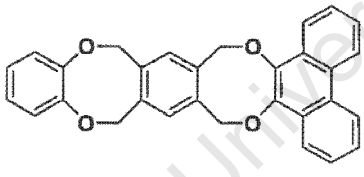

5a

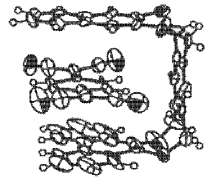

5b

University of Cape Town

Figure 1.3 Diagram illustrating molecular wheel and axle hosts **1** (1,1,6,6-tetraphenylhexa-2,4-diyne-1,6-diol, **TOD7**) and **2** (1,1,1,6,6,6-hexaphenylhexa-2,4-diyne), supramolecular wheel and axle host **3a** (gossypol) and the crystal structure of its acetone clathrate (**3b**)[27], supramolecular wheel and axle host **4a** (4-tritylbenzoic acid) and the crystal structure of its inclusion compound with xylene (mixed) (**4b**)[28], molecular tweezer host **5a** (9,13,18,22-tetraoxa-9,10,12,13,18,19,21,22-octahydrobenzo-9',10'-phenanthro[*e*,*e*']benzo[1,2-a:4,5-a']dicyclooctene and its inclusion compound with tetracyanoquinodimethane (**5b**)[28].

- **Hosts that possess cavities:**

Calixarenes[13,30,31] are made up of bridged units of the following:

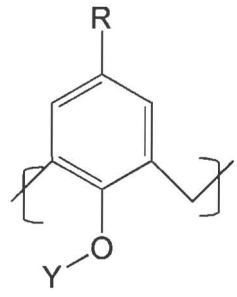

The shape of the calixarene depends on the number of units it contains. It is either cone or bowl- shaped or altenatively less well defined eg. calix[4]arene is bowl-shaped. Smaller calixarenes such as calix[4]arene and calix[5]arene have more structured cavities whereas the larger calixarenes, calix[6]arene up to calix[16]arene, are more flexible and thus have less well-defined cavities.

Cyclotriveratrylene (CTV) is a bowl-shaped host[32] consisting of a nine-membered cyclononatriene derived ring. The host shows conformational inversion from a stable bowl-shaped structure to a meta-stable saddle form, but this is very slow on the NMR time scale. In inclusion compounds involving CTV the host almost always adopts the crown conformation.

University of Cape Town

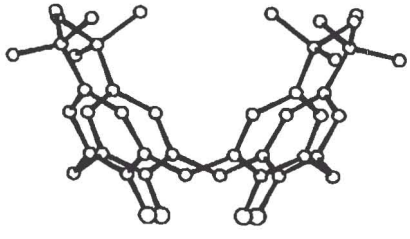

6

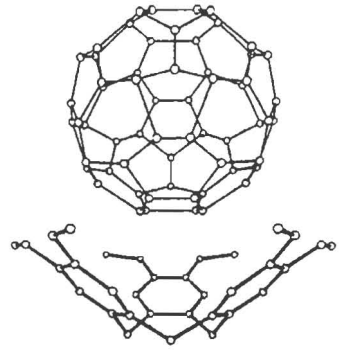

7

Figure 1.4. Crystal structures of p-tert-butylcalix[4]arene **6**[33] and the inclusion compound of CTV•C_{60} (**7**)[34].

PHYSICAL METHODS OF CHARACTERIZATION

THERMAL ANALYSIS

Thermal analysis is a very useful tool for the study of inclusion compounds[35-38]. The most common techniques are thermogravimetric analysis (TGA) and differential scanning calorimetry (DSC). A typical TGA experiment measures weight loss as a function of increasing temperature. Each individual weight loss is expressed as a percentage and this allows the calculation of the host to guest ratio. The reproducibility of the weight loss is generally of the order of ± 1%. The onset temperature cannot be determined by TGA because the commencement of weight loss is dependent on particle size and heating rate. TGA is also used extensively in the study of the kinetics of desolvation of host-guest compounds. Both isothermal and non-isothermal methods have been employed in this study and are described in Chapter 2.

DSC measures the enthalpy changes of a solid that occur during heating. These enthalpy changes are usually due to guest loss or a phase transformation. The area under the DSC peak is dependent on the particle size, heating rate, flow rate of the purging gas and the geometry of the calorimeter. In general, the onset temperatures for a given inclusion compound are dependent on the host-guest interactions and on the inherent physical properties of the guest included.

University of Cape Town

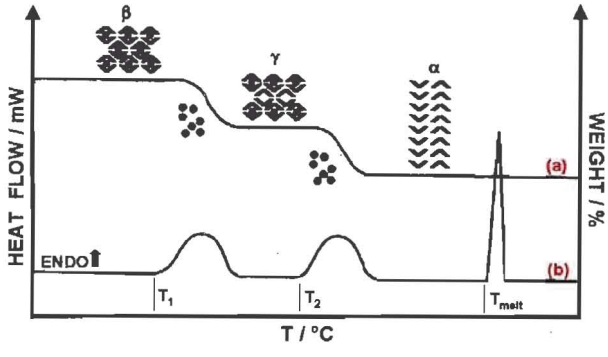

Figure 1.5 Schematic diagram[39] illustrating (a) TGA and (b) DSC traces.

GUEST EXCHANGE REACTIONS

These types of reactions can be represented by the general equation:

$$H{\bullet}G_1\,(s) \quad + \quad G_2\,(g) \leftrightarrow H{\bullet}G_2\,(s) \quad + \quad G_1\,(g)$$

In some cases the two crystal structures of the compounds $H{\bullet}G_1$ and $H{\bullet}G_2$ are isostructural and the shape and size of the two guests G_1 and G_2 are similar. An example is guest exchange between the host 1,4-bis(9-hydroxy-9-fluorenyl)benzene and the guests acetone and dimethylsulfoxide[40]. However guest exchange can also take place when the two compounds $H{\bullet}G_1$ and $H{\bullet}G_2$ have different crystal structures. This has been observed with the host 1,4-bis(9-hydroxy-9-fluorenyl)benzene and the guests acetone and isopropyl alcohol[40].

SOLID-SOLID REACTIONS

Solid-solid organic reactions were first studied by Schmidt[41], who developed the geometric rules for photocycloaddition. Many organic reactions can be performed in the absence of solvent or in the solid state. Certain reactions are even more efficient and take place faster in the solid state than in solution. Examples of these include the pinacol[42] and benzylic acid rearrangement[43] and certain Baeyer-Villager oxidation reactions[44]. These reactions are not fully understood and recent studies done by Cave et al. have proposed that certain solvent –free reactions proceed via a eutectic melt.[45,46]

Host-guest inclusion in the solid state is usually achieved by co-grinding of stoichiometric amounts of host and guest compounds. Successful experiments have been performed with the host 1,1,6,6-tetraphenylhexa-2,4-diyne-1,6-diol and the guests benzophenone[47]and the three isomers of aminobenzonitrile[48].

University of Cape Town

SEPARATION BY ENCLATHRATION

Selective inclusion or the preference of a host for one or more guests has important implications, especially in the separation of close isomers. This selectivity, or molecular recognition, is often due to a combination of factors such as the strength of the interaction between the host and the guest, shape, size and steric considerations as well as kinetic and thermodynamic effects. Successful separation of the lutidine isomers by the hosts 2,2'-dihydroxy-1,1'-binaphthyl[49], 1,4-bis(9-hydroxy-9-fluorenyl)benzene[50] and 1,1,6,6-tetraphenylhexa-2,4-diyne-1,6-diol[51] have been performed.

Separation by enclathration also has important industrial significance. Cyclodextrins can be used in the separation of isomers of different kinds including constitutional, diastereoisomers and enantiomers[52]. This has been widely exploited in many chromatographic techniques eg. high performance liquid chromatography (HPLC), capillary electrophoresis and gas-liquid chromatography (GLC) studies of the stoichiometry of cyclodextrin complexes.

Zeolites[53] are inorganic microporous materials of which the primary building blocks are SiO_2 and $[AlO_2]^{-1}$. The extra charge is generally countered by an alkali or alkaline earth metal cation. The tetrahedra form a network of channels, cavities and cages that are capable of including guest molecules. Zeolites are used in the separation of hydrocarbons in the petrochemical industry.

Molecules of urea form chiral, helical channels, which vary from 5.5-5.8 Å in diameter[54]. Urea also has potential industrial applications in separating linear and branched hydrocarbons in the petroleum industry.

University of Cape Town

MOLECULAR RECOGNITION AND CRYSTAL ENGINEERING

In living systems molecular organisation occurs when small units assemble into intricate superstructures[55]. Many of these are built by self-assembly ie. the basic units spontaneously combine to form a distinct entity. This recognition is determined largely by the chemical structure and geometry of the basic units involved and requires no external interference.

This has been mimicked by chemists and in particular supramolecular chemists in the hope of designing materials with novel and useful properties. Crystal engineering can be defined as the design and synthesis of solids with predefined physical properties using molecules or ions. Examples include:

- Polymeric conductors[56]: the transport of charges and spins along conjugated systems can be used for the storage of information on a molecular level.
- Superconducting charge transfer complexes: (bis(ethylenedithiotetrathiafulvalene))$_2$$ReO_4$ is a superconductor at 1.5K and 7 kbar.
- Photochemical devices[57]: capable of multielectron transfer, storage and catalysis. Molnar et al.[58] has reported the discovery of such a device.
- Light-conversion devices[59]: capable of absorbing light of one wavelength and re-emitting the maximum amount at another tuneable wavelength.
- Electrochemical sensors: Beer et al.[60] have developed a sensor for neutral molecules based on calixerene inclusion.
- Molecular wires[61]: conceptually, conduct an electric signal between two connected components. Arrhenius et al.[62] have prepared carotenoid type compounds for this purpose.

University of Cape Town

ASPECTS OF THIS STUDY

In this study, inclusion compounds of the hosts 1,1,6,6-tetraphenylhexa-2,4-diyne-1,6-diol (**TOD7**) and cyclotriveratrylene (**CTV**) were prepared and their physicochemical properties investigated. The two host compounds, **TOD7** and **CTV**, possess completely different geometries and functionality. This provides an interesting contrast in the type of interactions that occur between the hosts and the guest molecules as well as the packing arrangements of the crystal structures. The inclusion compounds formed provide intriguing examples in crystal engineering and molecular recognition.

The inclusion ability of the wheel and axle host, **TOD7,** was first discovered by Toda in 1968[26]. **CTV** was initially prepared by Mrs G. Robinson in 1915[63]. Robinson assigned the product she had synthesised as 2,3,6,7-tetramethoxy-9,10-dihydroanthracene with the molecular formula ~~$C_7H_{10}O_2$~~ $C_{18}H_{20}O_4$. In the 1950's it was again assigned as the hexamer before the correct trimeric formula was assigned in 1963.

Small organic molecules were used as guests and were chosen either because of their size, geometry or acceptor/donor capabilities. A wide variety of guests were included ranging from solid to liquid, polar to non-polar and symmetrical to non-symmetrical. Inclusion of these guests is significant in separation science for the isolation of organic molecules from aqueous solutions. This is especially important with respect to environmentally hazardous chemicals such as the chlorinated guests.

University of Cape Town

PHYSICAL PROPERTIES OF GUESTS STUDIED

The melting points, boiling points and densities of the guests are given below. The data were either obtained from the Merck Index[64] or from the reagent bottles themselves.

Guest	Molecular formula	m.p(°C)	b.p(°C)	Density (gcm^{-3})[a]
carbon tetrachloride	CCl_4	-23	77	1.589[a]
chloroform	$CHCl_3$	-63	61-62	1.484
dichloromethane	CH_2Cl_2	-95	40	1.325
acetonitrile	CH_3CN	-45	82	0.780-0.783
pyridine	C_5H_5N	-42	115	0.983
2-picoline	C_6H_7N	-70	128-129	0.944
3-picoline	C_6H_7N	-18	143-144	0.967
4-picoline	C_6H_7N	4	145	0.955
benzene	C_6H_6	5	80	0.879
toluene	C_7H_8	-95	111	0.866
mesitylene	C_9H_{12}	-45	165	0.864
N,N-Dimethyl formamide	C_3H_7NO	-61	153	0.950
dimethyl sulfoxide	C_2H_6OS	18	189	1.100
aniline	C_6H_7N	-6	184-186	1.022
o-nitroaniline	$C_6H_6N_2O_2$	69-71	284	0.901[a]
m-nitroaniline	$C_6H_6N_2O_2$	114	306	0.901[a]
2,2'-bipyridine	$C_{10}H_8N_2$	70	272-273	1.326
4,4'-bipyridine	$C_{10}H_8N_2$	111-112	305	1.232
1,1,1-trichloroethane	$C_2H_3Cl_3$	-33	74	1.338
1,1,2-trichloroethane	$C_2H_3Cl_3$	-35	113-114	1.442

a: at 25°C, all the rest are at 20°C.

University of Cape Town

REFERENCES

1. http://www.nobel.se/chemistry/index.html
2. J-M. Lehn, *Angew. Chem., Int. Ed. Engl. (*Nobel lecture), 27, 89, 1988.
3. L.F. Lindoy,and I.M. Atkinson, Monographs in Supramolecular Chemistry. No. 7.*Self-Assembly in Supramolecular Systems*, Royal Society of Chemistry, (ed) J.F. Stoddart, 2000.
4. H. Davy, *Philos. Trans. R. Soc. London*, 101, 1, 1811.
5. C. Schafhäutl, *J. Prakt. Chem*., 21, 129, 1841.
6. F. Wohler, *Ann. Chem. Liebigs*, 69, 297, 1849.
7. H. M. Powell, *J. Chem. Soc*., 61, 1948.
8. J. E. D. Davies, W. Kemula, H.M. Powell and N. O. Smith, *J. Incl. Phenom*., 1, 3, 1983.
9. A. P. Dianin, *J. Soc. Chem. Russe*, 46, 1310, 1914.
10. M. I. Hart, Jr., and N. O. Smith, *J. Am. Chem. Soc*., 84, 1816, 1962.
11. E. Weber and H.P. Josel, *J. Incl. Phenom*., 1, 61, 1983.
12. K.D.M. Harris, *Chemistry in Britain*, 132, 1993.
13. J. W. Steed and J. L. Atwood, *Supramolecular Chemistry*, (ed) John Wiley & Sons, 2000.
14. G.A. Jeffrey, *An Introduction to Hydrogen Bonding*, Oxford University Press, Oxford, 1997.
15. G.A. Saenger and W. Saenger, '*Hydrogen Bonding in Biological Structures'*, Springer, Berlin, 1991.
16. R. Taylor and O. Kennard, *J. Am. Chem. Soc*., 104, 5063, 1982.

University of Cape Town

17. G.R. Desiraju and T. Steiner, IUCR Monographs on Crystallography, Vol.9, '*The Weak Hydrogen Bond*', Oxford, 1999.

18. C.A. Hunter and J.K.M. Sanders, *J.Am. Chem. Soc.*,112, 5525, 1990.

19. J.F.Malone, C.M. Murray, M.H.Charlton, R. Doherty and A.J. Lavery, *J. Chem. Soc., Faraday Trans.*,93, 3429, 1997.

20. D. Braga, F. Grepioni and E. Tedesco, *Organometallics*, 17, 2669, 1998.

21. G.R. Desiraju and R. Parthasarathy, *J. Am. Chem. Soc.*, 111, 8725, 1989.

22. N. Ramasubba, R. Parthasarathy and P.Murray-Rust, *J. Am. Chem. Soc.*, 108, 4308, 1986.

23. S.C. Nyburg and W.Wong-Ng, *Proc. R. Soc. London Ser A*, 367, 29, 1979.

24. D.E. Williams and L.Y. Hsu, *Acta Crystallogr. , Sect A*, 41, 296, 1985.

25. G.R. Desiraju, 'Crystal Engineering. The Design of Organic Solids.', Elsevier, Amsterdam, 1989.

26. F. Toda, and K.Akagi, *Tetrahedron Lett.*, 3695, 1968.

27. G.R. Desiraju in Comprehensive Supramolecular Chemistry, Vol.6, Solid-state Supramolecular Chemistry, (eds) D.D. MacNicol, F. Toda and R. Bishop Pergamon, 1996.

28. H.Kurebayashi, T. Haino, S. Usui and Y. Fukuzawa, *Tetrahedron*, 57, 8667, 2001.

29. R.K.R. Jetti, F. Xue, T.C.W. Mak and A. Nangia, *J. Chem. Soc., Perkin. Trans 2*, 1223, 2000.

30. C. D. Gutsche, *Calixerenes*, Royal Society of Chemistry, Cambridge, 1989.

31. C. D. Gutsche, *Calixerenes 2*, Royal Society of Chemistry, Cambridge, 1989.

32. J.W. Steed, H. Zhang and J.L. Atwood, *Supramolecular Chemistry*, 7, 37, 1996.

33. Frontiers in Supramolecular Organic Chemistry and Photochemistry, (eds) H-J. Schneider and H. Dürr, Weinheim, pp.59, 1991.

University of Cape Town

34. J.W. Steed, P.C. Junk, J.L. Atwood, M.J. Barnes, C.L. Raston and R.S. Burkhalter, *J. Am. Chem. Soc.*,116, 10346, 1994.

35. M. E. Brown, *Introduction to Thermal Analysis*, Chapman & Hall, London, 1988

36. B. Wunderlicht, *Thermal Analysis*, Academic Press, San Diego, 1990.

37. P.J. Haines, Thermal Methods of Analysis. Principles, Application and Problems, Chapman & Hall, London, 1995.

38. H.K. Cammenga and M.Eppel, *Angew. Chem. Int. Ed. Engl.*, 34, 1171, 1995.

39. M.R. Caira, L.R. Nassimbeni, in Comprehensive Supramolecular Chemistry, Vol.6 Solid-state Supramolecular Chemistry (eds) D.D. MacNicol, F. Toda and R. Bishop, Pergamon, 1996.

40. M.R. Caira, L.R. Nassimbeni, D.Vujovic and E.Weber, *J.Chem. Soc., Perkin Trans.2*, 861, 2001.

41. G.M.J. Schmidt, *Pure Appl. Chem.*, 27, 674, 1971.

42. F. Toda, A. Kai, Y. Tagami and T.C.W. Mak, *Chem. Lett.*, 1393, 1987.

43. F. Toda, K. Tanaka, Y. Kagawa and Y. Sakaino, *Chem. Lett.*, 373, 1990.

44. F. Toda, M. Yagi and K. Kiyoshige, *J. Chem. Soc., Chem. Comm.*, 958, 1998.

45. G. Rothenberg, A.P. Downie, C.L. Raston and J.L. Scott, *J. Am. Chem. Soc.*, 123, 8701,, 2001.

46. G.W.V. Cave, C.L. Raston and J.L. Scott, *Chem. Comm.*, 2159, 2001.

47. D.R. Bond, L. Johnson, L.R. Nassimbeni and F. Toda, *J. Solid State Chem.*, 92, 68, 1991.

48. M.R. Caira, L.R. Nassimbeni, D.Vujovic and F. Toda, *J. Am. Chem. Soc.,122(39), 9367, 2000.*

49. E. de Vries, L.R. Nassimbeni and Hong Su, *Eur. J. Org. Chem.*, 1887, 2001.

University of Cape Town

50. M.R. Caira, L.R. Nassimbeni, D. Vujovic, E. Weber and A. Wierig, *Structural Chem.*, 10, 205, 1999.

51. M.R. Caira, L.R. Nassimbeni, D.Vujovic and F. Toda, *J. Chem. Soc., Perkin Trans.2*, 2681, 1999.

52. M. Asztemborska, R. Nowakowski and D. Sybilska, *J. Chromatog. A*, 902, 381, 2000.

53. P. Englezos, *Industrial and Engineering Chemical Research*, 32, 1251, 1993.

54. K.D.M. Harris, *J. Solid State Chem.*, 106, 83, 1993.

55. L. M. Greig and D. Philp, *Chem. Soc. Rev.*, 30, 287, 2001.

56. F. Vögtle, *Supramolecular Chemistry*, John Wiley & Sons, 1992.

57. V. Balzani, A. Juris, M. Venture et al., *Chem. Rev.*, 96, 759, 1996.

58. S.M. Molnar, G. Nallas., J.S. Bridgewater and K.J. Brewer, *J. Am. Chem. Soc.*, 116, 5206, 1994.

59. M.D. Ward, *Chem. Soc. Rev.*, 26, 365, 1997.

60. P. Beer, P.A. Gale and Z. Chen, *Supramol. Chem.*, 7, 241, 1996.

61. J-M. Lehn, *Supramolecular Chemistry: Concepts and Perspectives,* VCH:Weinheim, pp106-111, 1995.

62. T.S. Arrhenius, M. Blanchard-Desce, M. Dvolaitzky et al., Proc. Natl. Acad. Sci. USA, 83, 5355, 1986.

63. A. Collet, *'Cyclotriveratrylene' in Inclusion Compounds*, (eds) J.L Atwood, J.E.D. Davies and D.D. MacNicol, Academic Press: London, Vol.2, 97, 1984.

64. The Merck Index: An Encyclopedia of Chemical Drugs and Biologicals, Eleventh Edition, (ed) S.Budavari, Merck&Co., New Jersey, USA, 1989.

University of Cape Town

CHAPTER 2

University of Cape Town

CHAPTER 2 EXPERIMENTAL

HOST COMPOUNDS

Two host compounds were used in this study. The host compound 1,1,6,6-tetraphenylhexa-2,4-diyne-1,6-diol (**TOD7**) was synthesised and supplied by Professor Fumio Toda, from the Okayama University of Science, Japan. The host compound cyclotriveratrylene (2,3,7,8,12,13-hexamethoxy-5,10-dihydro-15*H*-tribenzo[a,d,g]cyclononene; **CTV**) was obtained from Dr. Leonard Barbour from the University of Missouri, United States of America.

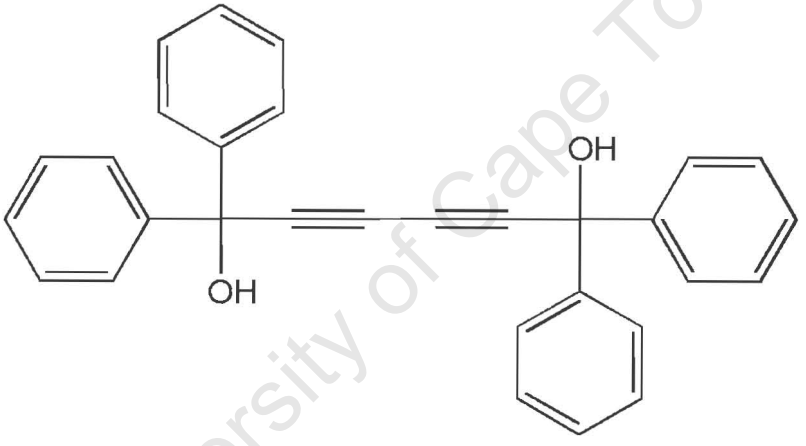

Figure 2.1 Schematic representation of **TOD7**.

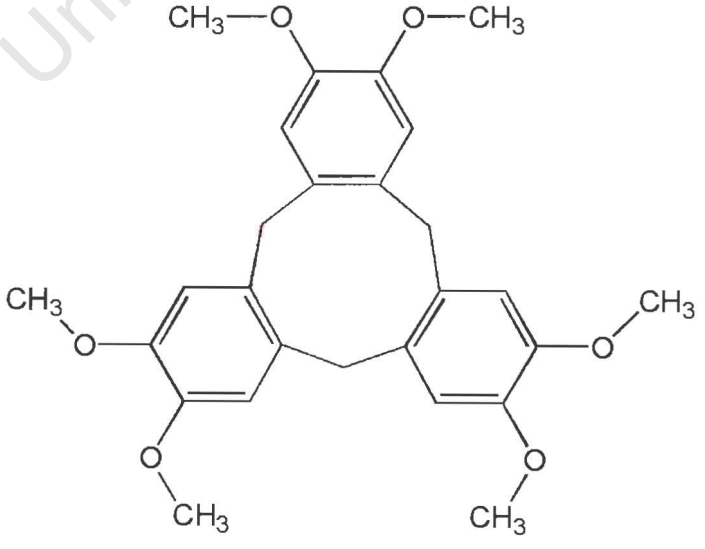

Figure 2.2. Schematic representation of **CTV.**

University of Cape Town

GUEST COMPOUNDS

The guests carbon tetrachloride, chloroform, dichloromethane, acetonitrile, pyridine, benzene, toluene, N,N- dimethylformamide, aniline and n-hexane were obtained from Saarchem-Holpro Analytic (Krugersdorp, RSA). The picolines, dimethyl sulfoxide and 1,1,2-trichloroethane were obtained from Merck (Darmstadt, Germany). BDH Chemicals (Poole, England) supplied the 1,1,1-trichloroethane. The solid guests nitroanilines, 2,2'-bipyridine and 4,4'-bipyridine were supplied by Sigma Chemical Company (St. Louis, USA). All chemicals were AR grade and were used without further purification.

CRYSTAL GROWTH

The host compound was dissolved in the hot liquid guest and the solutions were filtered through 0.45 μl teflon filter. Various methods of crystal growth were attempted to obtain suitable crystals. These included:

(a) slow evaporation: open vials containing solutions were left to evaporate slowly at room temperature.

(b) slow cooling: sealed vials containing solutions were placed in a thermoflask containing hot water and left to cool.

(c) crystal growth at elevated temperatures: brass blocks with holes to accommodate the vials were used in these experiments to maintain constant temperatures. The brass blocks were placed on hotplates at set temperatures and the temperature was monitored using a thermometer. The temperature that was most often successful in these experiments was 55°C. Vials were either sealed or were allowed to vent through small holes(≈1mm in diameter) in the lids.

University of Cape Town

For the solid guests, stoichiometric quantities of the host and the guest were dissolved in a common solvent. The hot solutions were filtered through 0.45 μl teflon filters and allowed to evaporate over a period of one week.

THERMAL ANALYSIS

Both thermogravimetric (TG) analysis and differential scanning calorimetry (DSC) are well-known techniques. TG and DSC were performed on Perkin-Elmer PC7 Series instruments. Crystals were blotted dry and crushed before analysis.

TG analysis was used to determine the host: guest ratios of the inclusion compounds with liquid guests. Calibration was done on the TG furnace. Curie point calibrations were performed with the standards nickel and alumel. A standard weight was used for the weight calibration.

DSC was used to monitor the decomposition of the inclusion compounds and to observe any phase changes that occur without an accompanying mass loss. The DSC instrumentation was calibrated using indium (onset temperature, T_{on}, = 156.6°C) and zinc (T_{on} = 419.5°C).

Both ramped TG and DSC traces were done at 10°C/min^{-1} and samples purged with nitrogen at a flow rate of 40ml/min^{-1}. TG and DSC results are affected by the particle size of the sample, the heating rate and the flow rate of the purging gas.[1]

KINETICS

The kinetics of decomposition of the host - guest compounds studied were determined using both isothermal and non-isothermal methods. Both these methods are well-known and have been studied extensively. Brief overviews of both methods are given below. Due to the limited amount of host compound, crystals were grown for kinetic

University of Cape Town

studies as opposed to powders from stirred solutions. The crystals were crushed to limit the effects of particle size on the results.

ISOTHERMAL KINETICS

A series of TG runs were performed at selected temperatures. The resultant TG runs were converted into α vs time curves, which were then fitted to various kinetic models. The α vs time curves are either acceleratory, deceleratory or sigmoidal[2]. Each of these types of curves can be described by certain rate expressions. An overview of these kinetic models has been taken from Brown[2] and is listed in Table 2.1. The Arrhenius equation was used to determine the activation energy of the reaction.

Arrhenius equation: $\ln k = -E_a / RT + \ln A$,

where k = rate constant,

E_a = activation energy,

A = pre-exponential factor

and T = absolute temperature.

$\alpha = \frac{m_o - m_t}{m_o - m_\infty}$

m = sample mass

University of Cape Town

NON-ISOTHERMAL KINETICS

A series of ramped TG runs ie. TG runs done over a selected temperature range, were performed at different heating rates. This method, developed by Flynn and Wall[3], analyses the thermogravimetric rate ie. the rate of weight loss with respect to temperature. The thermogravimetric rate can be described by the equation;

$dC / dT = (A / \beta) f(C) e^{-E / RT}$, where C = degree of mass loss and β = heating rate.

This equation can be reduced to: $d \log \beta / d\, 1/T \cong (0.457 / R) E$. An activation energy range can be obtained from plots of (-log β) vs 1/T.

A = pre exponential factor

Table 2.1. Broad overview of solid state rate equations.

	$f(\alpha) = kt$
1. Acceleratory	
P1 power law	$\alpha^{1/n}$
E1 exponential law	$\ln \alpha$
2. Sigmoidal	
A2 Avrami-Erofe'ev	$[-\ln(1-\alpha)]^{1/2}$
A3 Avrami-Erofe'ev	$[-\ln(1-\alpha)]^{1/3}$
A4 Avrami-Erofe'ev	$[-\ln(1-\alpha)]^{1/4}$
B1 Prout Tompkins	$\ln[\alpha/(1-\alpha)]$
3. Deceleratory	
Geometric Models	
R2 contracting area	$1-(1-\alpha)^{1/2}$
R3 contracting sphere	$1-(1-\alpha)^{1/3}$
Diffusion Controlled Models	
D1 one-dimensional	α^2
D2 two-dimensional	$(1-\alpha)\ln(1-\alpha) + \alpha$
D3 three-dimensional	$[1-(1-\alpha)^{1/3}]^2$
D4 Ginstling-Brounshtein	$(1-2\alpha/3) - (1-\alpha)^{2/3}$
"order of reaction"	
F1 first order	$-\ln(1-\alpha)$
F2 second order	$1/(1-\alpha)$
F3 third order	$[1/(1-\alpha)]^2$
Fn n-th order	$[1/(1-\alpha)]^n$

University of Cape Town

MICROANALYSIS

The host: guest ratios of the inclusion compounds formed with the selected solid guests were determined by microanalysis. Analyses were carried out on a Carlo Erba 1106 Elemental Analyser. Samples were analysed for carbon, hydrogen and nitrogen, and to prevent guest loss, were not placed under vacuum.

NUCLEAR MAGNETIC RESONANCE (NMR) SPECTROSCOPY

NMR was used to analyse inclusion compounds containing a mixture of guests and to confirm the purity of certain liquid guests believed to contain traces of contaminants. Prior to analysis, samples were dissolved in deuterated chloroform.

^{1}H-NMR spectra were recorded at 400MHz on a Varian VXR400, referenced relative to chloroform at 7.24 ppm.

HOT STAGE MICROSCOPY

Hot stage microscopy was used to follow the decomposition of the crystal and any physical changes that accompany it. This would include a change in the transparency or colour of the crystal and the crystal melt. Crystals were dried on filter paper and immersed in silicone oil. Guest loss was detected by the emergence of bubbles, which occurred upon heating. Hot stage microscopy was performed on a Linkam THMS600 apparatus mounted on a Nikon microscope. The temperature was controlled with a Linkam TP92 temperature controller. The crystal was monitored using a Sony Digital Hyper HAD video camera. The program analySIS[4] was used to observe and save the results.

Differences were observed in the onset temperatures of thermal events monitored using hot stage microscopy and DSC. This is due to differences in the physical instrumentation and differences in particle size of the samples analysed. Typically, crystals were monitored by hot stage microscopy and crushed crystals analysed using DSC.

University of Cape Town

COMPETITION EXPERIMENTS

2-, 3- and 4-component competition experiments were performed on selected host-guest systems. 2-component competition experiments are defined as competition between two guests, 3-component between three guests and 4-component between four guests.

In the 2-component competition, a series of 11 vials were set up containing mixtures of two guests such that the mole fraction of one guest was increased in the range from 0 to 1. The host compound was added and dissolved by heating. The total guest: host ratio was kept at least at 20:1 such that the guest was always in excess. The solutions were allowed to cool and evaporate slowly over a period of a few days. The resulting crystalline material was dried on filter paper and placed in vials with silicone seals. The vials were heated on a hotplate and the guests released were analysed by gas chromatography. The original mother liquors were also analysed by gas chromatography and the results plotted on graph paper.

University of Cape Town

This experiment was also extended to competition between 3 and 4 guests in certain cases. In the 3-component competition the three pure guests are represented on the apices of an equilateral triangle as shown in Figure 2.3(a). Points d. e. f and g represent the starting mixtures. In the 4-component competition the four pure guests are represented on the apices of a regular tetrahedron as shown in Figure 2.3(b). The blue dots in Figure 2.3(b) represent the starting mixtures.

(a) (b)

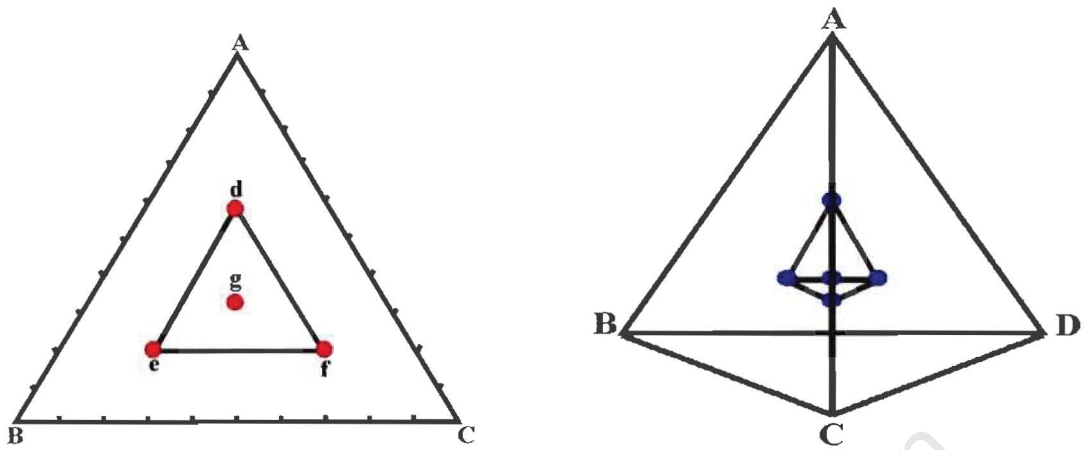

Figure 2.3. Diagram illustrating (a) 3-component competition and (b) 4-component competition experiments.

University of Cape Town

GUEST EXCHANGE

Host-guest inclusion was obtained by vapour diffusion of the liquid guest into the host in a sealed container. An excess of the guest was used. TG and DSC verified the formation of an inclusion compound. The resultant inclusion compound was exposed to an excess of vapour from a different guest. The reaction was monitored by TG or DSC over a time period which varied from a few hours to a few days. All experiments were performed at room temperature.

GAS CHROMATOGRAPHY

During competition experiments, vials containing mixtures of guests and those containing the original mother liquors were analysed on a Varian 3400 gas chromatograph. All analyses were performed on a polar Carbowax capillary column (0.25mm in diameter, 25mm in length). The computer package DELTA[5] was used to monitor and analyse the results. In the case of mixtures of guests which were not

isomers, the gas chromatograph was calibrated using mixtures of known concentrations.

X-RAY POWDER DIFFRACTION (XRD)

X-Ray powder diffraction (XRD) traces were recorded on a Phillips PW1050/25 goniometer mounted on a Philips PW1130/90 X-ray generator. The generator was operated at 25mA and 40kV and nickel-filtered CuK_α radiation (λ=1.5418Å) was used. Powdered samples were packed into aluminium or glass sample holders. All samples were scanned over a 2θ range of 5°-40° with a step size of 0.1° and 2s counts.

CRYSTAL STRUCTURE ANALYSIS

Suitable crystals of size 0.1 to 0.5mm in all dimensions were selected and mounted, either on glass fibres or in 0.3 or 0.5mm diameter Lindemann capillary tubes containing mother liquor. The latter method would prevent desolvation and was often used on unstable crystals.

Preliminary unit cell dimensions and Laue symmetry were obtained from oscillation and Weissenberg photographs. X-ray photographs were taken on a Stoë goniometer using Ni-filtered CuK_α radiation of wavelength 1.5418Å.

Data were collected on a Nonius-Kappa-CCD diffractometer using graphite-monochromated MoK_α radiation (λ = 0.7107Å). An ENRAF-NONIUS FR590 generator was used. Data collections were either done at room temperature, typically at 293-295K, or at low temperature (173K). The low temperature was maintained by an Oxford Cryostream cooler. The strategies for the data collections were evaluated

University of Cape Town

using COLLECT software[6]. Each data set was scaled and reduced using DENZO-SMN[7]. All data were corrected for Lorentz and polarisation effects. Absorption corrections are described in the relevant chapters.

All the structures were solved by direct methods using SHELXS-97[8]. Subsequent refinement by full-matrix least-squares methods on F^2 were performed using SHELXL-97[8]. The degree of agreement between the calculated (F_c) and observed (F_o) structure factors is given by the residual index, R_1:

$$R_1 = \frac{\sum \left| |F_o| - |F_c| \right|}{\sum |F_o|}$$

However, the R-indices based on F^2 are larger than those based on F. Thus, both the R-factor based on F values and that based on F^2, wR_2, will be given.

$$wR_2 = \left[\frac{\sum w(F_o^2 - F_c^2)^2}{\sum w(F_o^2)^2} \right]^{1/2}$$

A simplified default weighting scheme (w) was used in which a and b were refined for each structure.

$$w = 1 / \left[\sigma^2(F_o^2) + (aP)^2 + bP \right]$$

$$P = \left[\max(0, F_o^2) + 2F_c^2 \right] / 3$$

University of Cape Town

The Goodness of Fit (S) is also based on F^2:

$$S = \left[\frac{\sum (w(F_o^2 - F_c^2)^2}{(n - p)} \right]^{1/2}$$

where n is the number of reflections and p is the total number of parameters refined.

COMPUTATION

X-ray powder patterns for inclusion complexes were calculated using LAZY PULVERIX[9]. All the crystal packing diagrams were produced with Pov-Ray[10]. The program LAYER[11] was used to check for systematic absences and space group symmetry. SECTION[12] was used to slice through cross sections of the unit cell to determine the type of voids occupied by guest molecules. In a typical example the host molecules were represented in van der Waals radii with the guests omitted.

X-SEED[13] was used as a graphical interface for the programs SHELXS-97, SHELXL-97, LAZY PULVERIX, Pov-Ray, LAYER and SECTION.

PLATON[14] was used to analyse all host-host, host-guest and guest-guest interactions.

WinGX32[15] was used as an interface for PLATON.

The Cambridge Structural Database[16] (CSD) was used to search and analyse published crystal structures.

University of Cape Town

LATTICE ENERGY CALCULATIONS

The atom-atom potential method was used to perform lattice energy calculations. Intermolecular non-bonded interactions were determined using the program HEENY[17]. HEENY is a modified version of EENY[18]. A force field given by equation (1) was used.

$$V(r) = a \exp(-br) / r^d - c/r^6 \qquad (1)$$

where r is the distance between any pair of atoms (Å) and a, b, c and d are coefficients calculated by Gavezzotti[19]. Pertsin and Kitaigorodskii[20] reviewed these coefficients with V(r) in kcal mol^{-1}. Hydrogen bonding potentials were introduced into the calculations. A simplified version of these, given by Vedani and Dunitz[21] was used and is shown below:

$$V_{ab} = \left[\left(A/R^{16} \right) - \left(C/R^{10} \right) \right] \cos^2\theta$$

where V_{ab} is the energy associated with the hydrogen bond, R is the distance between the hydrogen atom and the acceptor, θ is the donor—H•••acceptor angle, A and C are the constants related to the well-depth V_{min} and the equilibrium distance R_o by $A = -5\ R_o^{12} V_{min}$ and $C = -6\ R_o^{10} V_{min}$.

University of Cape Town

Table 2.2. Host-guest compounds studied in this thesis.

Host(H)	Guest(G)	H:G ratio	Code name
TOD7	carbon tetrachloride	1: ½	**T7CCL4**
	chloroform	1: ½	**T7CHCL3**
	dichloromethane	1: ½	**T7CH2CL2**
	acetonitrile	1: 2	**T7CH3CN**
	pyridine	1: 2	**T7PYR**
	2-picoline	1: 2	**T72PIC**
	3-picoline	1: 2	**T73PIC**
	4-picoline	1: 2	**T74PIC**
	benzene	1: 1	**T7BENZ**
	toluene	1: ¾	**T7TOL**
	mesitylene	1: 1	**T7MESI**
	N,N-dimethylformamide	1: 2	**T7DMF**
	dimethyl sulfoxide	1: 2	**T7DMSO**
	aniline	1: 2	**T7ANI**
	o-nitroaniline	1: 2	**T7ONA**
	m-nitroaniline / n-hexane	1: 2: ¼	**T7MNA**
	2,2-bipyridine	1: 2	**T72BIPY**
	4,4-bipyridine	1: ½	**T74BIPY**
CTV	carbon tetrachloride	1: 1	**CTVCCL4**
	1,1,1-trichloroethane / 1,1,1-trichloropropane	1: 1: 1	**CTV111**
	1,1,2-trichloroethane	1: 2	**CTV112**

University of Cape Town

REFERENCES

1. M.R. Caira, and L.R. Nassimbeni, "Phase transformation in inclusion compounds, kinetics and thermodynamics of enclathration" in D.D. MacNicol, F.Toda and R.Bishop (eds.), Comprehensive Supramolecular Chemistry, Vol 6. Solid State Supramolecular Chemistry: Crystal Engineering, Pergamon, Elsevier Science Ltd., Oxford, pp825-850, 1996.
2. M. E. Brown, *Introduction to Thermal Analysis*, Chapman & Hall, London, 1988.
3. J.H. Flynn, L.A.Wall, *Polymer Letters,* Vol.4, 323-328, 1966.
4. Soft Imaging System GmbH: Digital Solutions for Imaging and Microscopy, Version 3.1 for Windows.
5. Delta chromatography data system for windows, Version 5.0, © 1995-1998.
6. COLLECT, data collection software, Nonius, 1998.
7. Z. Otwinowski, W. Minor, *Methods in Enzymology*, (eds) C. W. Carter and R. M. Sweet, Academic Press, New York, 276, 307, 1996.
8. G. M. Sheldrick, SHELX-97, University of Göttingen, 1997.
9. K. Yvon, W. Jeitschko and E. Parthe, *J. Appl. Cryst.*, 10, 73, 1977.
10. Pov-Ray for Windows, Version 3.1e.watcom.win32, The persistence of vision development team, © 1991-1999.
11. L.J. Barbour, LAYER, A computer program for the graphic display of intensity data as simulated precession photographs, *J. Appl. Cryst.*, 32, 351, 1999.
12. L.J. Barbour, SECTION, A computer program for the graphic display of cross sections through a unit cell, *J. Appl. Cryst.*, 32, 351, 1999.
13. L.J. Barbour, X-SEED, *A graphical interface to SHELX*, University of Missouri, Columbia, USA, 1999.

University of Cape Town

14. A.L. Spek, PLATON, *A multipurpose crystallographic tool*, Version 10500 © 1980-2000.

15. L.J. Farrugia, WinGX, An integrated system of windows programs for the solution, refinement and analysis of single crystal X-ray diffraction data, Version 1.63, *J. Appl. Cryst.*, 32, 837, 1999.

16. Cambridge Structural Database and Cambridge Structural Database System, Version 5.22 (2001), Cambridge Crystallographic Data Centre, University Chemical Laboratory, Cambridge, England.

17. C.F Marais, *HEENY-Modification of EENY to allow H-bonding calculations*, University of Cape Town, 1990.

18. W.D.S. Motherwell, *EENY, Potential Energy Program*, Cambridge University, England, 1973.

19. A. Gavezzotti, *Crystallogr. Rev.*, 7, 5, 1998.

20. A.J. Pertsin and A.I. Kitaigorodski, *The Atom-atom Potential Method, Chemical Physics 43*, Springer, Berlin, 1987.

21. A. Vedani and J.D Dunitz, *J. Amer. Chem. Soc.*, 107, 7653, 1985.

University of Cape Town

CHAPTER 3

University of Cape Town

CHAPTER 3. TOD7 AND ITS INCLUSION COMPOUNDS

TOD7

A series of small organic guests were included with the host, **TOD7** (1,1,6,6-tetraphenylhexa-2,4-diyne-1,6-diol). The structure and reactivity of these inclusion compounds were investigated. Reactivity was restricted to desolvation reactions ie. the loss of guest and in certain cases exchange reactions between guests.

The host numbering scheme is given below:

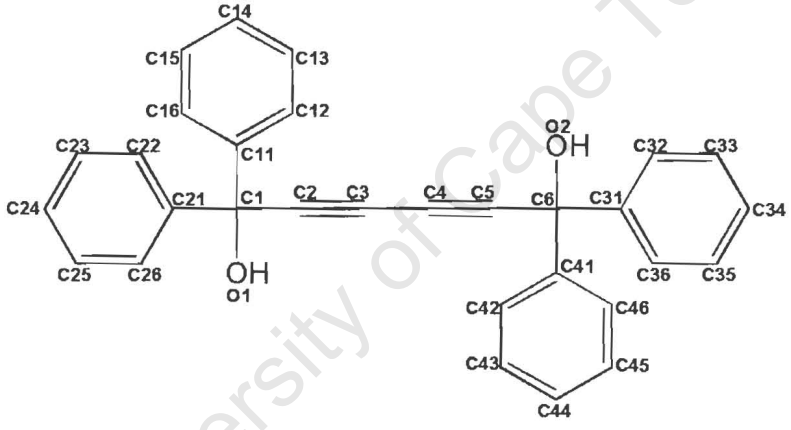

In cases where there are two host molecules in the asymmetric unit, the first molecule is labelled as shown above and the second molecule is labelled with the suffix A.

Guests included by **TOD7** and discussed in this study:

- carbon tetrachloride, chloroform, dichloromethane and acetonitrile.
- pyridine and 2-, 3-, and 4-picoline.
- aromatic guests——▶benzene, toluene and mesitylene.
- dimethyl formamide and dimethyl sulphoxide
- aniline and o- and m-nitroaniline / n-hexane.
- bipyridines.

University of Cape Town

CHAPTER 3.1 INCLUSION OF CHLORINATED GUESTS AND ACETONITRILE.

In this chapter, inclusion compounds formed between the host, **TOD7**, and the guests carbon tetrachloride, chloroform, dichloromethane and acetonitrile will be discussed. Crystal structures were obtained for all the above inclusion compounds. Thermal analysis was performed and an activation energy for desolvation was determined for one of the compounds.

The crystals **T7CCL4** and **T7CH3CN** were grown at room temperature by slow evaporation whereas **T7CHCL3** and **T7CH2CL2** were grown at 4°C. In all cases dilute solutions were prepared, typically 20mg host dissolved in 5 ml guest.

University of Cape Town

Table 3.1.1 Crystal data, experimental and refinement parameters.

	T7CCL4	T7CHCL3	T7CH2CL2	T7CH3CN
Compound	$C_{30}H_{22}O_2 \cdot ½CCl_4$	$C_{30}H_{22}O_2 \cdot ½CHCl_3$	$C_{30}H_{22}O_2 \cdot ½CH_2Cl_2$	$C_{30}H_{22}O_2 \cdot 2CH_3CN$
M_W , $gmol^{-1}$	491.38	473.66	456.94	496.58
Temperature/ K	200(2)	173(2)	173(2)	200(2)
Crystal system	monoclinic	monoclinic	monoclinic	monoclinic
Space group	C2/c	C2/c	$P2_1/n$	$P2_1/n$
a, Å	22.190(10)	22.270(5)	17.083(3)	10.847(2)
b, Å	13.775(3)	13.869(3)	13.629(3)	8.251(2)
c, Å	17.38(3)	16.934(3)	22.274(5)	15.364(3)
α, °	90	90	90	90
β, °	107.49(7)	107.71(3)	108.02(3)	91.05(3)
γ, °	90	90	90	90
V, $Å^3$	5067(9)	4982(2)	4931(2)	1374.8(5)
Z	8	8	8	2
Absorption coefficient, mm^{-1}	0.282	0.232	0.180	0.075
F(000)	2040	1972	1912	524
Crystal size, mm	0.31× 0.25 × 0.47	0.44 × 0.30 × 0.22	0.61 × 0.51 × 0.33	0.28× 0.39 × 0.31
Index ranges	h: 26,25; k: 0,16; l: 0,20	h: -26,20; k: ±16; l:-19,17	h: ±22; k: -17, 15; l: -26, 28	h: ±12; k: 0, 9; l: -5, 18
Reflections collected / unique	4628 / 4465	12323 / 4356	23756 / 11092	2577 / 2416
Data/ restraints/ Parameters	4465 / 4 / 320	4356 / 4 / 333	11092 / 8 / 620	2416 / 2 / 177
Goodness-of-fit	0.923	1.052	1.038	0.990
ρ_{calc}, $g \cdot cm^{-3}$	1.288	1.263	1.231	1.200
Final R indices [$I > 2\sigma(I)$]	$R_1 = 0.0637$, $wR_2 = 0.1687$	$R_1 = 0.0668$, $wR_2 = 0.1691$	$R_1 = 0.0744$, $wR_2 = 0.1933$	$R_1 = 0.0479$, $wR_2 = 0.1243$
R indices (all data)	$R_1 = 0.1530$, $wR_2 = 0.1906$	$R_1 = 0.1148$, $wR_2 = 0.1956$	$R_1 = 0.1089$, $wR_2 = 0.2198$	$R_1 = 0.0780$, $wR_2 = 0.1339$
Largest difference peak and hole, $eÅ^{-3}$	0.340 and -0.321	0.460 and -0.451	0.843 and –1.161	0.164 and -0.258

University of Cape Town

T7CCL4

$C_{30}H_{22}O_2 \cdot ½CCl_4$
Guest : carbon tetrachloride
Space Group : C2/c
a = 22.190(10)Å α =90°
b = 13.775(3)Å β =107.49(7)°
c = 17.38(3)Å γ =90°
Volume = 5067(9)Å^3
Z = 8

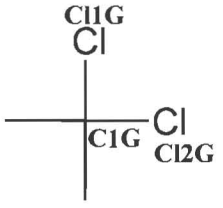

Crystal Structure and Refinement

Preliminary oscillation and Weissenberg photography indicated that **T7CCL4** belonged to the monoclinic system. A host: guest ratio of 1: ½ was established by TG and this was confirmed by the crystal structure. The following reflection conditions were observed :

hkl : h + k = 2n

h0l : h , l = 2n

0k0 : k = 2n

The above conditions indicate the space groups Cc and C2/c. The centrosymmetric space group C2/c was assigned based on the mean $|E^2 - 1|$ values. This was vindicated by the solution of the crystal structure in this space group. The data were corrected for absorption (min. correction factor: 0.9013, max. correction factor: 0.9962, ave. correction factor: 0.9606).

All the non-hydrogen atoms of the host and the guest were obtained by direct methods. The unit cell consists of eight host molecules and four guest molecules (Z=8). The guest is situated on a two-fold axis (Wyckoff position e). The non-hydrogen atoms of the host and the guest were refined anisotropically. The aromatic hydrogens of the host were obtained in the electron density maps but were

University of Cape Town

geometrically constrained with the C-H distances fixed at 0.93Å. The hydroxyl hydrogens were located in the difference electron density maps, and were refined isotropically. The hydroxyl hydrogens were then placed in geometrically calculated positions based on the relationship between O—H distances and O•••O distances[1]. The bond lengths and angles of the host molecule are all within the accepted ranges[2], except for selected aromatic bond lengths, which are lower than expected. This is due to the relatively high temperature factors of: C25 (U_{eq} = 0.10Å^2), C42 (U_{eq} = 0.12Å^2), C43 (U_{eq} = 0.13Å^2) and C45 (U_{eq} = 0.11Å^2) compared to the average U_{eq} (aromatic carbon atoms) = 0.07Å^2. Details of the host geometry are discussed in Chapter 5. Both the carbon and the chlorine atoms of the guest refined with very high temperature factors. At the end of the refinement U_{eq}(C1G) = 0.12Å^2, U_{eq}(Cl1G)=0.13Å^2 and U_{eq}(Cl2G) = 0.25Å^2. The geometry of the carbon tetrachloride molecule is defined by two unique bond distances (C—Cl = 1.728(5)Å and 1.740(5)Å) and four unique bond angles (Cl—C—Cl = 108.3(1)°, 108.3(5)°, 109.0(1)° and 113.8(5)°). The bond angles and distances differ from those expected due the poor refinement of the guest molecule. The final R factor was R_1 = 0.0637.

Crystal Packing

The crystal packing of **T7CCL4** is illustrated in Figure 3.1.1. The hydroxyl groups of the host molecule are in the gauche configuration. The host molecules pack in a zigzag pattern when viewed down [100]. The guest molecules lie in cages located at centres of symmetry at Wyckoff position e. Each cage, of size approximately 9.8Å × 9.5Å × 6.7Å, contains one guest molecule. The word cryptate can be used to describe the structure.

University of Cape Town

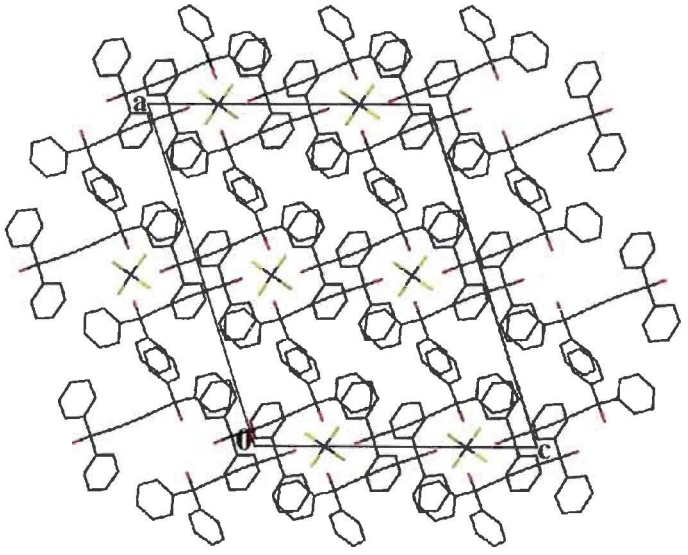

Figure 3.1.1(a). Packing diagram of **T7CCL4** down [010].

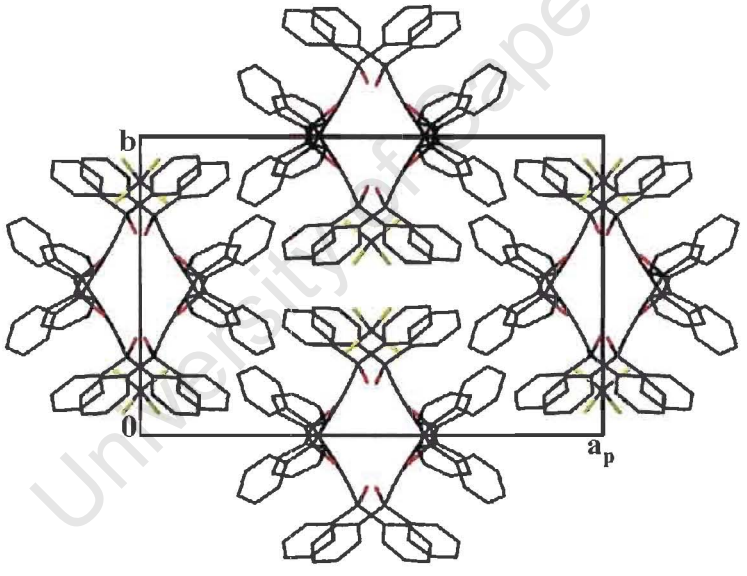

Figure 3.1.1(b). Packing diagram of **T7CCL4** down [001].

University of Cape Town

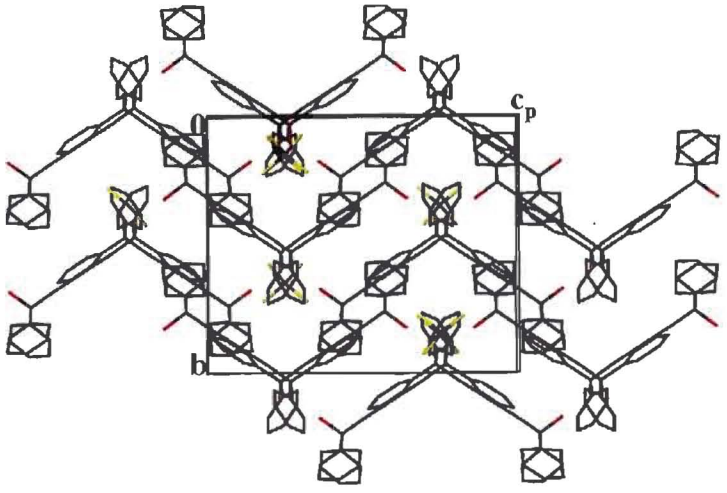

Figure 3.1.1(c). Packing diagram of **T7CCL4** down [100].

Figure 3.1.2 shows the view down [001] when sections are sliced through the crystal. The guest has been omitted to show the cavities created by the host framework. The guests occupy positions 0, 0.15, ¼; 0, 0.85, ¾; ½, 0.65, ¼; ½, 0.35, ¾; 1, 0.15, ¼ and 1, 0.85, ¾ in the unit cell.

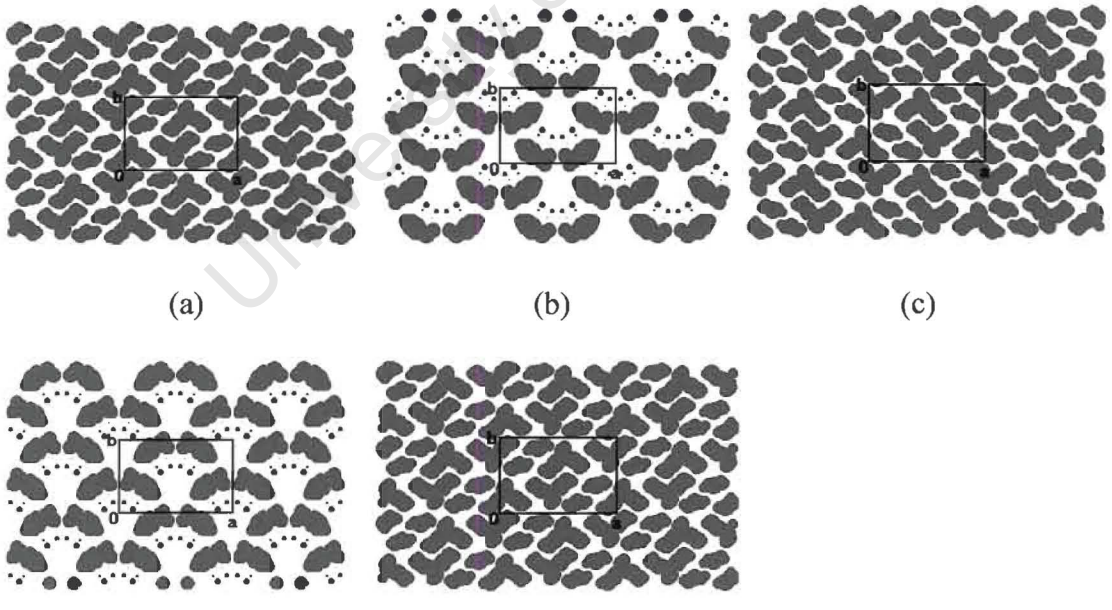

Figure 3.1.2. Section plot of **T7CCL4** down [001] at sections (a) z=0, (b) z= ¼, (c) z=½, (d) z=¾ and (e) z=1

University of Cape Town

The hydrogen bonding scheme is illustrated in Figure 3.1.3. Hydrogen bonding occurs between the hydroxyl groups of adjacent host molecules[3]. Four hydroxyl ~~moeities~~ moieties on four distinct host molecules form a four-centre hydrogen bond ~~network~~ tetramer. This results in the host stacking in zigzag layers parallel to [100]. The guest molecules fit in the hydrophobic cavities between the layers. The hydrogen bonding details are listed in Table 3.1.2. In addition weak C—H•••π interactions, with distances shorter than 3.05Å, also exist between certain aromatic C—H bonds of the host and the phenyl rings of another host molecule. This type of interaction is well-documented[4,5] and has been referred to as aromatic C—H•••π interactions[6].

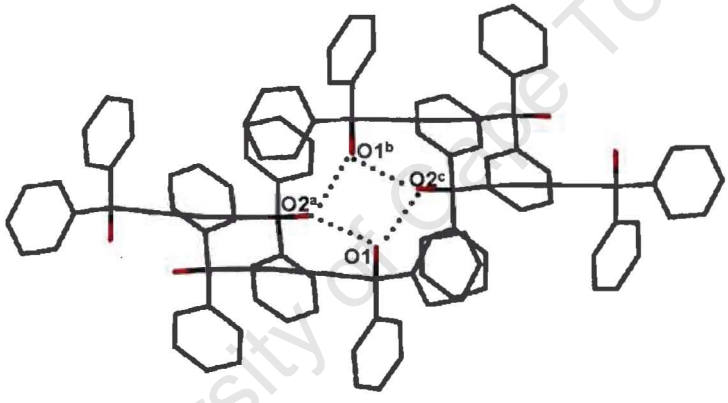

a: 1-x, -y, -z

b: 1-x, y, -z - ½

c: x, -y, z - ½

Figure 3.1.3. Hydrogen bonding scheme of **T7CCL4**

Table 3.1.2. Hydrogen bonding details of **T7CCL4**.

Donor (D)	Acceptor (A)	D—H / Å	D•••A / Å	D—H•••A / °
O1	O2[d]	0.98(3)	2.721(4)	155(1)
O2	O1[e]	0.98(1)	2.710(4)	139(1)

d: -x+1, -y, -z

e : x, -y, z+½

University of Cape Town

Thermal Analysis

The DSC curve shows three endotherms of which the first (T_{on} = 107.0°C) corresponds to the loss of guest. The last two endotherms (T_{on} = 147.1°C, peaks at 144.4°C and 148.5°C) correspond to a phase change and melt of the host. This phase change was not visible on the hot stage because it occurs too close to the host melt.

The TG curve shows two steps which individually do not correspond to a stoichiometric loss of guest. The first step is consistent with the loss of 0.38 of the total guest and the second step corresponds to the loss of 0.62 of the total guest. The experimental guest loss was 16.2 % (calculated guest loss = 15.7 %). Above 170°C decomposition occurs.

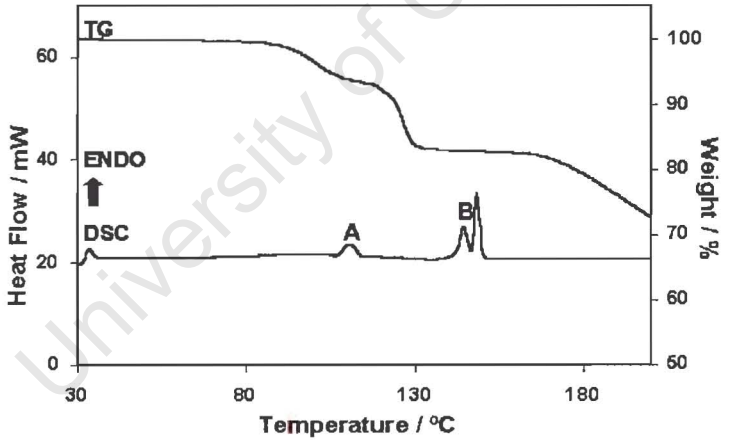

Figure 3.1.4. TG and DSC curves for **T7CCL4**.

University of Cape Town

T7CHCL3

$C_{30}H_{22}O_2 \cdot ½CHCl_3$		
Guest : chloroform		
Space Group : C2/c		
a = 22.270(5)Å	α =90°	
b = 13.869(3)Å	β =107.71(3)°	
c = 16.934(3)Å	γ =90°	
Volume = 4982(2)Å^3		
Z = 8		

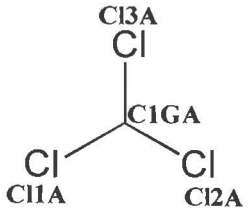

Crystal Structure and Refinement

The host: guest ratio of 1: ½ was confirmed by TG analysis. The conditions for observed reflections were the same as those found for **T7CCL4**. The centrosymmetric space group C2/c was assigned based on the mean $|E^2 - 1|$ values obtained from direct methods. This was confirmed by the successful solution of the crystal structure in this space group.

The host atoms were located in general positions and were refined anisotropically. The aromatic and the hydroxyl hydrogen atoms of the host were located in the difference electron density maps but were geometrically constrained as for the previous structure. The hydroxyl hydrogens of the host molecule are oriented in the gauche conformation. The host molecule refined with all bond lengths and angles in the typical range[2]. The U_{eq} values for two of the phenyl carbon atoms were slightly large (U_{eq}(C15) = 0.11Å^2 and U_{eq}(C16) = 0.10Å^2) compared to the average value of U_{eq} = 0.06Å^2 obtained for the remainder of the aromatic carbon atoms. This affected certain aromatic bond lengths, which refined to shorter values than expected. The host conformation is described in detail in Chapter 5.

University of Cape Town

The carbon and chlorine atoms of the guest were found to be disordered over two positions via a twofold rotation axis (Wyckoff position e). The non-hydrogen atoms of the guest were refined anisotropically. Even though the data collection was done at low temperature (-100°C) the thermal parameters for the guest atoms were still quite large. At the end of the refinement U_{eq}(Cl1A) = 0.14Å^2, U_{eq}(Cll2A) = 0.30Å^2 and U_{eq}(Cl3A) = 0.12Å^2. All the guest hydrogen atoms were omitted from the final model.

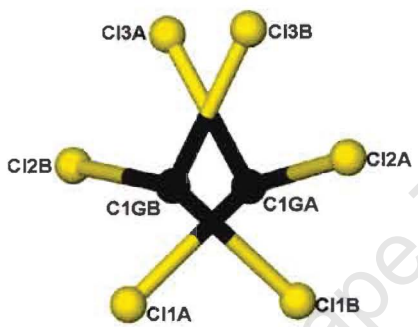

Figure 3.1.5. Disorder in the chloroform guest molecule.

The bond lengths of the chloroform molecule (C1GA—Cl1A = 1.719(9)Å, C1GA—Cl2A = 1.707(11)Å and C1GA—Cl3A = 1.753(9)Å) are shorter than those expected and this can be ascribed to the disorder. The bond angles refined to Cl1A—C1GA—Cl2A = 105.6(5)°, Cl2A—C1GA—Cl3A = 109.2(6)° and Cl1A—C1GA—Cl3A = 109.5(5)°.

Crystal Packing

T7CHCL3 and **T7CCL4** are isostructural with respect to the host (similar unit cell dimensions, space group C2/c and closely matching coordinates). A similar packing motif is observed as for the previous structure. The guest molecules are situated in cages of approximate size 6.5Å × 6.3Å × 5.5Å located at Wyckoff position e. The host framework forms a zigzag pattern when viewed down [100]. The crystal packing of **T7CHCL3** is shown in Figure 3.1.6.

University of Cape Town

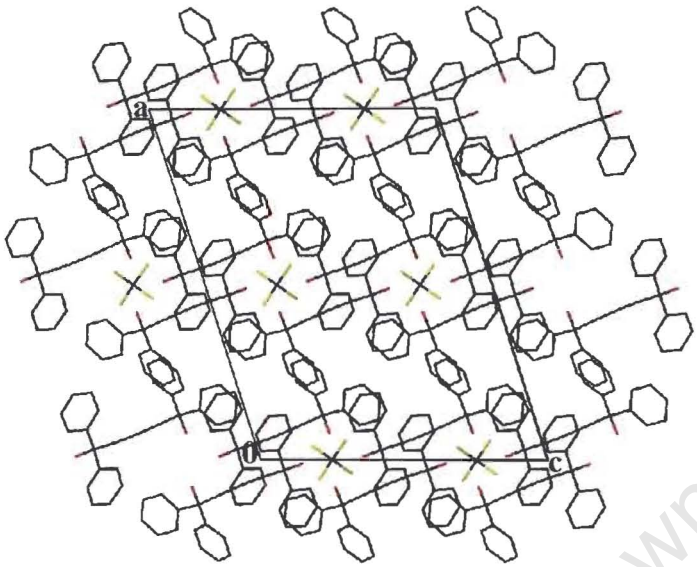

Figure 3.1.6(a). Packing diagram of **T7CHCL3** down [010].

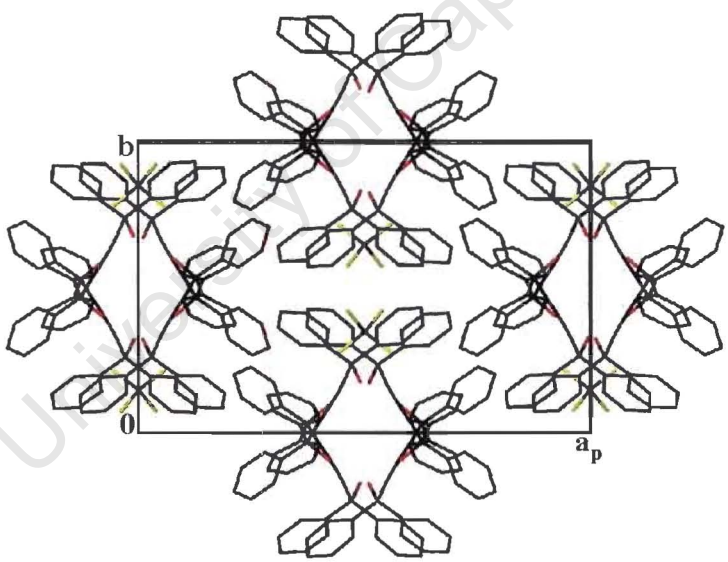

Figure 3.1.6(b). Packing diagram of **T7CHCL3** down [001].

University of Cape Town

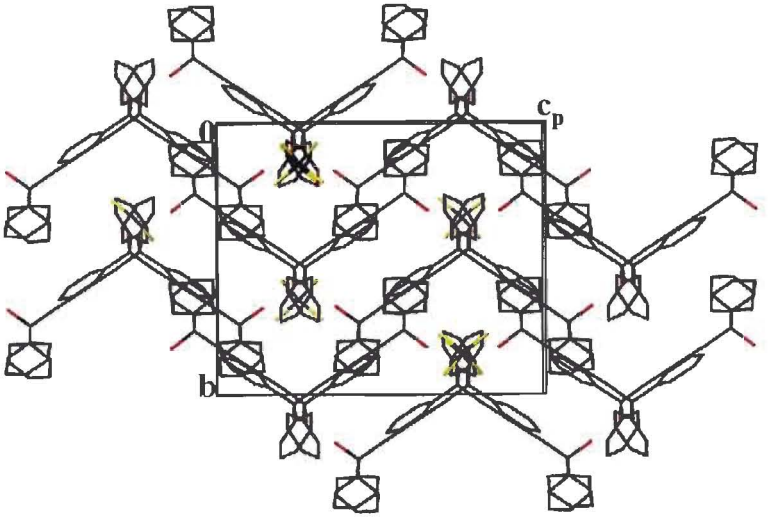

Figure 3.1.6(c). Packing diagram of **T7CHCL3** down [100].

Once again hydrogen bonding occurs between four hydroxyl groups on four adjacent host molecules. The details of the hydrogen bonding are given in Table 3.1.3. Again, aromatic C—H•••π interactions[5] are present.

Table 3.1.3. Hydrogen bonding details of **T7CHCL3**.

Donor (D)	**Acceptor (A)**	**D—H / Å**	**D•••A / Å**	**D—H•••A / °**
O1	O2[a]	0.98(1)	2.689(1)	158(2)
O2	O1[b]	0.98(1)	2.702(1)	150(3)

a: x, -y, z+½

b : -x+1, -y, -z

University of Cape Town

Thermal Analysis

The TG shows a two step mass loss. The individual mass losses are non-stoichiometric, with the first step corresponding to the loss of 0.20 of the total guest and the second step corresponding to the loss of 0.80 of the total guest present. The total experimental mass loss of 12.6% (calculated 12.6%) is consistent with a host:guest ratio of 1:½.

The DSC results are similar to those of the previous compound. The first endotherm corresponds to the loss of guest (T_{on} = 93.9°C) with the last two endotherms due to a phase change and subsequent melt of the host (T_{on} = 147.5°C, peaks at 145.0°C and 148.8°C). These results are consistent with the hot stage microscopy, where guest loss is already taking place at ca. 90°C and is followed by the host melt.

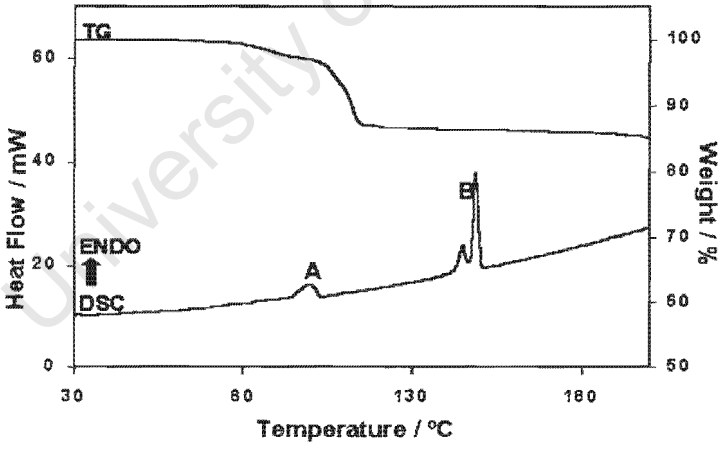

Figure 3.1.7. TG and DSC of **T7CHCL3**.

University of Cape Town

Hot stage Microscopy

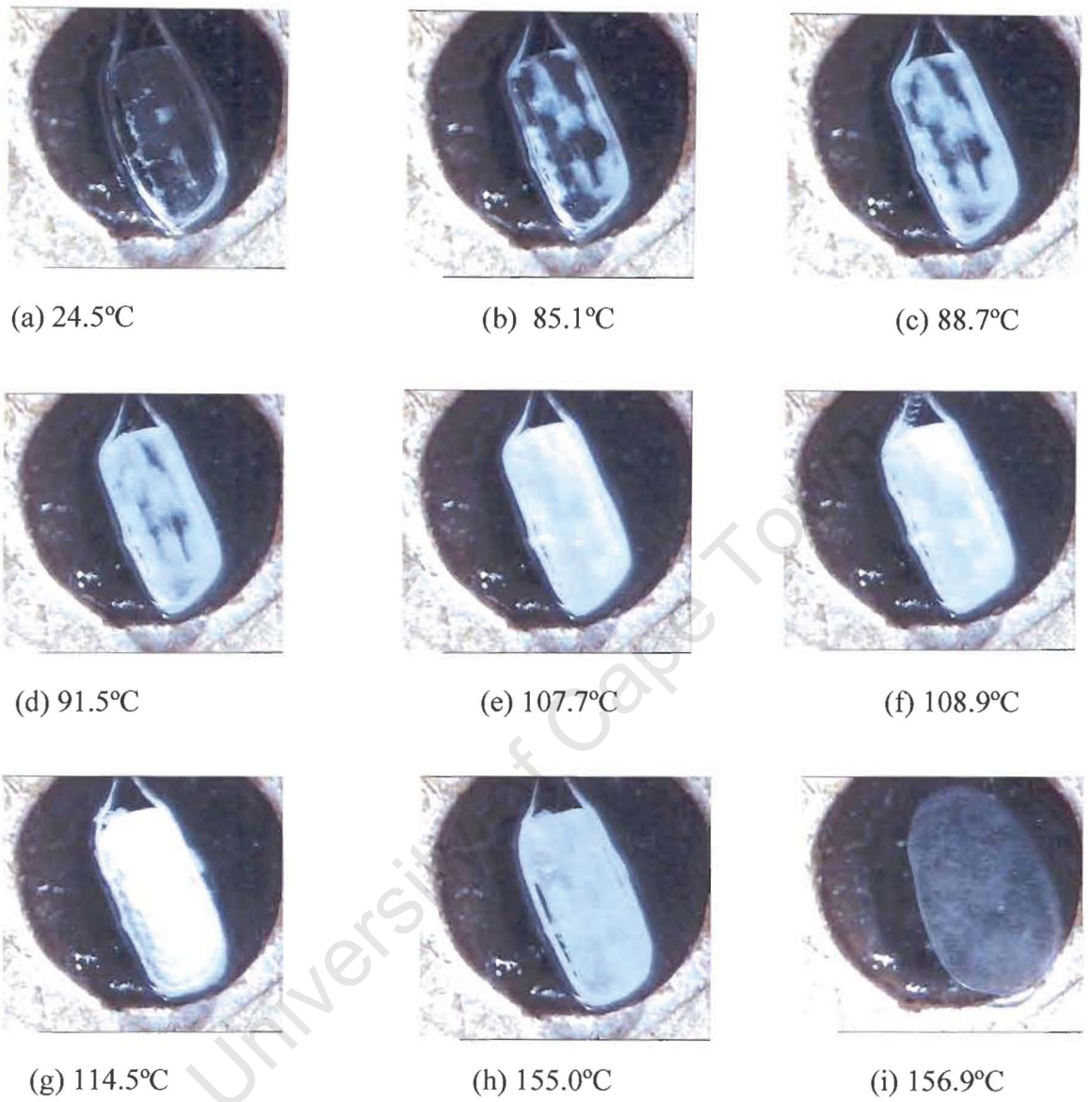

(a) 24.5°C (b) 85.1°C (c) 88.7°C

(d) 91.5°C (e) 107.7°C (f) 108.9°C

(g) 114.5°C (h) 155.0°C (i) 156.9°C

University of Cape Town

Figure 3.1.8. Changes observed in a crystal of **T7CHCL3** during heating:

(a) T**7CHCL3** at room temperature, (b) crystal starts turning opaque at 85.1°C, (e) crystal is completely opaque at 107.7°C, (f) bubbles are visible at 108.9°C, (h) host melt occurs at 155.0°C and (i) host is completely melted at 156.9°C.

T7CH2CL2

$C_{30}H_{22}O_2 \cdot ½CH_2Cl_2$
Guest : dichloromethane
Space Group : $P2_1/n$
a = 17.083(3)Å α =90°
b = 13.629(3)Å β =108.02(3)°
c = 22.274(5)Å γ =90°
Volume = 4931(2)Å^3
Z = 8

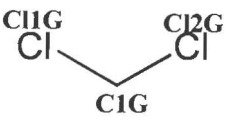

Crystal Structure and Refinement

TG analysis indicated a host:guest ratio of 1:½. The monoclinic space group $P2_1/n$ was assigned based on the following hkl reflections observed:

h0l : h + l = 2n , (h00 : h = 2n), (00l : l = 2n)

0k0 : k = 2n

All the non-hydrogen atoms of the host and guest were located after the first direct methods run. Both the host and guest molecules were found in general positions. The hydroxyl groups of the host molecule are in a gauche conformation. During the refinement both the host and guest non-hydrogen atoms were treated anisotropically. The asymmetric unit consists of two independent host molecules and one guest molecule. There are eight host molecules and four guest molecules in each unit cell. Inspection of the difference electron density maps revealed the positions of the hydrogen atoms of the host, but in the final refinement, the aromatic hydrogens were geometrically constrained. The hydroxyl hydrogen was placed in geometrically calculated positions relating O—H distances to O•••O distances[1]. Bond lengths and angles of the host are in the expected ranges[2]. The non-hydrogen atoms of the guest refined with the following U_{eq} values: U_{eq}(C1G) = 0.23Å^2, U_{eq}(Cl1G) = 0.12Å^2 and U_{eq}(Cl2G) = 0.16Å^2.

University of Cape Town

Unique bond lengths of the dichloromethane refined to C1G—Cl1G = 1.678(9)Å and C1G—Cl2G = 1.797(11)Å with the unique bond angle Cl1G—C1G— Cl2G of 109.2(4)°. The hydrogen atoms of the guest were geometrically constrained and were assigned common isotropic temperature factors.

Crystal Packing

Once again the packing of **T7CH2CL2** is similar to **T7CCL4** and **T7CHCL3.** The guest molecules are situated in cages of approximate dimensions 5.2Å × 6.1Å × 6.7Å.

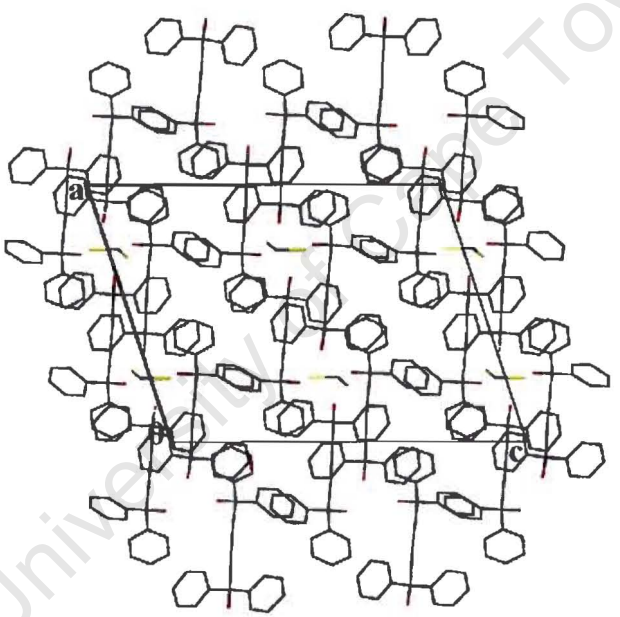

University of Cape Town

Figure 3.1.9. Packing diagram of **T7CH2CL2** down [010].

Once again the hydrogen bonding is similar to that described in the previous two structures. These are listed in Table 3.1.4. The structure is also stabilised by short aromatic C—H•••π contacts[5] less than 3.05Å and interactions between one of the guest C—H bonds and a phenyl group of the host. The C1G—H2G•••π interaction is

defined by the following : (a) the distance between H2G and the centroid of the phenyl ring of the host is 3.26Å and (b) the angle C1G—H2G•••π is 141.85°.

Table 3.1.4. Hydrogen bonding details of **T7CH2CL2**.

Donor (D)	**Acceptor (A)**	**D—H / Å**	**D•••A / Å**	**D-H•••A / °**
O1	O2A[a]	0.98(1)	2.711(1)	155(2)
O2	O1[b]	0.98(1)	2.689(1)	154(3)
O1A	O2	0.98(2)	2.677(1)	156(3)
O2A	O1A[C]	0.98(1)	2.673(1)	158(3)

a: x-1, y, z

b : -x, -y+1, -z

c : -x+1, -y+1, -z

University of Cape Town

Thermal Analysis

Once again the individual mass loss steps are non-stoichiometric. The first step corresponds to the loss of 0.43 of the total guest and the second step correponds to the loss of 0.57 of the total guest. The total mass loss does however correspond to the loss of 0.5 mol of guest per mol of complex. The experimental mass loss is 9.3% (calculated 9.3%).

The guest is released at T_{on} = 96.5°C followed by a phase change and host melt (T_{on} = 147.6°C, peaks at 144.6°C and 148.7°C). The TG and DSC results are shown in Figure 3.1.10.

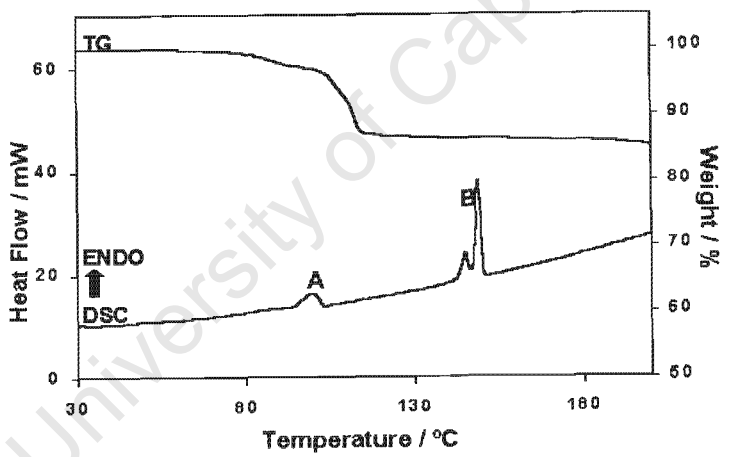

Figure 3.1.10. TG and DSC for **T7CH2CL2**.

University of Cape Town

Hot stage Micoscopy

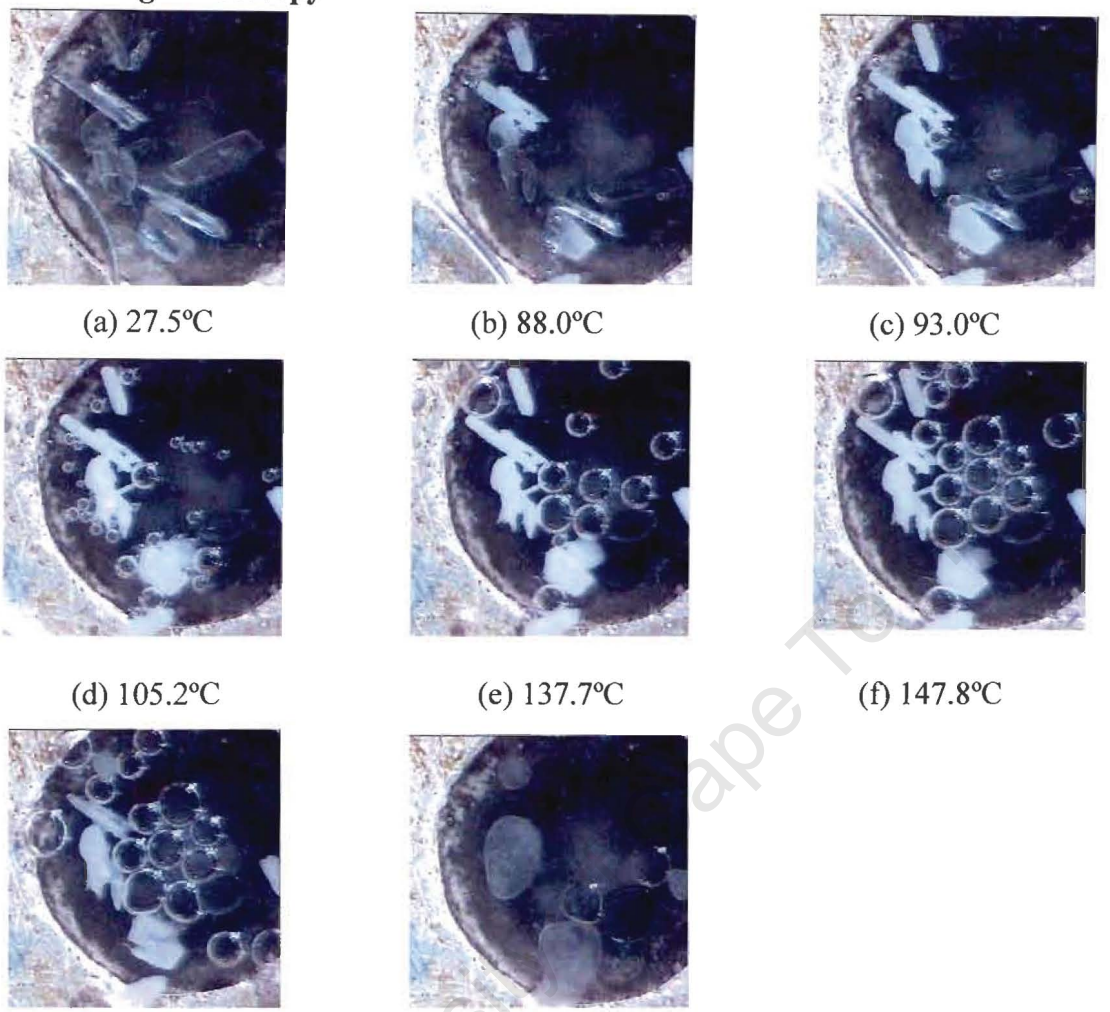

(a) 27.5°C (b) 88.0°C (c) 93.0°C

(d) 105.2°C (e) 137.7°C (f) 147.8°C

(g) 151.2°C (h) 152.4°C

Figure 3.1.11. Crystals of **T7CH2CL2** (a) at room temperature, (b) crystals start becoming opaque at 88.0°C, (c), (d), (e) bubbles are released, (f), (g) host starts to melt at 147.8°C and (h) crystal is completely melted at 152.4°C.

University of Cape Town

T7CH3CN

$C_{30}H_{22}O_2 \cdot 2CH_3CN$		
Guest : acetonitrile		
Space Group : $P2_1/n$		
a = 10.847(2)Å	$\alpha = 90°$	
b = 8.251(2)Å	$\beta = 91.05(3)°$	
c = 15.364(3)Å	$\gamma = 90°$	
Volume = 1374.8(5)Å^3		
Z = 2		

Crystal Structure and Refinement

Preliminary oscillation and Weissenberg photography indicated that **T7CH3CN** possessed 2/m Laue symmetry and therefore belonged to the monoclinic system. The centrosymmetric space group $P2_1/n$ was assigned based on the hkl reflections observed and $|E^2 - 1|$ statistics. The host molecules are situated on centres of inversion (Wyckoff position a) and the guest molecules were found in general positions. There are 2 host molecules and 4 guest molecules in each unit cell (Z=2).

All the non-hydrogen atoms of the host and guest were obtained by direct methods and refined anisotropically. It was difficult to distinguish between the guest carbon and nitrogen atoms based solely on the peak heights, hence the distances between the atoms were used to establish the position of the nitrogen. Due to symmetry, the hydroxyl hydrogens of the host are trans and subsequently one of them was located in the difference electron density maps and refined isotropically. The hydroxyl hydrogens were fixed 0.97Å from the oxygen atoms of the host. The electron density maps revealed the positions of the aromatic hydrogens of the host and the methyl hydrogens of the guest but these were geometrically constrained (C-H distance for aromatic hydrogens = 0.93Å, C-H distance for methyl hydrogens = 0.96Å) for

a consequence of energy

University of Cape Town

consistency. The host:guest ratio of 1:2 established by TG was confirmed by the crystal structure.

Crystal Packing

Symmetry dictates that the hydroxyl groups of the host molecule are in the trans configuration. The acetylenic backbones of the host pack in wavy layers which lie close to the (002) planes. The guest molecules lie in channels parallel to [010]. The cross-sectional areas of the channels vary in size from approximately 5.4Å × 3.9 Å to 7.7Å × 4.9Å.

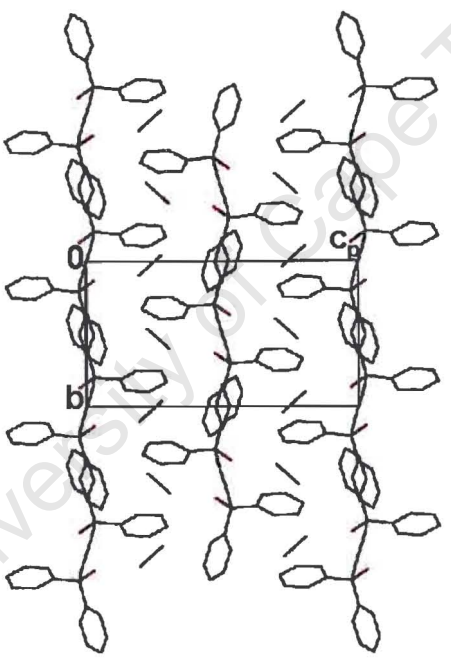

Figure 3.1.12(a). Crystal packing diagram of **T7CH3CN** down [100].

University of Cape Town

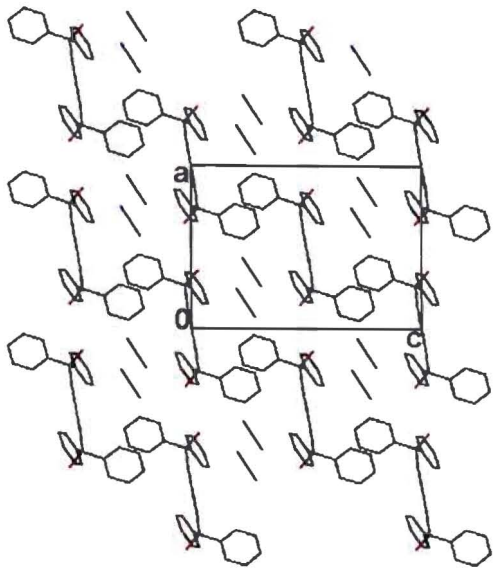

(b)

Figure 3.1.12(b). Crystal packing diagram of **T7CH3CN** down [010].

The channels occupied by the guest molecules are widest at y=0, ½ and 1; and narrowest at y=¼ and y= ¾. This is shown by a SECTION plot (Figure 3.1.13).

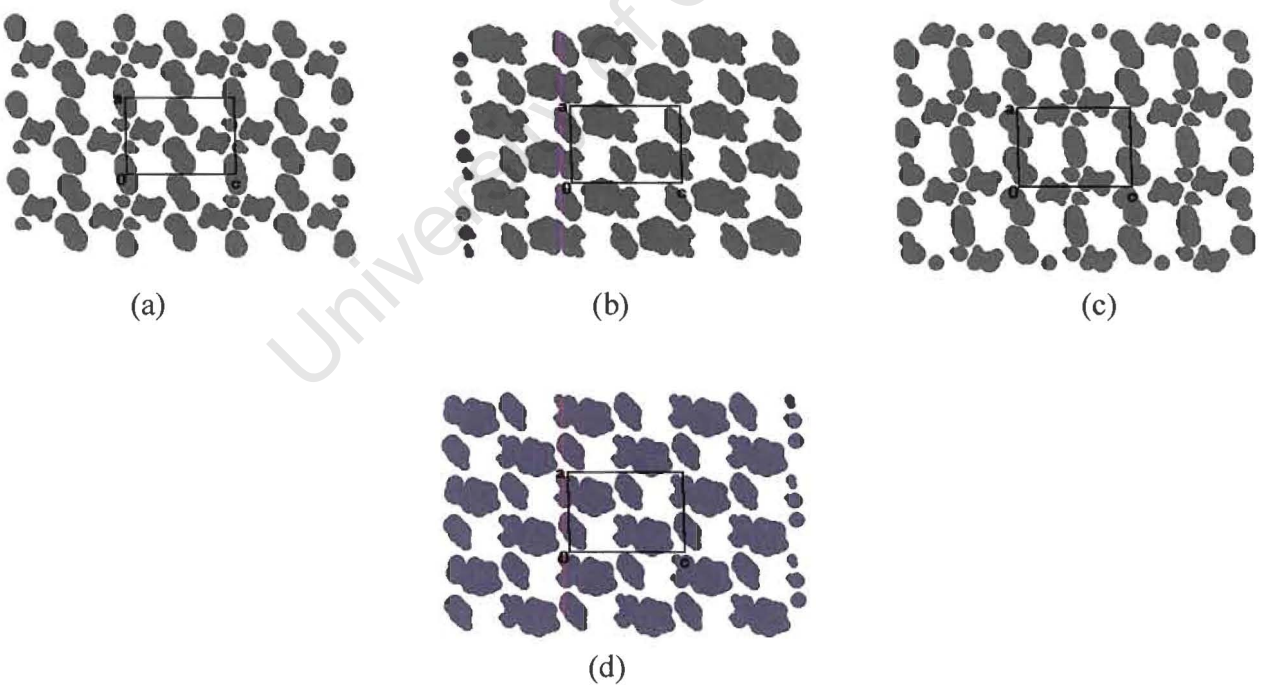

(a) (b) (c)

(d)

Figure 3.1.13. SECTION plot illustrating the constricted channels of **T7CH3CN**. The view is down [010] at sections (a) y=0, (b) y= ¼, (c) y=½, (d) y=¾.

University of Cape Town

Unlike the previous structures the crystal structure is stabilised by hydrogen bonding between the hydroxyl hydrogens of the host and the nitrogen of the acetonitrile guest.

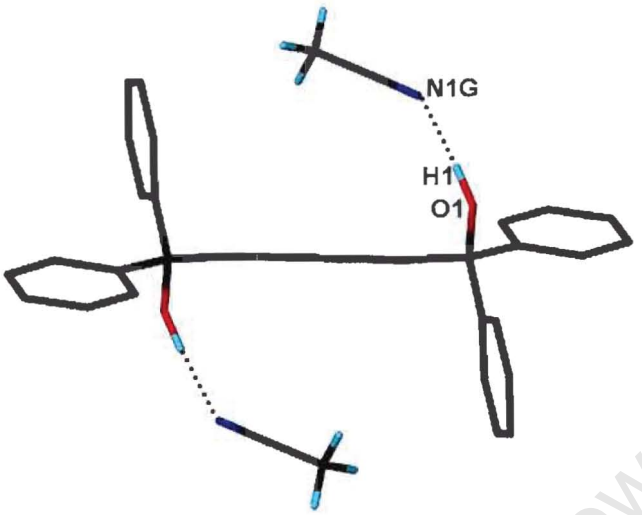

Figure 3.1.14. Hydrogen bonding in **T7CH3CN**.

Table 3.1.5. Hydrogen bonding details of **T7CH3CN**.

Donor (D)	**Acceptor (A)**	**D—H / Å**	**D•••A / Å**	**D—H•••A / °**
O1	N1G	0.97(1)	2.888(1)	175(2)

University of Cape Town

Thermal Analysis

The first endotherm in the DSC curve (T_{on}= 89.0°C) corresponds to the loss of guest. The last two endotherms (T_{on}= 146.6°C, peaks at 144.2°C and 147.9°C) correspond to a phase change and subsequent host melt.

The TG curve shows two steps, which similar to the previous structures show a non-stoichiometric mass loss for each individual step. The total mass loss was 16.2% (calculated 16.5%). The first step corresponds to the loss of 40% of the total guest present and the second step corresponds to the mass loss of 60% of the total guest present. Overall the total mass loss is consistent with the host:guest ratio of 1:2.

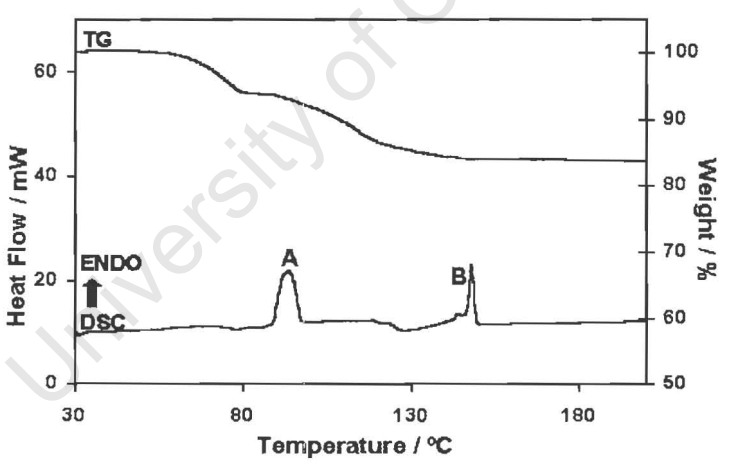

Figure 3.1.15. TG and DSC of **T7CH3CN**.

University of Cape Town

Hot stage Microscopy

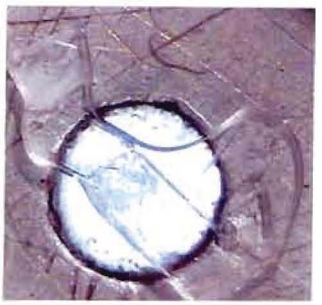

(a) 26.4°C

(b) 55.4°C

(c) 65.2°C

(d) 93.7°C

(e) 132.3°C

(f) 147.5°C

(g) 151.2°C

University of Cape Town

Figure 3.1.16. Thermal decomposition of **T7CH3CN** at (a) at room temperature, (b) crystals start becoming opaque at 55.4°C, (c) crystals completely opaque at 65.2°C, (d), (e) bubbles released, (f) melt of host at 147.5°C and (g) crystal completely melted at 151.2°C.

Kinetics of decomposition

Due to insufficient sample of the host, crystals of **T7CH3CN** were crushed and a series of isothermal runs performed. Ideally powders of the complex are preferred as the kinetics of decomposition is influenced by the particle size as well as the reaction conditions. Usually, once a powder is obtained an X-ray powder diffraction pattern, which provides a unique fingerprint, is used to verify that it is indeed the required complex. Unfortunately a limited amount of host made this impossible.

Isothermal Thermogravimetry

In the TG two distinct desolvation steps could be distinguished and these were analysed separately. In the first step isothermal TG experiments were conducted over a temperature range of 50-63°C at intervals of 3-5°C. The resulting α - time curves were deceleratory. Various deceleratory kinetic models were fitted to the data. The best fit curve was obtained with the first order model, F1: $-\ln(1-\alpha) = kt$ over the α range 0.10-0.90. The plot of ln k vs 1/T is shown in Figure 3.1.17(a). An activation energy of 174(6) $kJmol^{-1}$ was obtained.

In the second step, isothermal TG experiments were carried out over the temperature range of 100-120°C at intervals of 5°C. Similar to the first step, the α - time curves thus obtained were deceleratory. However, the data could best be described by the three dimensional diffusion controlled model, D3: $kt = [1-(1-\alpha)^{1/3}]^2$ over the α range 0.10-0.90. The Arrhenius plot is shown in Figure 3.1.17(b). An activation energy 84(5) $kJmol^{-1}$ was obtained.

University of Cape Town

Thermal decomposition of solids predominantly occurs at the surface of the reacting phase. The higher activation energy obtained in the first desolvation step is probably due to a higher diffusion barrier that has to be overcome as a result of the crystallite size.

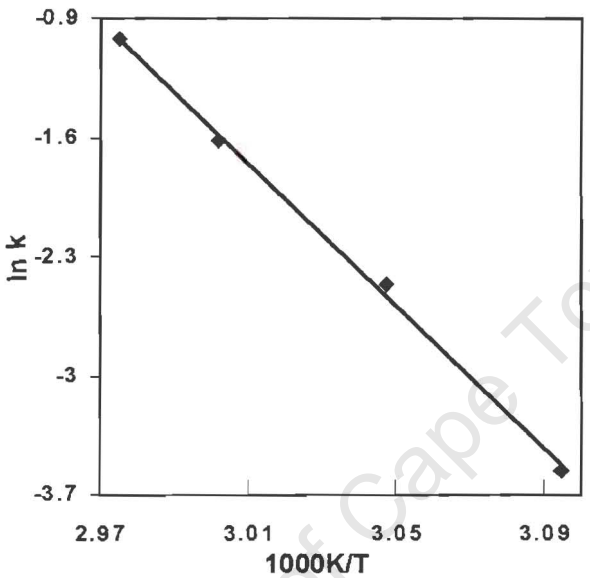

Figure 3.1.17(a). Plot of ln k versus 1/T for the first step in the desolvation of **T7CH3CN.**

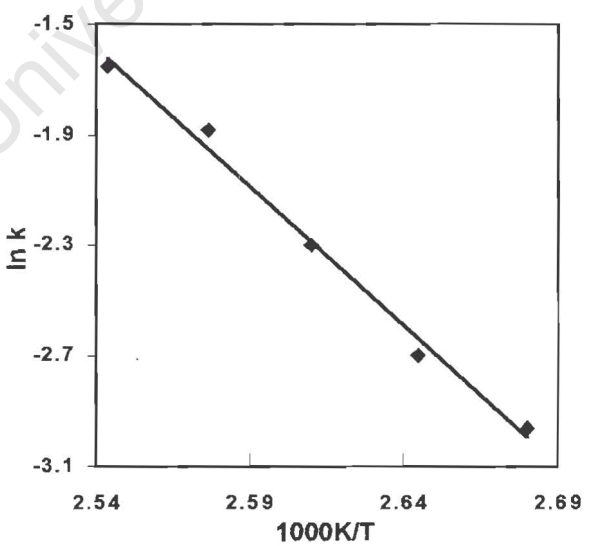

Figure 3.1.17(b). Plot of ln k versus 1/T for the second step in the desolvation of **T7CH3CN.**

University of Cape Town

Discussion

T7CCL4 and **T7CHCL3** crystallize in the space group C2/c with similar unit cell dimensions and packing motifs. In addition the fractional co-ordinates of corresponding host atoms (which form the bulk of the crystal structure) are also similar. According to the definition by Kalman *et al.*[7,8] they are therefore isostructural with respect to the host framework.

T7CH2CL2 crystallizes in the space group $P2_1/n$ with similar unit cell parameters (a and c interchanged) and interestingly, an analogous molecular packing arrangement to **T7CCL4** and **T7CHCL3**. In all of these structures the host molecules are not situated on a centre of symmetry and consequently the hydroxyl groups adopt a gauche conformation. The hydrogen bonding networks between adjacent host molecules resulting in the guests occupying cages, are comparable in all three structures.

The guests studied in this series $CCl_4 \longrightarrow CHCl_3 \longrightarrow CH_2Cl_2$ differ in the successive loss of a chlorine atom from the parent carbon atom. The introduction of a cyano group in the form of acetonitrile results in a totally different packing arrangement with the host located on a centre of inversion. In **T7CH3CN** the hydroxyl groups of the host are trans and hydrogen bonding occurs between the host and the guest.

University of Cape Town

Table 3.1.6. Summary of thermal analysis data for the structures studied in this chapter.

Inclusion compound			**T7CCL4**	**T7CHCL3**	**T7CH2CL2**	**T7CH3CN**
H : G ratio			1 : ½	1: ½	1 : ½	1 : 2
TG results	Calc. % mass loss		15.7	12.6	9.3	16.5
	Exp. % mass loss		16.2	12.6	9.3	16.2
DSC results	T_{on} (°C) :	A*	107.1	93.9	96.5	88.9
		B*	147.1	147.5	147.6	146.6
Normal boiling points T_b (°C)			76.7	61.5	39.8	81.6
T_{on} / T_b			1.396	1.527	2.425	1.089

*: A and B refer to the endotherms illusrated in previous DSC diagrams.

In all four structures the DSC shows the loss of guest followed by a phase change and subsequent melt of the host. The loss of guest in **T7CH3CN** takes place at T_{on} = 88.9° C, lower than that of the other compounds. This is expected since in **T7CH3CN** the guests are situated in channels whereas in the other structures the guests lie in cages. A smaller energy barrier has to be overcome when the guests are released from channels than when they are in cages. Also, a good indicator of how strongly the guest is held in the crystal is given by the ratio, T_{on} / T_b , where T_{on} = the onset temperature of guest release and T_b = the normal boiling point of the guest.

The higher value of T_{on} / T_b = 2.425 obtained for **T7CH2CL2** implies that it is more strongly held by the host structure than **T7CCL4** and **T7CHCL3**.

This could be explained by the additional C—H•••π interaction which exists between the dichloromethane guest and the host. This shows the importance of the C—H•••π interaction in determining the stability of inclusion compounds[4].

University of Cape Town

References

1. I. Olovsson and P. Jönsson, *The Hydrogen Bond* – Structure and Spectroscopy, P.Schuster, G. Zundel and C. Sardefy (eds.), North-Holland Publishing Company, USA, 1975.

2. International Tables For Crystallography, Vol. C, (ed.) A.J.C. Wilson, Kluwer Academic Publishers, Dordrecht, pp.691, 1992.

3. M.R. Caira, L.R. Nassimbeni, F. Toda and D. Vujovic, *J. Chem. Soc., Perkin Trans. 2*, 2119-2124, 2001.

4. F. Cozzi and J.S. Siegel, *Pure Applied Chem.*, 67, 683, 1995.

5. E. Kim, S. Paliwal and C.S. Wilcox, *J. Am. Chem. Soc.*, 120, 11192, 1998.

6. H. Suezawa et al., *J. Chem. Soc., Perkin Trans. 2*, 2053-2058, 2001.

7. A.Kálmán and L. Párkányi, in "Advances in Molecular Structure Research", JAI Press Inc., pp.189-226, 1997.

8. L. Fabián and A. Kálmán, *Acta Crystallogr. Sect. B, Struct. Sci.*, 55, 1039,1999.

University of Cape Town

CHAPTER 3.2 INCLUSION OF PYRIDINE AND PICOLINES

In this chapter inclusion compounds formed between the host, **TOD7**, and pyridine and picoline isomers will be presented. The structures of these inclusion compounds and their lattice energies have been determined.

Crystals of **TOD7** and guests pyridine, 3-picoline and 4-picoline were obtained after approximately 5 days. It was however very difficult to grow crystals of the complex between **TOD7** and 2-picoline. Many crystal growth techniques were attempted including slow evaporation, slow cooling, low temperature, high temperature experiments and mixed solvent systems. During an experiment to grow the powder of **TOD7** and 2-picoline by continuous stirring at room temperature, crystals formed after the resultant suspension was left overnight.

The selectivity of the host for a particular guest has been measured by competition experiments and the results are rationalised in terms of the structural features of the host-guest compounds.

University of Cape Town

Table 3.2.1. Crystal data, experimental and refinement parameters

	T7PYR	**T72PIC**	**T73PIC**	**T74PIC**
Compound	$C_{30}H_{22}O_2 \cdot 2C_5H_5N$	$C_{30}H_{22}O_2 \cdot 2C_6H_7N$	$C_{30}H_{22}O_2 \cdot 2C_6H_7N$	$C_{30}H_{22}O_2 \cdot 2C_6H_7N$
M_W , $gmol^{-1}$	572.68	600.73	600.73	600.73
Temperature / K	295(2)	173(2)	293(2)	295(2)
Crystal System	monoclinic	triclinic	monoclinic	monoclinic
Space group	$P2_1/c$	$P\bar{1}$	$P2_1/c$	$P2_1/c$
a, Å	8.245(2)	6.716(1)	8.700(2)	13.278(3)
b, Å	17.276(4)	9.473(2)	15.458(3)	6.764(1)
c, Å	11.131(2)	13.611(3)	12.985(3)	18.964(4)
α, °	90	104.06(3)	90	90
β, °	91.94(3)	90.14(3)	106.00(3)	98.79(3)
γ, °	90	99.81(3)	90	90
V, $Å^3$	1584.6(5)	826.8(3)	1678.6(6)	1683.2(6)
Z	2	1	2	2
Absorption coefficient, mm^{-1}	0.074	0.074	0.073	0.072
F(000)	604	318	636	636
Crystal size, mm	0.12 × 0.30 × 0.20	0.27 × 0.45 × 0.39	0.30 × 0.50 × 0.28	0.08 × 0.40 × 0.17
Index ranges	h:±9; k: ±20; l:-6, 13	h:-8,4; k:±10; l:±16	h:0,12; k:0, 21; l:-18, 16	h:±16; k:-4,8; l:-14, 24
Reflections collected / unique	5912 / 2786	3238 / 2569	4557 / 4557	3866 / 3665
Data/ restraints/ Parameters	2786 / 2 / 201	2569 / 2 / 210	4557 / 2 / 213	3665 / 2 / 213
Goodness-of-fit	1.005	1.027	0.997	1.017
ρ_{calc}, $g \cdot cm^{-3}$	1.200	1.206	1.189	1.185
Final R indices [$I > 2\sigma(I)$]	$R_1 = 0.0550$, $wR_2 = 0.1475$	$R_1 = 0.0682$, $wR_2 = 0.1764$	$R_1 = 0.0780$, $wR_2 = 0.1897$	$R_1 = 0.0475$, $wR_2 = 0.1272$
R indices (all data)	$R_1 = 0.1458$, $wR_2 = 0.1815$	$R_1 = 0.1039$, $wR_2 = 0.2008$	$R_1 = 0.1858$, $wR_2 = 0.2452$	$R_1 = 0.1077$, $wR_2 = 0.1494$
Largest difference peak and hole, $eÅ^{-3}$	0.424 and -0.496	0.666 and -0.584	0.383 and -0.433	0.170 and -0.217

University of Cape Town

T7PYR

$C_{30}H_{22}O_2 \cdot 2C_5H_5N$
Guest : pyridine
Space Group : $P2_1/c$
a = 8.245(2)Å $\alpha = 90°$
b = 17.276(4)Å $\beta = 91.94(3)°$
c = 11.131(2)Å $\gamma = 90°$
Volume = 1584.6(5)Å^3
Z = 2

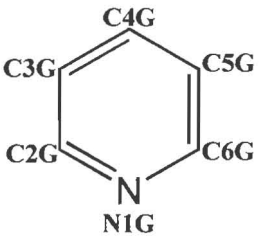

Crystal Structure and Refinement

A host:guest ratio of 1:2 was established by TG and this was confirmed by the crystal structure. The centrosymmetric space group $P2_1/c$ was assigned based on the mean $|E^2 - 1|$ values and the reflection conditions that were observed. viz

h0l : l = 2n

0k0 : k = 2n

This was vindicated by the solution of the crystal structure in this space group. The host molecules were located on a centre of inversion at Wyckoff position b. The guests were placed in general positions.

Direct methods were used successfully to obtain all the non-hydrogen atoms of the host and the guest. All the non-hydrogen atoms of the host and the guest were refined anisotropically. The hydroxyl hydrogens were located in the difference electron density maps and were refined isotropically. The hydroxyl hydrogens were then placed in geometrically calculated positions[1]. The aromatic hydrogens were fixed in position as described earlier. The bond lengths and angles of both molecules were all in acceptable ranges[2]. The carbon atoms of the pyridine guest refined with the

University of Cape Town

following U_{eq} values: $U_{eq}(C2G) = 0.12Å^2$, $U_{eq}(C3G) = 0.12Å^2$, $U_{eq}(C4G) = 0.10Å^2$, $U_{eq}(C5G) = 0.11Å^2$, $U_{eq}(C6G) = 0.10Å^2$.

Crystal Packing

Symmetry (energy) requires that the hydroxyl hydrogens of the host adopt the trans configuration. The acetylenic backbone of the host lie close to the (020) planes. The phenyl groups of neighbouring host molecules overlap to form channel-like voids. The guest molecules lie in these channels parallel to [001]. The channels vary in size from approximately 4.9Å × 5.8Å to 5.6Å × 7.1Å. This type of inclusion compound is referred to as tubulate.

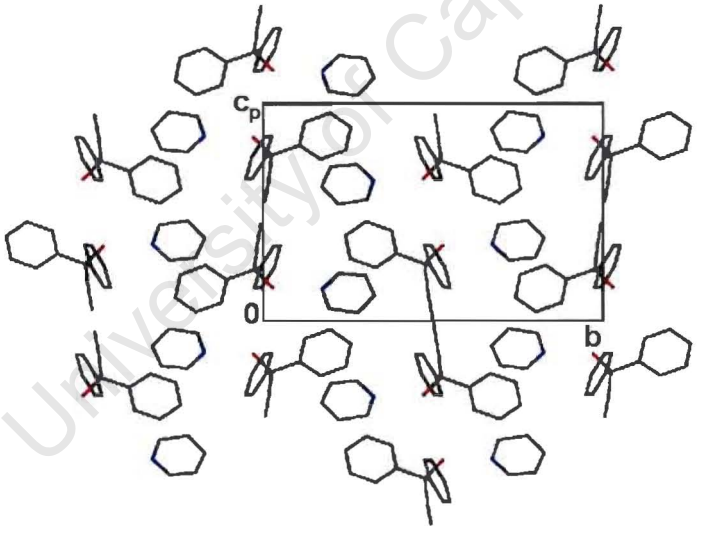

Figure 3.2.1. Packing diagram of **T7PYR** down [100].

University of Cape Town

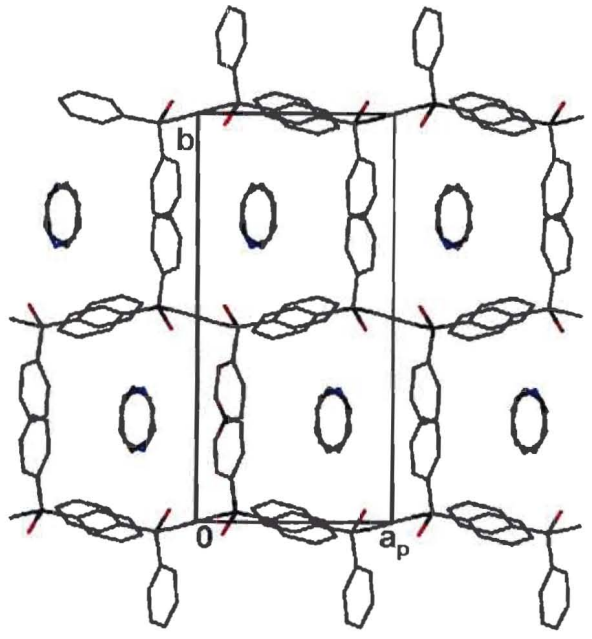

(a)

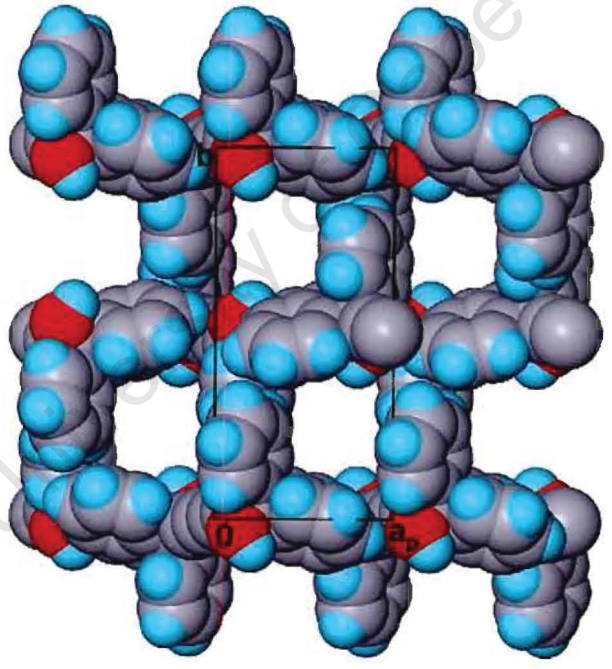

(b)

University of Cape Town

Figure 3.2.2. Packing diagram of **T7PYR** down [001] with (a) both the host and guest molecules represented in stick form and (b) the guests removed and the host atoms in van der Waals radii.

The structure is stabilised by hydrogen bonding between the hydroxyl groups of the host molecules and nitrogen of the guest. Each host molecule is hydrogen bonded to two guest molecules. The hydrogen bonding scheme is depicted in Figure 3.2.3.

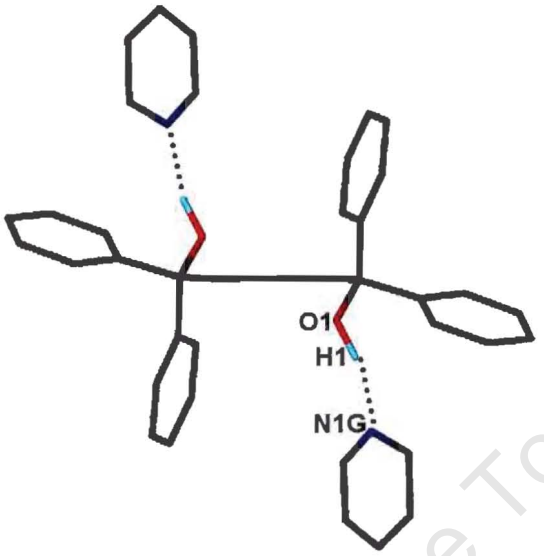

Figure 3.2.3. Hydrogen bonding scheme of **T7PYR**

University of Cape Town

Table 3.2.2. Hydrogen bonding details of **T7PYR**.

Donor (D)	**Acceptor (A)**	**D—H / Å**	**D•••A / Å**	**D—H•••A / °**
O1	N1G[a]	0.97(1)	2.746(2)	165(2)

a : -x, y+½, -z+½

Thermal Analysis

Both the TG and the DSC curves for **T7PYR** are illustrated in Figure 3.2.4. The DSC curve shows a single endotherm, A, (T_{on} = 99.2°C). This corresponds to desolvation accompanied by dissolution of the host in the liquid guest.

The TG shows a single mass loss step (expected mass loss = 27.6%, observed mass loss = 27.2%) which is consistent with the host:guest ratio of 1:2.

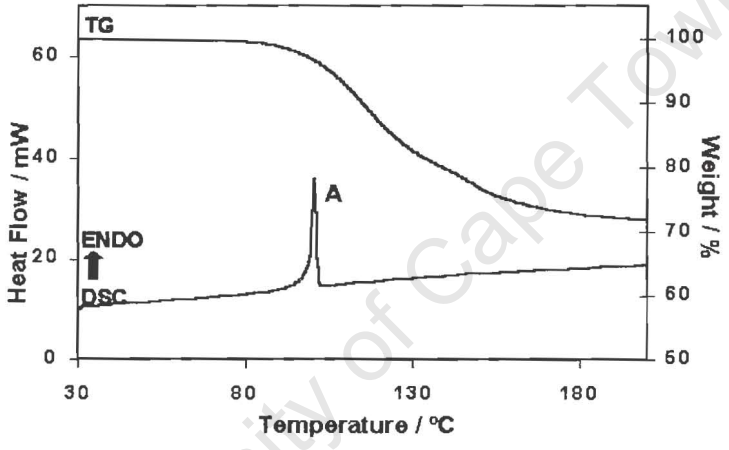

Figure 3.2.4. TG and DSC of **T7PYR**.

University of Cape Town

T72PIC

$C_{30}H_{22}O_2 \cdot 2C_6H_7N$
Guest : 2-picoline
Space Group : P $\bar{1}$
a = 6.716(1)Å $\alpha = 104.06(3)°$
b = 9.473(2)Å $\beta = 90.14(3)°$
c = 13.611(3)Å $\gamma = 99.81(3)°$
Volume = 826.8(3)Å^3
Z = 1

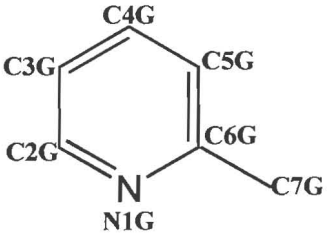

Crystal Structure and Refinement

A host to guest ratio of 1:2 was established by TG and this was confirmed by the crystal structure. There were no conditions limiting observed reflections. The mean $|E^2 - 1|$ values indicated a centrosymmetric space group and P $\bar{1}$ was assigned. This was confirmed by the successful solution of the crystal structure in this space group. The host molecules were located on a centre of inversion at Wyckoff position e and the guests were placed in general positions.

All the non-hydrogen atoms of the host and guest were obtained by direct methods. The nitrogen of the guest could be distinguished from the rest of the carbon atoms by its peak height and the preliminary bond lengths. Anisotropic refinement of all the non-hydrogen atoms of the host and the guest was performed. Upon further refinement the hydroxyl hydrogens were located in the difference electron density maps, and were refined isotropically. The hydroxyl hydrogens were then placed in geometrically calculated positions[1]. A residual electron density of 0.67eÅ^{-3} was observed in the region of the guest but could not be modelled. The bond lengths and angles of the host and guest were in acceptable ranges[2]. The structure refined successfully to $R_1 = 0.0682$.

University of Cape Town

Crystal Packing

The crystal packing of **T72PIC** is shown in Figure 3.2.5. Once again the phenyl groups act as spacers creating voids in the host lattice. The guest molecules lie in channels parallel to [100]. The channels vary in size from 6.0Å × 7.6Å at the narrowest regions to 8.5Å × 11.1Å at the widest regions.

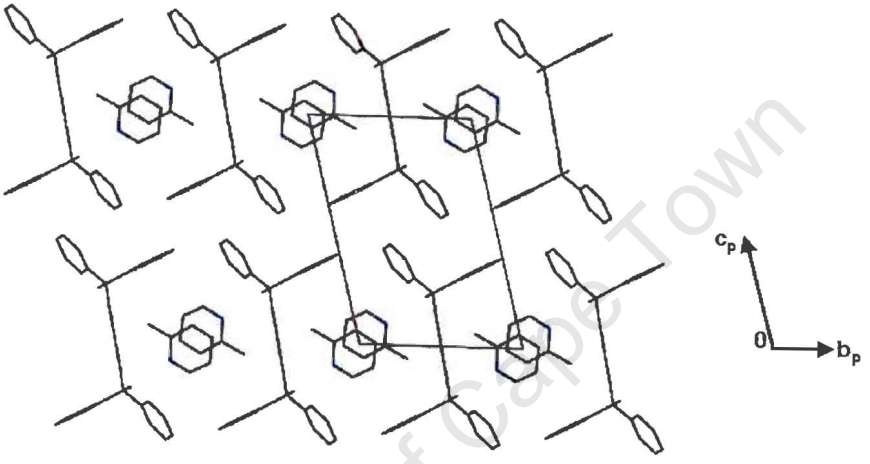

Figure 3.2.5. View down [100] showing the crystal packing in **T72PIC**.

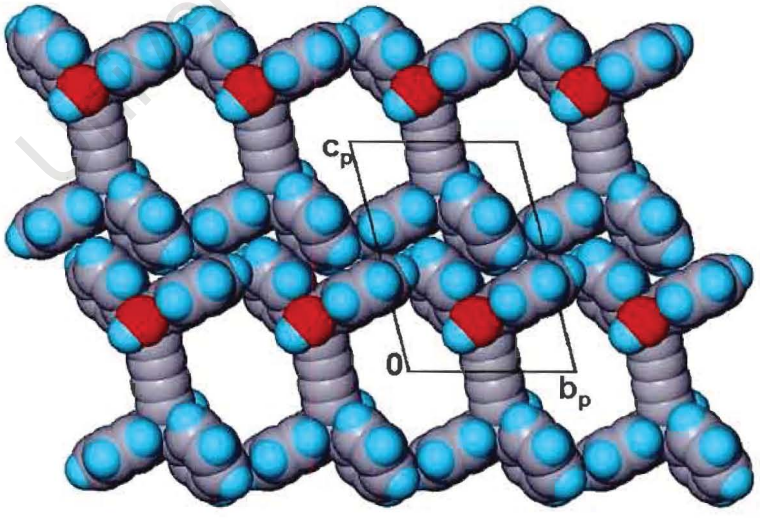

Figure 3.2.6. View down the channels of **T72PIC** with the guest omitted. The host is represented with van der Waals radii.

University of Cape Town

As was seen in **T7PYR** the hydroxyl groups of the host molecule, which are trans to each other, are hydrogen bonded to the nitrogen atoms of the guests. The hydrogen bonding details are given in Table 3.2.3.

Table 3.2.3. Hydrogen bonding details of **T72PIC**.

Donor (D)	Acceptor (A)	D—H / Å	D•••A / Å	D—H•••A / °
O1	N1G	0.97(1)	2.743(1)	167(2)

Thermal Analysis

The DSC curve shows two endotherms, A and B, which have onset temperatures 77.5°C and 114.8°C (peaks at 115.5°C and 117.5°C) respectively.

The TG shows two mass loss steps which are not clearly defined and individually correspond to a non-stoichiometric mass loss. The first step corresponds to the loss of 0.43 of the total guest present and the second step corresponds to the loss of 0.57 of the total guest. The total experimental mass loss of 29.9% compares with the calculated value of 31.0% expected for a host: guest ratio of 1:2.

University of Cape Town

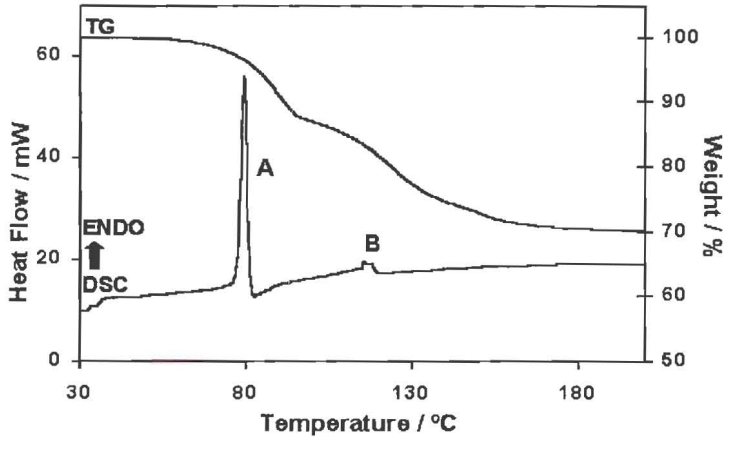

Figure 3.2.7. TG and DSC of **T72PIC**.

T73PIC

$C_{30}H_{22}O_2 \cdot 2C_6H_7N$
Guest : 3-picoline
Space Group : $P2_1/c$
a = 8.700(2)Å $\alpha = 90°$
b = 15.458(3)Å $\beta = 106.00(3)°$
c = 12.985(3)Å $\gamma = 90°$
Volume = 1678.6(6)Å^3
Z = 2

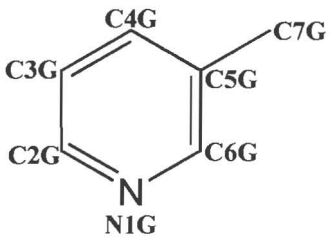

Crystal Structure and Refinement

Preliminary oscillation and Weissenberg photography indicated that **T73PIC** belonged to the monoclinic system. TG results indicated a host: guest ratio of 1: 2 and this was confirmed by the crystal structure. The centrosymmetric space group $P2_1/c$ was assigned. The host molecules were located on a centre of inversion (Wyckoff position c) and the guests were placed in general positions.

All the non-hydrogen atoms of the host and the guest were obtained by direct methods and treated anisotropically. The hydroxyl hydrogens were located in the difference electron density maps and refined isotropically. The hydroxyl hydrogens were then placed in geometrically calculated positions[1]. The aromatic hydrogens were geometrically constrained with the carbon to hydrogen distances equal to 0.93Å.

University of Cape Town

Crystal Packing

The host molecules stack to form zigzag layers perpendicular to [001]. Unlike the previous two structures, the guest molecules lie in cages located at centres of inversion at Wyckoff position c. The cages are approximately 6.5Å × 7.5Å × 7.5Å in size and each contains two guest molecules.

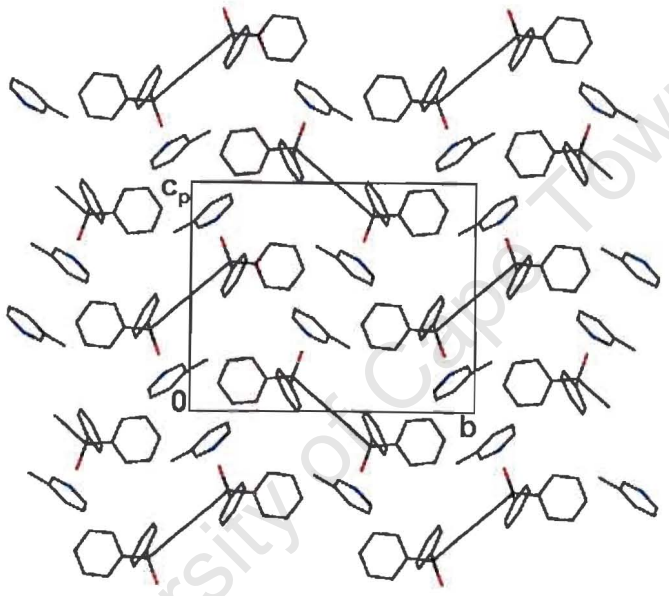

Figure 3.2.8. Crystal packing of **T73PIC** down [100].

University of Cape Town

Once again hydrogen bonding occurs between the hydroxyl groups of the host molecules and the nitrogen of the guest. Each host molecule is hydrogen bonded to two guest molecules.

Table 3.2.4. Hydrogen bonding details of **T73PIC**.

Donor (D)	Acceptor (A)	D—H / Å	D•••A / Å	D—H•••A / °
O1	N1G[a]	0.97(1)	2.757(1)	158(2)

a: -x+2, y-½, -z+1½

Thermal Analysis

The DSC curve shows a single endotherm, A, (T_{on} = 102.3°C) and the hot stage confirmed that the host melted in the hot guest.

The TG shows a single mass loss step (calculated mass loss = 31.0%, observed mass loss = 30.8%) which is consistent with the host: guest ratio of 1:2.

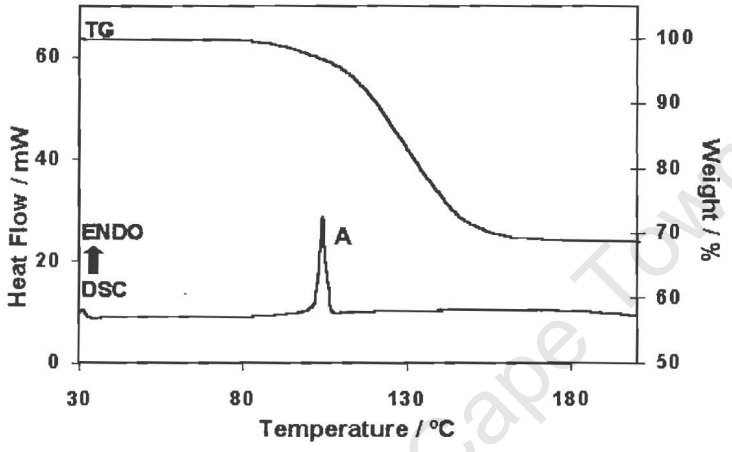

Figure 3.2.9. TG and DSC results for **T73PIC.**

University of Cape Town

Hot stage Microscopy

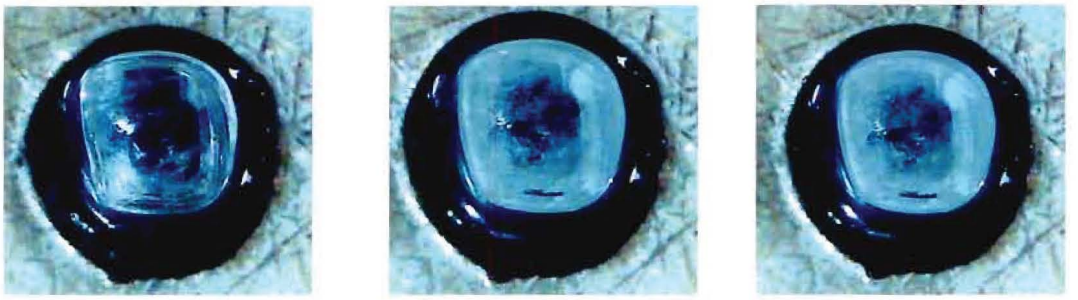

(a) 23.7°C (b) 90.8°C (c) 97.2°C

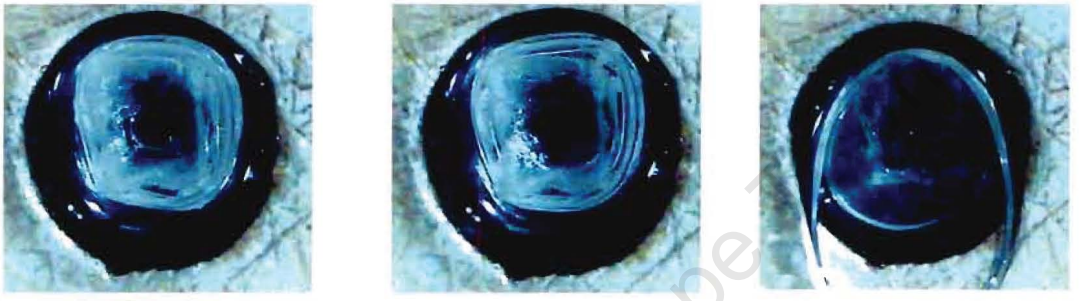

(d) 108°C (e) 110°C (f) 114°C

Figure 3.2.10. Hot stage microscopy results for a crystal of **T73PIC** at: (a) room temperature, (b) guest loss commences at 90.8°C, (c) melt occurs as the guest is released (d), (e) melt progresses and (f) crystal almost completely melted at 114°C.

University of Cape

T74PIC

$C_{30}H_{22}O_2 \cdot 2C_6H_7N$
Guest : 4-picoline
Space Group : $P2_1/c$
a = 13.278(3)Å $\alpha = 90°$
b = 6.764(1)Å $\beta = 98.79(3)°$
c = 18.964(4)Å $\gamma = 90°$
Volume = 1683.2(6)Å^3
Z = 2

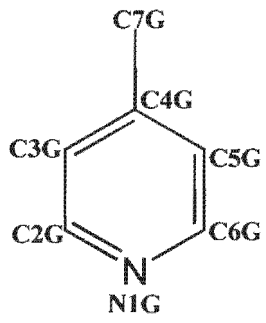

Crystal Structure and Refinement

Oscillation and Weissenberg photography showed that **T74PIC**, like **T7PYR** and **T73PIC** belonged to the monoclinic system. Once again the structure solved successfully in the space group $P2_1/c$. A host to guest ratio of 1: 2 was established by TG and was confirmed by the crystal structure. As was observed for all the above structures in this series the host molecules were located on a centre of inversion (Wyckoff position b) and the guests were placed in general positions.

The non-hydrogen atoms were refined anisotropically. The hydroxyl hydrogens were located in the difference electron density maps and were allowed to refine isotropically. The hydroxyl hydrogens were then constrained at a distance of 0.97Å from the parent oxygen atom[1]. Bond lengths and angles for both the host and the guest were in the expected ranges[2]. The structure refined successfully to $R_1 = 0.0475$.

Crystal Packing

The crystal packing of **T74PIC** is shown in Figure 3.2.11. The packing of the host molecules in **T74PIC** is very similar to that of **T72PIC**. The guest molecules lie in channels parallel to [010].

The channels vary in size from approximately 6.5Å × 6.8 Å to 7.6Å × 15.9Å.

University of Cape Town

In addition the cell parameters of **T7PYR** and **T74PIC** are comparable. Similarities can be seen between: (a) the lengths of the a axis of **T72PIC** and the b axis of **T74PIC**, (b) the lengths of the c axis of **T72PIC** and the a axis of **T74PIC**, (c) the b axis of **T72PIC** is approximately twice the length of the c axis of **T74PIC** and (d) the angles α and γ are larger in **T72PIC** than in **T74PIC.**

Hydrogen bonding details for **T74PIC** are given in Table 3.2.5.

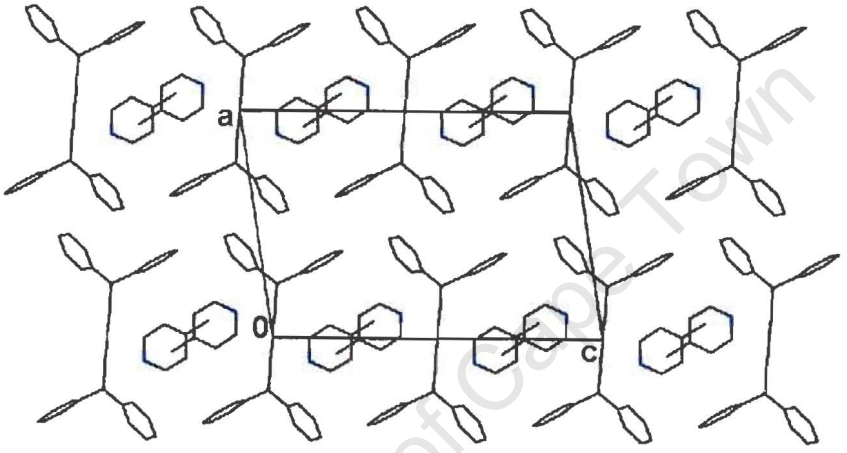

Figure 3.2.11. Crystal packing diagram of **T74PIC**.

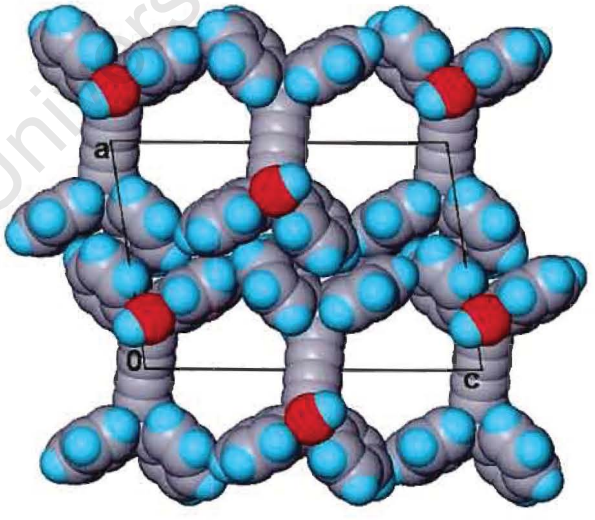

Figure 3.2.12. Space filling diagram down [010], with the guests omitted, illustrating the channels of **T74PIC**.

University of Cape Town

Table 3.2.5. Hydrogen bonding details of **T74PIC**.

Donor (D)	Acceptor (A)	D—H / Å	D•••A / Å	D—H•••A / °
O1	N1G[a]	0.97(2)	2.768(1)	169(2)

a : -x+1, -y+1, -z

Thermal Analysis

The DSC curve shows a single endotherm, A (T_{on}= 99.2°C) which once again is associated with the dissolution of the host in the released guest and includes the contribution due to desolvation.

The TG shows a single mass loss step (expected mass loss: 31.0%, observed mass loss: 31.1%) which is consistent with the host:guest ratio of 1:2.

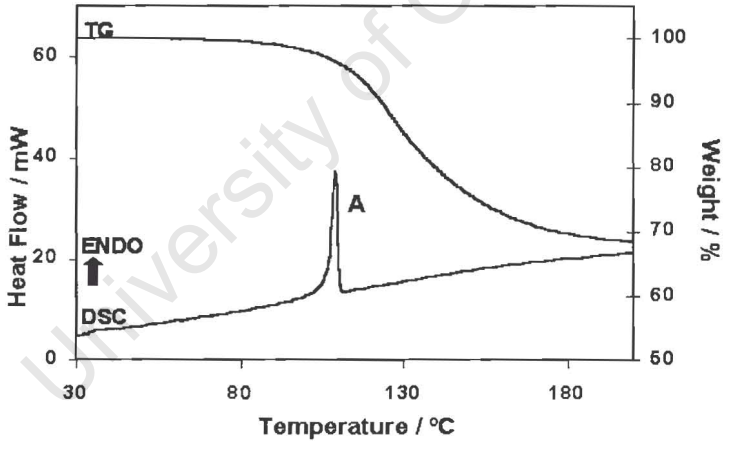

Figure 3.2.13. TG and DSC curves for **T74PIC**.

Competition Experiments

Competition experiments have been performed to determine which of the pyridine and picoline guests are preferentially included by the host **TOD7**. A series of 2-, 3- and 4-component competition experiments have been carried out and the results are shown in Figures 3.2.14. and 3.2.15.

University of Cape Town

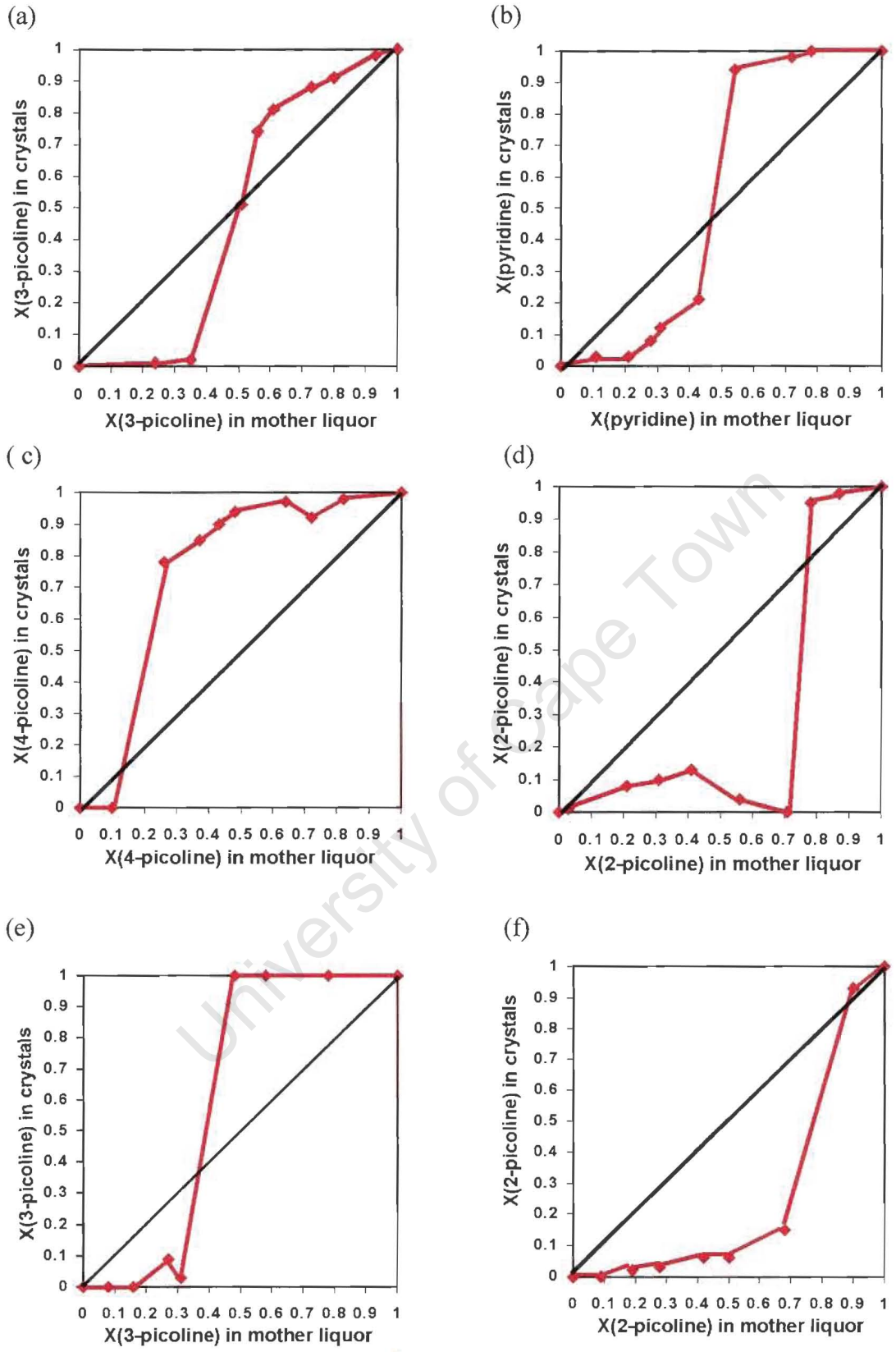

University of Cape Town

Figure 3.2.14. 2- component competition experiments: (a) pyridine vs 3-picoline, (b) pyridine vs 2-picoline, (c) pyridine vs 4-picoline, (d) 2-picoline vs. 4-picoline, (e) 3-picoline vs. 4-picoline and (f) 2-picoline vs. 3-picoline.

2- component competition

Some of the results shown below are similar to those obtained by Toda[3] who conducted similar experiments using different host: guest ratios. Concentration dependent behaviour is observed for the pyridine / 3-picoline and the pyridine / 2-picoline systems. In both cases the selectivity of the host for pyridine is increased whenever the percentage of pyridine in the mixture exceeds 50%.

In the competition experiments between pyridine and 4-picoline the latter is preferred when the mol fraction of 4-picoline in the mixture is greater than 0.2.

Similarly in the competition experiments between 2-picoline and 4-picoline, 4-picoline is preferentially enclathrated when the mol fraction of 4-picoline is larger than 0.3.

In the case of 3-picoline versus 4-picoline the former is selected when the mol fraction of 3-picoline in the mother liquor exceeds 0.40.

The competition experiments between 2-picoline and 3-picoline indicate that the latter is favoured whenever the percentage of 3-picoline in the mixture is larger than 30%.

3-component competition

3-component competition experiments have been carried out between the host, **TOD7**, and the following combinations of guests:

(i) pyridine, 3-picoline and 4-picoline

(ii) 2-picoline, 3-picoline and 4-picoline.

In both cases concentration dependent selectivity is observed. Thus mixtures which contain mol fractions of pyridine larger than 0.5, will strongly enrich the pyridine guest in the crystals. Similarly 4-picoline is selectively enclathrated when the

University of Cape Town

percentage of 4-picoline in the mother liquor exceeds 45%. In the remaining cases 2-picoline and 3-picoline are preferred.

4-component competition

In the 4-component competition experiments there is a clear migration of points away from 2-picoline and towards the pyridine, 3-picoline, 4-picoline baseline. The majority of the points have migrated towards 4-picoline which indicates that 4-picoline is preferred in a mixture of all four guests.

(a)

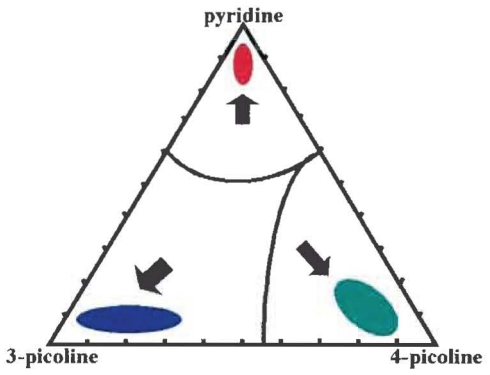

(b)

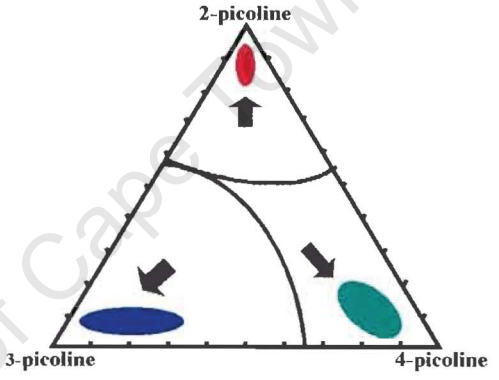

(c)

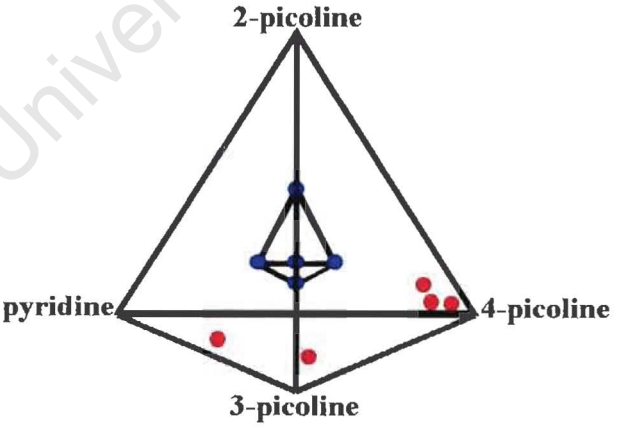

Figure 3.2.15. 3-, and 4-component competition experiments: (a) pyridine vs 3-picoline vs 4-picoline, (b) 2-picoline vs 3-picoline vs 4-picoline and (c) pyridine vs 2-picoline vs 3-picoline vs 4-picoline. Starting materials defined by the boundaries result in concentrations given by the coloured areas.

University of Cape Town

Potential Energy Calculations

Lattice energies were calculated using the program HEENY. HEENY is generally used to compare lattice energies between inclusion compounds where the guests are isomers. However in this case the results can be normalised by dividing the lattice energy by the molecular weights of the respective complexes. The results are listed in Table 3.2.6.

Table 3.2.6. Lattice energy results for **T7PYR**, **T72PIC**, **T73PIC** and **T74PIC**.

Compound	**Lattice Energy(LE) / kJmol^{-1}**	**LE / M_W(kJg^{-1})**
T7PYR	–603.3	-1.053
T72PIC	-419.8	-0.699
T73PIC	–588.2	-0.979
T74PIC	–616.3	-1.026

University of Cape Town

Discussion

T7PYR, **T73PIC** and **T74PIC** crystallise in the space group $P2_1/c$. **T72PIC** exhibits lower symmetry and crystallises in the space group $P\bar{1}$.

However, **T7PYR**, **T72PIC** and **T74PIC** exhibit similar packing motifs with the acetylenic spacers of the host molecules parallel to one unit cell axis and bulky phenyl groups of the host creating voids which are occupied by guest molecules. In all three structures the guests lie in relatively open channels. **T73PIC** has a different packing arrangement with the guest lying in cages.

In all four structures in this series the host is situated on a centre of inversion resulting in the hydroxyl groups of the host being trans. Hydrogen bonding occurs between the host hydroxyl groups and the nitrogen atom of the guests.

A comparison of the lattice energies can be made between the picoline isomers. The lattice energies indicate that **T74PIC** is the most stable structure of the inclusion compounds containing the three picoline isomers. This result is supported by the competition experiments where overall, 4-picoline is preferentially included when all four guests are present. In the 2- and 3-component competition experiments it appears that it is not only the stability of the compounds that are important but also kinetic effects which play a role in determining which complex crystallizes in a mixture.

T72PIC has the least negative lattice energy which implies that it is the least stable structure. This result is consistent with the great difficulty experienced in growing

University of Cape Town

crystals of this particular inclusion compound. The competition experiments also indicated that 2-picoline was the least favoured of all the guests.

Table 3.2.7. Summary of thermal analysis data for the structures studied in this chapter.

Inclusion compound			**T7PYR**	**T72PIC**	**T73PIC**	**T74PIC**
H : G ratio			1 : 2	1: 2	1 : 2	1 : 2
TG results	Calc. % mass loss		27.6	31.0	31.0	31.0
	Exp. % mass loss		27.2	29.9	30.8	31.1
DSC results	T_{on} (°C) :	A	99.2	77.5	102.3	106.2
		B	—	114.8	—	—
Normal boiling points, T_b (°C)			115.2	128.5	143.5	145.0
T_{on}/ T_b			0.861	0.603	0.713	0.732

The larger value of T_{on}/ T_b obtained for **T7PYR** is consistent with the normalised lattice energy results which favour **T7PYR** as the most stable compound.

University of Cape Town

References

1. I. Olovsson and P. Jönsson, *The Hydrogen Bond* – Structure and Spectroscopy, P.Schuster, G. Zundel and C. Sardefy (eds.), North-Holland Publishing Company, USA, 1975.

2. International Tables for crystallography, Vol. C, (ed.) A.J.C. Wilson, Kluwer Academic Publishers, Dordrecht, pp.691, 1992.

3 K. Doki, K. Tanaka, F. Toda, Nippon Kagaku Kaishi, 7(1986)927.

University of Cape Town

CHAPTER 3.3. INCLUSION OF AROMATIC GUESTS

The inclusion compounds formed between the host, **TOD7**, and the aromatic guests benzene, toluene and mesitylene have been studied. Their crystal structures have been solved. The inclusion compounds formed between **TOD7** and the guests benzene and toluene were grown from dilute solutions by slow evaporation. The crystals of the inclusion compound between **TOD7** and mesitylene were grown unexpectedly from a mixture of **TOD7**, mesitylene and o-nitroaniline. Later in Chapter 3.5, complexation between **TOD7** and o-nitroaniline in a mixture of diethyl ether/n-hexane is discussed.

University of Cape Town

Table 3.3.1. Crystal data, experimental and refinement parameters

	T7BENZ	**T7TOL**	**T7MESI**
Compound	$C_{30}H_{22}O_2 \cdot C_6H_6$	$C_{30}H_{22}O_2 \cdot ¾C_7H_8$	$C_{30}H_{22}O_2 \cdot C_9H_{12}$
M_w, $gmol^{-1}$	492.58	481.56	534.66
Temperature/ K	173(2)	173(2)	173(2)
Crystal system	triclinic	triclinic	monoclinic
Space group	$P\bar{1}$	$P\bar{1}$	C2/c
a, Å	13.001(3)	12.922(3)	23.750(5)
b, Å	15.284(3)	15.159(3)	8.475(2)
c, Å	16.744(3)	16.562(3)	17.760(4)
α, °	99.26(3)	68.12(3)	90
β, °	105.22(3)	73.99(3)	123.40(3)
γ, °	115.04(3)	66.00(3)	90
V, $Å^3$	2764(1)	2720.4(9)	2984(1)
Z	4	4	4
Absorption coefficient, mm^{-1}	0.072	0.072	0.072
F(000)	1040	1014	1136
Crystal size, mm	0.35 × 0.34 × 0.30	0.50 × 0.22 × 0.12	0.35 × 0.30 × 0.25
Index ranges	h: 0, 17; k: -20, 18; l: -22,21	h: ±16; k: ±19; l: -21,20	h: ±29; k: -9,10; l: ±22
Reflections collected / unique	13613 / 13613	19748 / 12439	5159/ 3016
Data/ restraints/ Parameters	13613 / 14 / 696	12439 / 8 / 702	3016 / 1 / 192
Goodness-of-fit	1.022	0.930	1.063
ρ_{calc}, $g \cdot cm^{-3}$	1.184	1.176	1.190
Final R indices [$I > 2\sigma(I)$]	$R_1 = 0.0957, wR_2 = 0.2956$	$R_1 = 0.0509, wR_2 = 0.1216$	$R_1 = 0.0512, wR_2 = 0.1360$
R indices (all data)	$R_1 = 0.1578, wR_2 = 0.3490$	$R_1 = 0.1106, wR_2 = 0.1475$	$R_1 = 0.0810, wR_2 = 0.1507$
Largest difference peak and hole, $eÅ^{-3}$	0.477 and -0.483	0.251 and -0.237	0.390 and -0.213

University of Cape Town

T7BENZ

$C_{30}H_{22}O_2 \cdot C_6H_6$
Guest : benzene
Space Group : $P\bar{1}$
a = 13.001(3)Å
b = 15.284(3)Å
c = 16.744(3)Å
Volume = 2764(1)Å^3
Z = 4

α = 99.26(3)°
β = 105.22(3)°
γ = 115.04(3)°

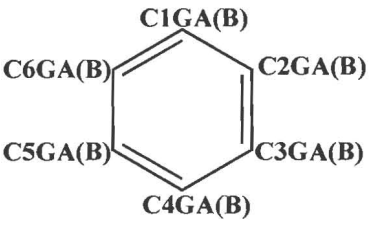

Crystal Structure and Refinement

The centrosymmetric space group $P\bar{1}$ was assigned based on symmetry considerations and the mean $|E^2 - 1|$ values. Both the host and the guest molecules occupy general positions. All the non-hydrogen atoms of the host and the guest were obtained by direct methods. All the non-hydrogen atoms of the host and the guest were refined anisotropically. There are two host molecules and two guests in the asymmetric unit. Two of the hydroxyl hydrogens were located in the difference electron density maps, refined isotropically and subsequently placed in geometrically calculated positions[1]. The other two were fixed in position with torsion angles chosen to match the maximum electron density in the difference map. Thereafter the hydroxyl hydrogens were geometrically constrained[1]. The bond lengths and angles of the host molecules and one of the guests (guest B: identified by the atoms C1GB, C2GB, C3GB, C4GB, C5GB, C6GB) are in the expected ranges[2]. The atoms of the other guest, guest A (identified by the atoms C1GA, C2GA, C3GA, C4GA, C5GA, C6GA) were restrained to lie in a common plane. The U_{eq} values of guest A refined to the following: U_{eq}(C1GA) = 0.17Å^2, U_{eq}(C2GA) = 0.15Å^2, U_{eq}(C3GA) = 0.16Å^2, U_{eq}(C4GA) = 0.27Å^2, U_{eq}(C5GA) = 0.48Å^2 , and U_{eq}(C6GA) = 0.38Å^2, compared to the average U_{eq} of the atoms of guest B which refined to 0.11Å^2.

University of Cape Town

The bond lengths of guest A were shorter than expected due to its poor refinement. The structure was solved with a final $R_1 = 0.0957$.

Crystal Packing

As was observed for all the structures where the host was located in general positions, the hydroxyl groups are in the gauche conformation. The guests lie in restricted channels parallel to [100]. The size of the channels varies from 5.6Å × 6.4Å at the narrowest parts to 10.6Å × 8.5Å at the widest parts. The host forms wavy chains that are held together by hydrogen bonding between adjacent host molecules. The hydrophobic phenyl groups point inwards to encircle the guests.

(a) (b)

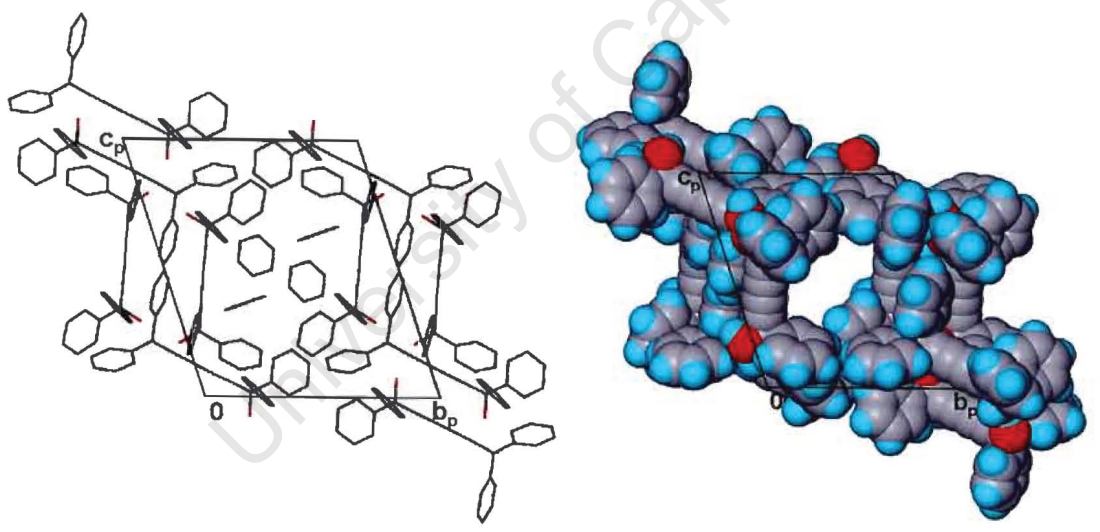

Figure 3.3.1 (a) Crystal packing of **T7BENZ** down [100]; (b) Space-filling diagram down [100] with the guest removed.

University of Cape Town

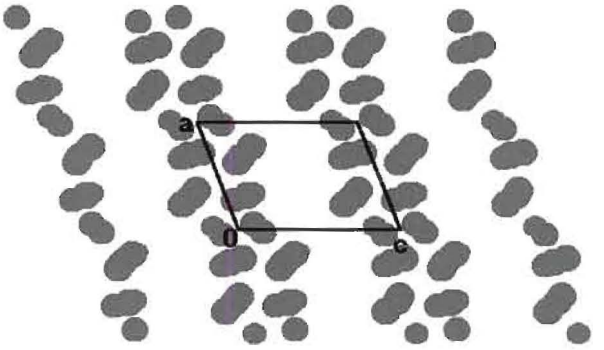

Figure 3.3.2. SECTION plot of **T7BENZ** down [010], guest omitted, sectioned at y = ½, showing the channels parallel to [100].

As in the **T7CCL4** structure, hydrogen bonding in **T7BENZ** occurs between hydroxyl groups on adjacent host molecules forming a four-centre hydrogen bond. Aromatic C—H•••π distances of less than 3.05Å are also present[3,4].

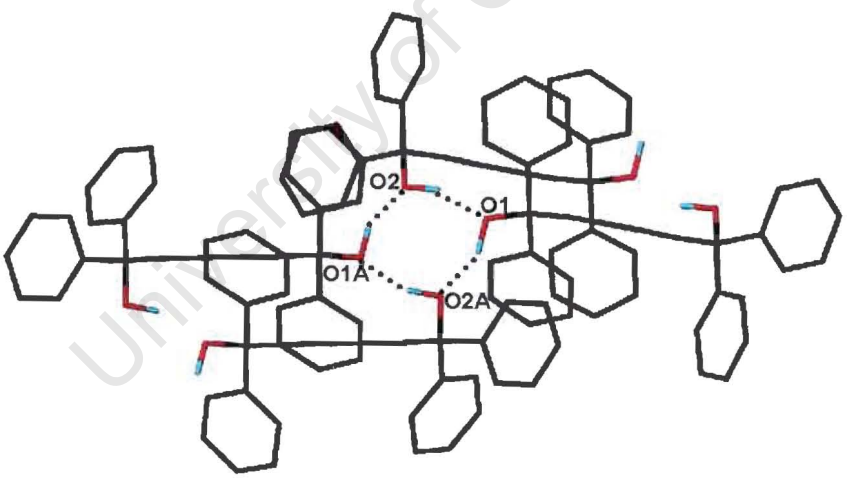

Figure 3.3.3. Hydrogen bonding in **T7BENZ**.

University of Cape Town

Table 3.3.2. Hydrogen bonding details of **T7BENZ**.

Donor (D)	Acceptor (A)	D—H / Å	D•••A / Å	D—H•••A / °
O1	O2A[a]	0.98(1)	2.667(1)	157(4)
O2	O1[b]	0.99(3)	2.676(1)	156(7)
O1A	O2	0.98(1)	2.667(1)	157(3)
O2A	O1A[c]	0.98(1)	2.725(1)	159(2)

a: x, y, z +1

b: -x+2, -y+2, -z

c: -x+2, -y+2, -z-1

Thermal Analysis

The TG curve shows a multistep pathway in which the mass losses are not well defined. This is indicative of the guest molecules being situated in different environments in the host framework (there are two independent guest molecules in the asymmetric unit). The total mass loss of 14.9% (calculated 15.9%) confirms the host: guest ratio of 1:1 obtained in the crystal structure.

The DSC curve shows a very complicated decomposition pathway and is characterised by four endotherms and an exotherm. Endotherms A (T_{on} = 79.5°C), B (T_{on} = 92.4°C) and exotherm C (T_{on} = 102.8°C) correspond to the loss of guest. As was observed in the previous structures, the last two endotherms, collectively referred to as D (T_{on} = 145.8°C, peaks at 142.1°C and 147.5°C), represents a phase change followed by the host melt.

University of Cape Town

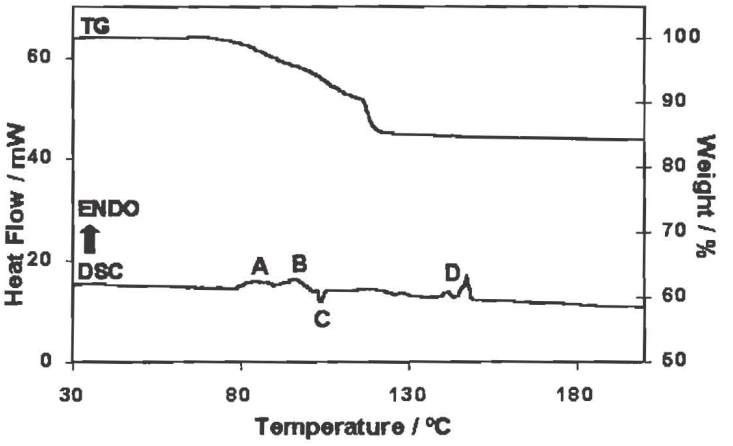

Figure 3.3.3. TG and DSC curves for **T7BENZ**.

University of Cape Town

T7TOL

$C_{30}H_{22}O_2 \cdot 1\frac{1}{2}C_7H_8$		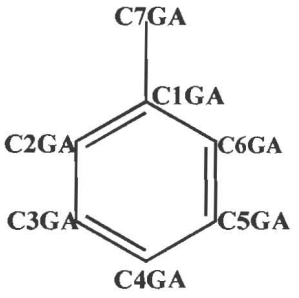
Guest : toluene		
Space Group : $P\bar{1}$		
a = 12.922(3)Å	α = 68.12(3)°	
b = 15.159(3)Å	β = 73.99(3)°	
c = 16.562(3)Å	γ = 66.00(3)°	
Volume = 2720.4(9)Å^3		
Z = 4		

Crystal Structure and Refinement

The crystal structure was refined in the triclinic space group $P\bar{1}$. Two host molecules were located in general positions, as was the case in the previous structure. One of the guests was also situated in general positions (guest A) with the other guest on a centre of inversion at Wyckoff position b (guest B). The carbon atoms of guest B were found to be disordered and refined with the following site occupancy factors of C1GB: 0.5, C2GB: 1.0, C3GB: 0.5, C4GB: 0.5 and C5GB: 1.0 as shown in Figure 3.3.4. The hydrogens of guest B were omitted from the final model. All the non-hydrogen atoms were refined with anisotropic temperature factors. All the hydroxyl hydrogens of the host were found in the difference maps but were geometrically constrained as before. The bond lengths and angles of the host and guest A all fall within the expected ranges[2].

University of Cape Town

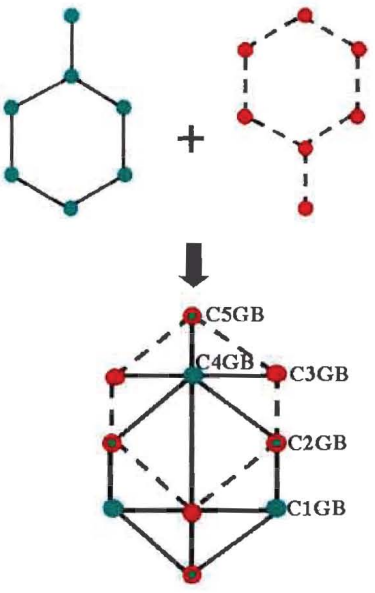

Figure 3.3.4. Disorder in guest B.

Crystal Packing

As was observed in the previous structure the guest molecules lie in channels parallel to [100]. This is illustrated in Figure 3.3.5. The channels vary in size from approximately 6.2Å × 5.6Å to 11.2Å × 10.2Å. The hydrogen bonding in **T7TOL** is similar to that described in **T7BENZ** and details are given in Table 3.3.3.

University of Cape Town

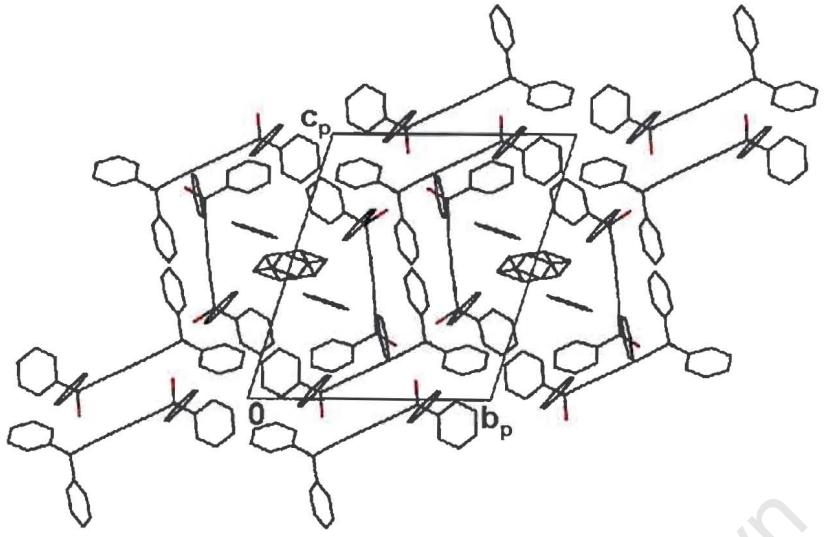

(a)

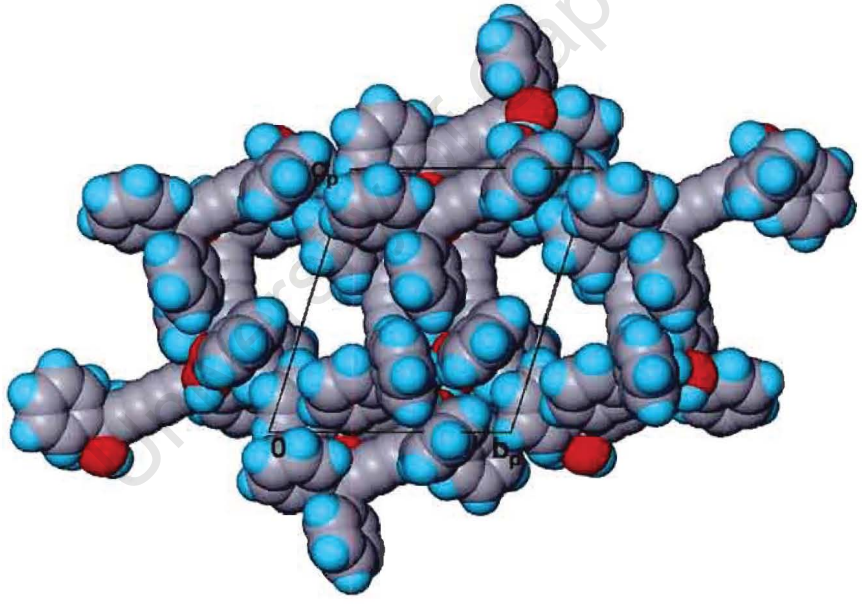

(b)

Figure 3.3.5(a) Crystal packing in **T7TOL** down [100]; (b) Space-filling diagram down [100] with the guest omitted.

University of Cape Town

The hydrogen bonding in **T7TOL** is similar to that of **T7BENZ.** These are listed in Table 3.3.3. Again, aromatic C—H•••π short contacts are present to stabilise the structure.

Table 3.3.3. Hydrogen bonding details of **T7TOL**.

Donor (D)	Acceptor (A)	D—H / Å	D•••A / Å	D—H•••A / °
O1	O2A[a]	0.98(1)	2.693(1)	145(6)
O2	O1[b]	0.98(3)	2.672(1)	155(5)
O1A	O2	0.99(1)	2.656(1)	160(3)
O2A	O1A[c]	0.98(1)	2.708(1)	164(7)

a: x, y, z +1

b: -x+1, -y+1, -z

c: -x+1, -y+1, -z-1

Thermal Analysis

A single mass loss step was observed in the TG. The mass loss (experimental: 14.3%, calculated: 14.3%) is consistent with the host: guest ratio of 1: ¾.

The DSC shows a loss of guest at T_{on} = 89.5°C. This is consistent with the hot stage results which show that the crystal has turned opaque at 88.5°C. Once again a phase change followed by the host melt occurs in the expected region (T_{on} = 146.2°C, peaks at 143.1°C and 147.6°C).

University of Cape Town

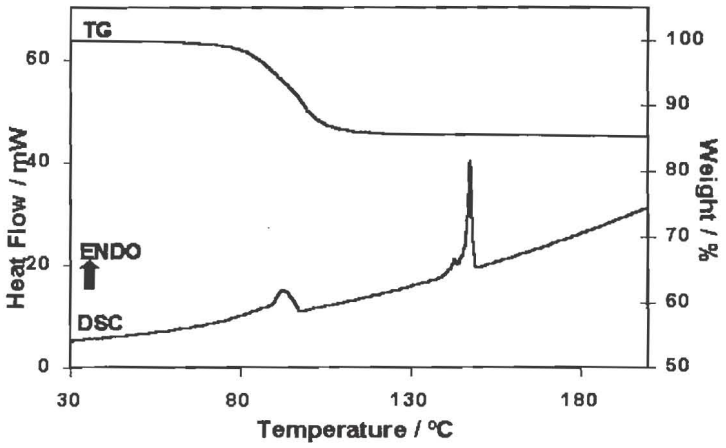

Figure 3.3.6. TG and DSC curves for **T7TOL**.

Hot stage Microscopy

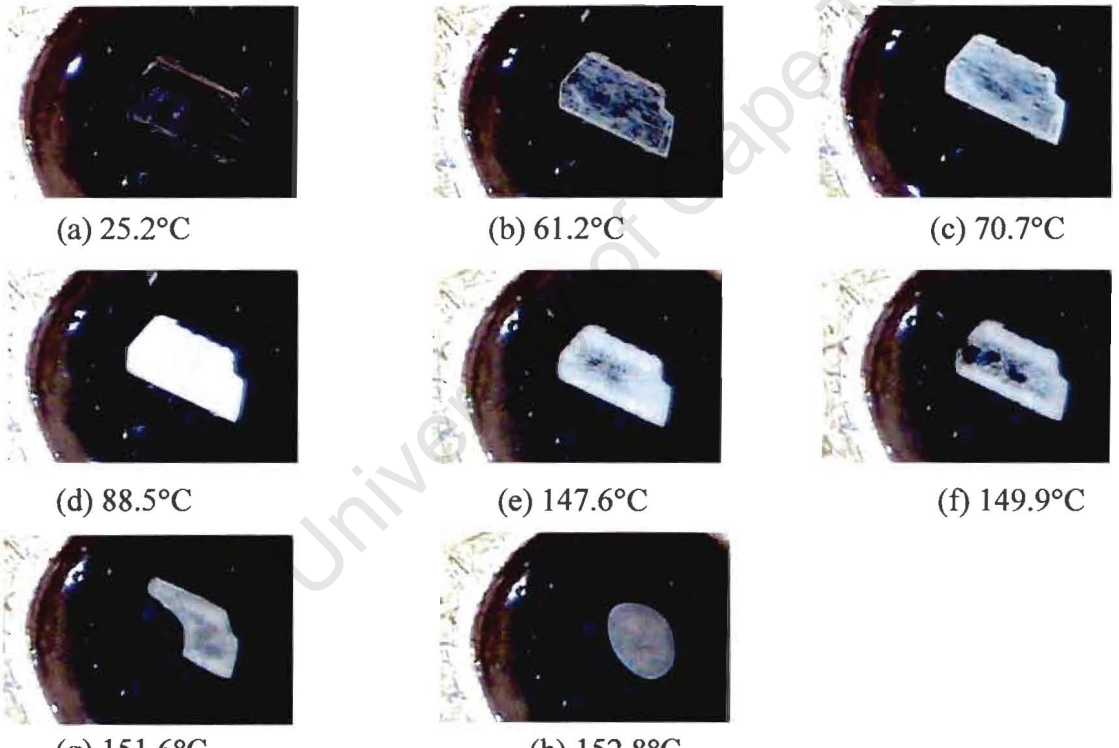

(a) 25.2°C (b) 61.2°C (c) 70.7°C

(d) 88.5°C (e) 147.6°C (f) 149.9°C

(g) 151.6°C (h) 152.8°C

Figure 3.3.7. Hot stage microscopy of a single crystal of **T7TOL** at (a) room temperature, (b) crystal starts turning opaque at 61.2°C; (c) crystal at 70.7°C, (d) crystal is totally opaque at 88.5°C; (e) melt starts at 147.6°C ; (f), (g) crystal melt at 149.9°C and 151.6°C and (h) melt is complete at 152.8°C.

University of Cape Town

T7MESI

$C_{30}H_{22}O_2 \cdot C_9H_{12}$
Guest : mesitylene
Space Group : C2/c
a = 23.750(5)Å $\alpha = 90°$
b = 8.475(2)Å $\beta = 123.40(3)°$
c = 17.760(4)Å $\gamma = 90°$
Volume = 2984(1)Å^3
Z = 4

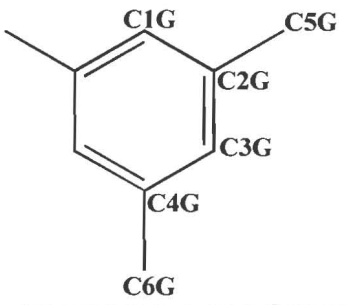

Crystal Structure and Refinement

A host:guest ratio of 1:1 was determined by TG and verified by the crystal structure. The space group C2/c was assigned in preference to the Cc space group due to the mean $|E^2-1|$ statistics which indicated that the structure was centrosymmetric.

Direct methods yielded all the non-hydrogen atoms of the host and the guest. The host was located on a centre of inversion (Wyckoff position d) and the guest was found on a two fold axis at Wyckoff position e. During the refinement all the non-hydrogen atoms were made anisotropic. The following carbon atoms of the guest were refined with site occupancy factors of 0.5: C1G, C4G and C6G. The aromatic hydrogen atoms of the host and the guest were geometrically constrained with C—H distances of 0.93Å. The methyl hydrogens on C5G were inserted with C—H distances of 0.96Å, whereas those on C6G were omitted from the final model. The hydroxyl hydrogen of the host was located in the difference electron density maps and fixed a distance of 0.97Å from the parent oxygen atom. All bond lengths and angles obtained were consistent with known and accepted values[2].

University of Cape Town

Crystal Packing

The guests are situated in channels parallel to [010]. The channels are constricted and vary in size from approximately 4.4Å × 5.1Å to 12.8Å × 4.4Å.

(a) (b)

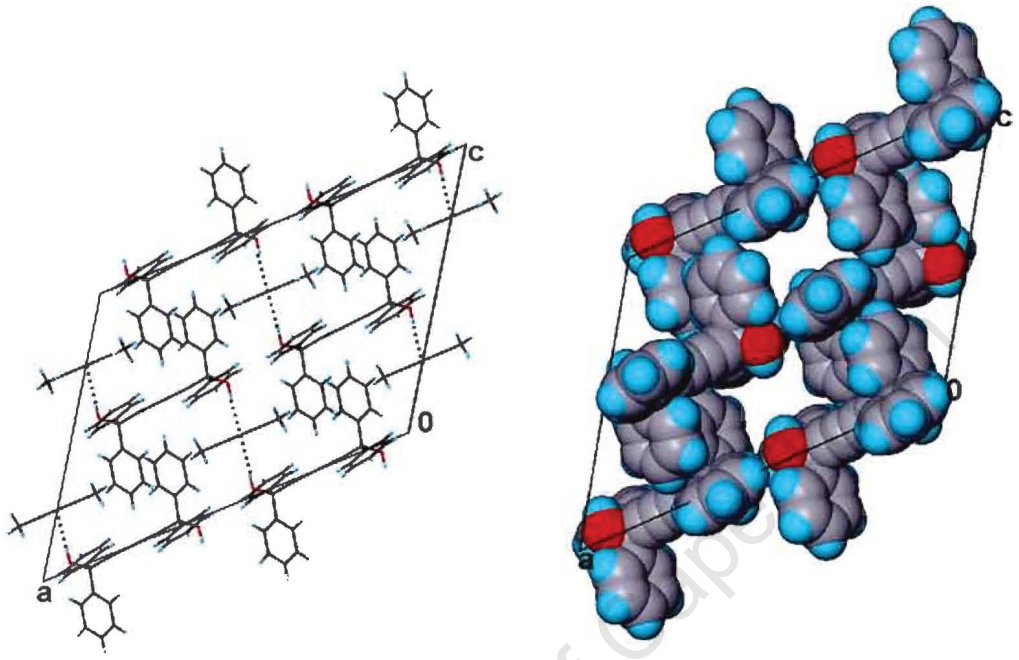

Figure 3.3.8. (a) Crystal packing in **T7MESI** down [010], indicating the hydrogen bonding and (b) Space-filling diagram down [010] with the guest omitted.

The crystal structure is stabilised by weak hydrogen bonding between the hydroxyl hydrogen of the host and the phenyl ring of the guest ie. O—H•••π hydrogen bonding. Table 3.3.4 lists both the O and the H distances to each atom in the aromatic ring (including the centroid). The O—H•••π hydrogen bonding is mostly directed towards the centroid of the guest.

University of Cape

Table 3.3.4. O—H•••π hydrogen bonding for **T7MESI**.eg. O1•••C1G = 3.619Å.

	O1	H1	O—H•••π(°)
C1G	3.619	2.974	125.00
C2G	3.781	3.046	133.58
C3G	3.716	2.827	152.90
C4G	3.525	2.557	175.44
C2G*	3.422	2.725	129.28
C3G*	3.359	2.484	149.89
Centroid	3.293	2.405	152.06

*: -x, y, ½-z

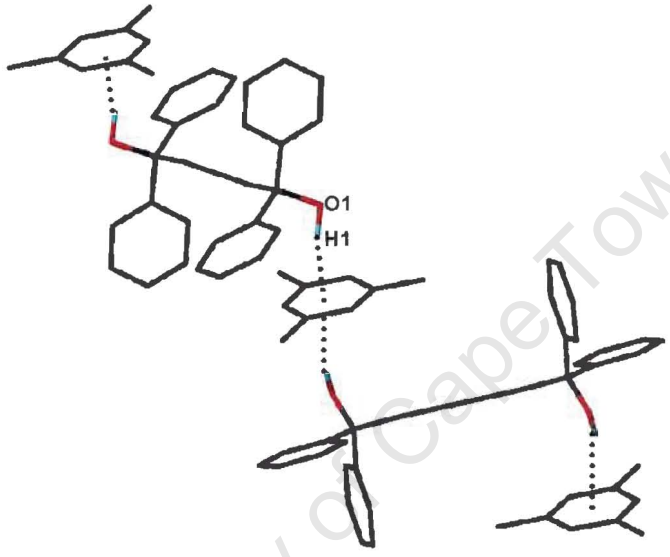

University of Cape Town

Figure 3.3.9. O—H•••π hydrogen bonding in **T7MESI**.

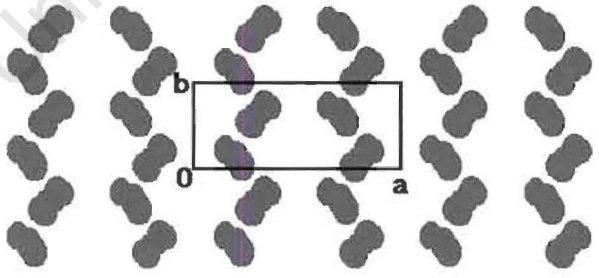

Figure 3.3.10. SECTION plot of **T7MESI** down [001] sectioned at c = ¼, with the guest omitted, showing the channels parallel to [010].

Thermal Analysis

The TG shows a single mass loss (experimental: 22.4%, calculated: 22.5%). This is in agreement with the host: guest ratio of 1: 1 obtained from the crystal structure.

The DSC indicates that guest loss occurs at an onset temperature of 80.7°C. A phase change and host melt occurs at T_{on} = 134.9°C (peaks at 136.0°C and 138.1°C).

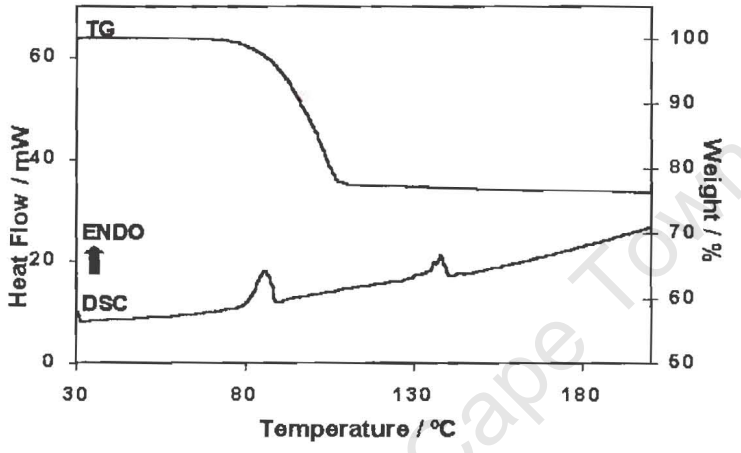

Figure 3.3.10. TG and DSC curves for **T7MESI**.

University of Cape Town

Hot stage microscopy

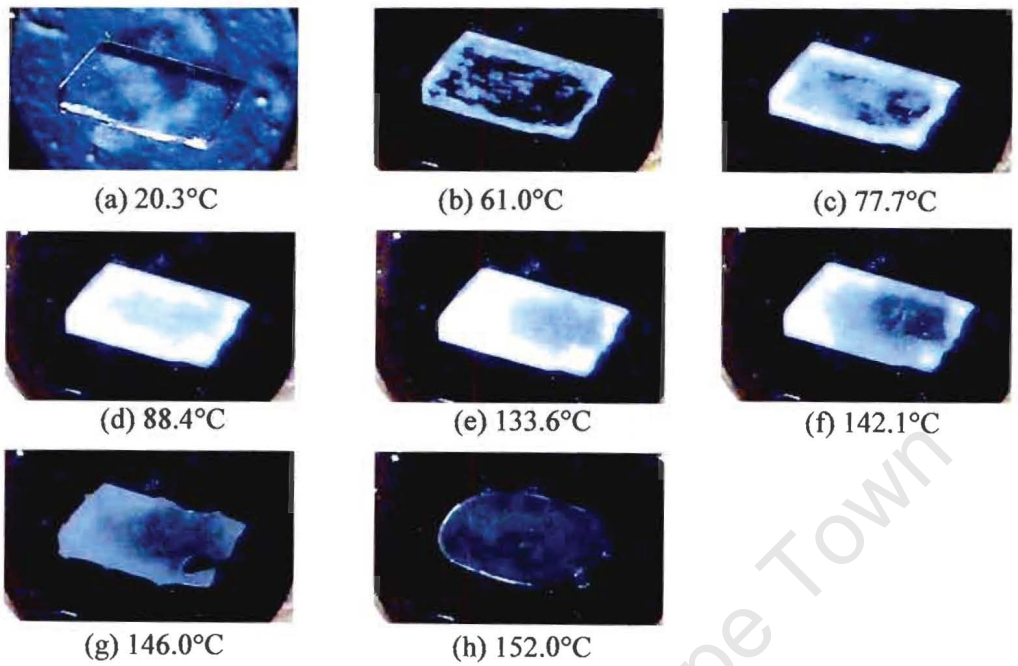

(a) 20.3°C (b) 61.0°C (c) 77.7°C

(d) 88.4°C (e) 133.6°C (f) 142.1°C

(g) 146.0°C (h) 152.0°C

Figure 3.3.11. Thermal decomposition of **T7MESI** at (a) room temperature, (b) crystal starts becoming opaque at 61.0°C (c), (d) crystal at 77.7°C and 88.4°C, (e) melt starts at 133.6°C, (f), (g) melt progresses at 142.1°C and 146.0°C and (h) melt complete at 152.0°C.

University of Cape Town

Discussion

Both **T7BENZ** and **T7TOL** crystallise in the space group $P\bar{1}$ with similar unit cell parameters although the angles in **T7BENZ** are significantly larger. The asymmetric unit of **T7BENZ** consists of two independent host molecules and two independent guest molecules. This is in contrast to **T7TOL**, which has two independent host molecules and one and a half guest molecules in its asymmetric unit. The crystal packing is similar in both structures with the guests situated in relatively open channels. The hydrophobic parts of the host framework point inwards, surrounding the hydrophobic guests. Both structures are stabilised by hydrogen bonding between adjacent host molecules. The hydrogen bonding is similar to that found in Chapter 3.1 between **TOD7** and the chlorinated guests. However in those structures the host framework formed cages which were occupied by guest molecules.

T7MESI crystallises in the space group C2/c. The asymmetric unit contains one half of a host molecule and one half of a guest molecule. The guests lie in slightly more constricted channels. The structure is stabilised by weak O—H•••π hydrogen bonding between the host and the guest.

In all three structures guest release is followed by the host melt. A detailed summary of the thermal analysis data is given in Table 3.3.5.

Table 3.3.5. Summary of thermal analysis data

Inclusion compound		**T7BENZ**	**T7TOL**	**T7MESI**
H : G ratio		1 : 1	1: ¾	1 : 1
TG results	Calc. % mass loss	15.9	14.3	22.5
	Exp. % mass loss	14.9	14.3	22.4
DSC results	T_{on} (° C) :	79.5, 92.4, 102.8	89.5	80.7
		145.8	146.2	134.9
Normal boiling points T_b (° C)		80.1	110.6	164.7
T_{on} / T_b		0.993, 1.153, 1.283	0.809	0.819

University of Cape Town

References

1. I. Olovsson and P. Jönsson, *The Hydrogen Bond* – Structure and Spectroscopy, P.Schuster, G. Zundel and C. Sardefy (eds.), North-Holland Publishing Company, USA, 1975.

2. International Tables For Crystallography, Vol. C, (ed.) A.J.C. Wilson, Kluwer Academic Publishers, Dordrecht, pp.691, 1992.

3. F. Cozzi and J.S. Siegel, *Pure Applied Chem.*, 67, 683, 1995.

4. E. Kim, S. Paliwal and C.S. Wilcox, *J. Am. Chem. Soc.*, 120, 11192, 1998.

University of Cape Town

CHAPTER 3.4 INCLUSION OF DMF AND DMSO.

In this chapter the inclusion compounds formed between **TOD7** and guests N, N-dimethylformamide (DMF) and dimethyl sulfoxide (DMSO) will be discussed. Both crystal structures have been solved and the results correlated with thermal analysis, kinetics of desolvation, competition experiments and guest exchange reactions. Crystals of **T7DMF** were grown by slow evaporation of a dilute solution of host, **TOD7** and guest DMF. **TOD7** proved to be only slightly soluble in DMSO. Thus in a typical experiment, 10-15 ml of DMSO was added to 50 mg of **TOD7**. When stirred on a hotplate, a cloudy suspension formed which cleared when 1-2 ml of 2-picoline was added. In Chapter 3.2 it was shown that complexation takes place between **TOD7** and 2-picoline. However in this instance the molar ratios are in favour of DMSO which is in excess (mols of 2-picoline:mols of DMSO is approximately 1:10). Plate-like crystals of **T7DMSO** formed by slow evaporation of this solution.

University of Cape Town

Table 3.4.1. Crystal data, experimental and refinement parameters.

	T7DMF	**T7DMSO**
Compound	$C_{30}H_{22}O_2 \cdot 2C_3H_7NO$	$C_{30}H_{22}O_2 \cdot 2C_2H_6SO$
M_w , $gmol^{-1}$	560.67	570.73
Temperature / K	293(2)	173(2)
Crystal system	orthorhombic	orthorhombic
Space group	Pbca	Pbca
a, Å	11.564(2)	11.377(2)
b, Å	16.393(3)	15.982(3)
c, Å	16.793(3)	16.191(3)
α, °	90	90
β, °	90	90
γ, °	90	90
V, $Å^3$	3183(1)	2944(1)
Z	4	4
Absorption coefficient, mm^{-1}	0.076	0.218
F(000)	1192	1208
Crystal size, mm	0.50 × 0.45 × 0.44	0.27 × 0.33 × 0.12
Index ranges	h: 0, 14; k: ±20; l: -20,21	h: ±13; k: ±19; l: ±19
Reflections collected /unique	9742 / 3248	5047 / 2694
Data/restraints/Parameters	3248 / 2 / 196	2694 / 2 / 184
Goodness-of-fit	1.032	1.226
ρ_{calc}, $g \cdot cm^{-3}$	1.170	1.288
Final R indices [$I > 2\sigma(I)$]	$R_1 = 0.0666$, $wR_2 = 0.1802$	$R_1 = 0.0970$, $wR_2 = 0.2060$
R indices (all data)	$R_1 = 0.0979$, $wR_2 = 0.2048$	$R_1 = 0.1096$, $wR_2 = 0.2108$
Largest difference peak and hole, $eÅ^{-3}$	0.348 and -0.214	0.496 and -0.449

University of Cape Town

T7DMF

$C_{30}H_{22}O_2 \cdot 2C_3H_7NO$	
Guest : dimethyl formamide	
Space Group : Pbca	
a = 11.564(2)Å	$\alpha = 90°$
b = 16.393(3)Å	$\beta = 90°$
c = 16.793(3)Å	$\gamma = 90°$
Volume = 3183(1)Å^3	
Z = 4	

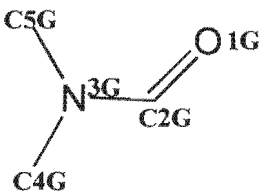

Crystal Structure and Refinement

Preliminary oscillation and Weissenberg photography indicated that **T7DMF** belonged to the orthorhombic system. A host to guest ratio of 1:2 was established by TG and this was confirmed by the crystal structure. The following conditions limiting certain reflections were observed:

0kl: k=2n (0k0: k=2n)

h0l: l=2n (00l: l=2n)

hk0: h=2n (h00: h=2n)

The centrosymmetric space group Pbca was assigned based on these conditions and confirmed by the mean $|E^2 - 1|$ values. The four host molecules were located on centres of inversion (Wyckoff position a) and the eight guests were placed in general positions.

All the non-hydrogen atoms of the host and all but one carbon atom of the guest were obtained by direct methods. Subsequent refinement revealed the last carbon atom. All the non-hydrogen atoms of the host and the guest were refined anisotropically. The hydroxyl hydrogen of the host was located in the difference electron density maps, and was refined isotropically. The hydroxyl hydrogens were then placed in geometrically calculated positions based on the relationship between the O—H

University of Cape Town

distance and O•••O distance[1]. The bond lengths and angles of the host were in the typical ranges[2]. The bond lengths and angles of the guest were shorter than expected due to the poor refinement of the guest molecule. No sensible disorder model could be proposed and the residual electron density was only 0.35eÅ^{-3}. At the end of the refinement U_{eq} values for the guest atoms were as follows: U_{eq}(O1G) = 0.16Å^2, U_{eq}(C2G) = 0.11Å^2, U_{eq}(C4G) = 0.16Å^2 and U_{eq}(C5G) = 0.21Å^2. The structure refined to a final R_1 = 0.0666.

Crystal Packing

Symmetry (energy) requires that the hydroxyl hydrogens of the host molecules adopt the trans ~~configuration~~ information. The host molecules form a wave-like pattern when viewed along [001]. The bulky phenyl groups act as spacers between the layers of host molecules. The guest molecules lie in channels parallel to [100]. The channels vary in size from approximately 5.2Å × 5.6Å to 7.0Å × 6.2Å. This type of inclusion compound is referred to as tubulate.

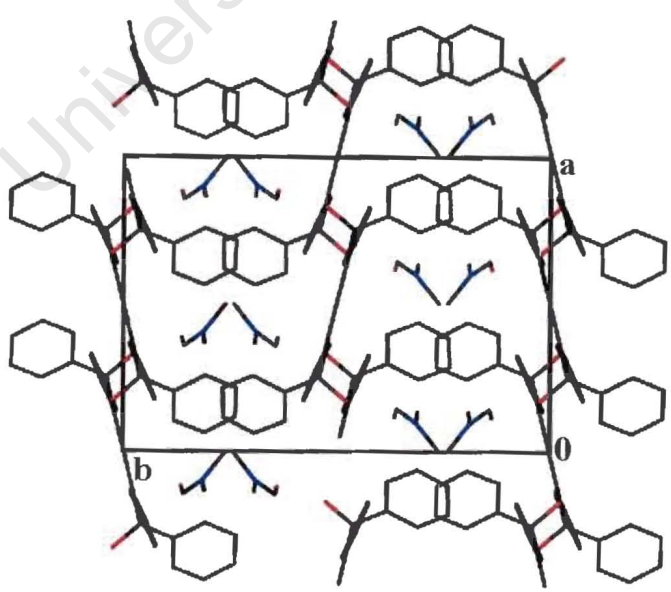

Figure 3.4.1. Crystal packing of **T7DMF** down [001].

University of Cape Town

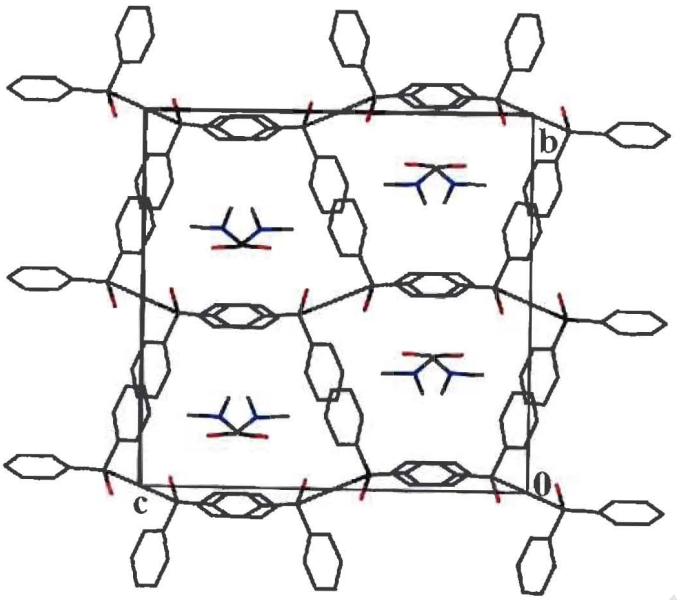

Figure 3.4.2. Packing diagram of **T7DMF** down [100].

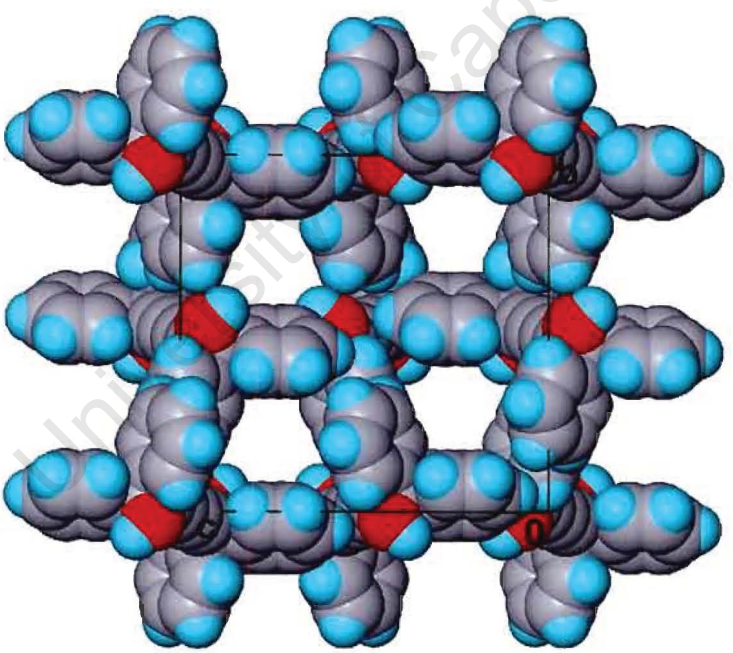

Figure 3.4.3. Packing diagram viewed down [100] with the atoms represented with van der Waals radii. Guests were omitted to show the channels, which they occupy.

University of the Western Cape Town

(a) (b)

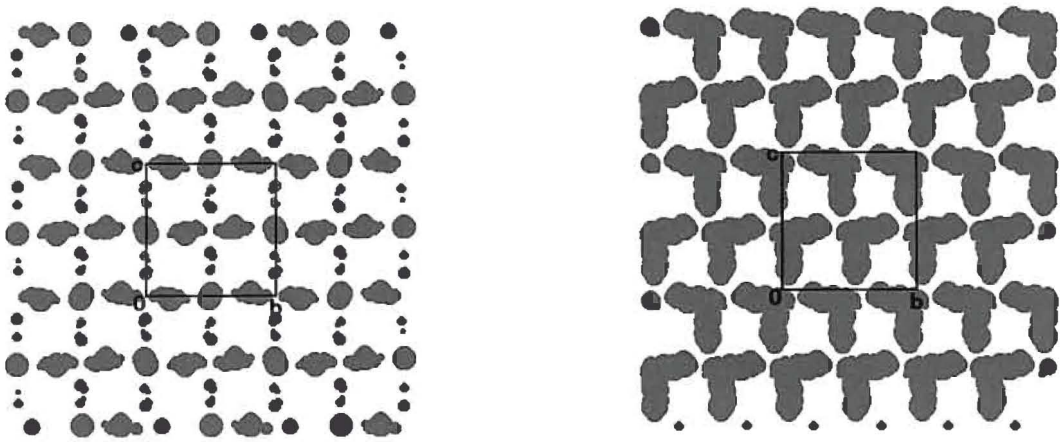

Figure 3.4.4. SECTION Plot of **T7DMF** viewed down [100], sectioned at (a) x =½ and (b) x = ¾.

Hydrogen bonding occurs between the hydroxyl groups of the host molecules and the oxygen of the guest. As observed in previous structures each host is hydrogen bonded to two guest molecules.

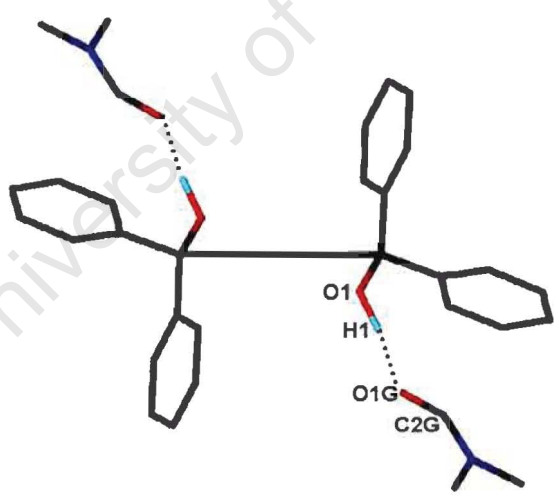

Figure 3.4.5. Hydrogen bonding in **T7DMF**.

Table 3.4.2. Hydrogen bonding details of **T7DMF**.

Donor (D)	Acceptor (A)	D—H / Å	D•••A / Å	D—H•••A / °
O1	O1G[a]	1.00(2)	2.611(1)	170(1)

a : -x+½, y+½, z

University of Cape Town

Thermal Analysis

The DSC curve shows a single endotherm (T_{on} = 105.0°C). Observation of the crystal under the hot stage microscope verified that the complex desolvated and the host melted in the hot guest.

The TG shows a single mass loss step (calculated mass loss: 26.1%, observed mass loss: 26.2%) which is consistent with the host to guest ratio of 1:2.

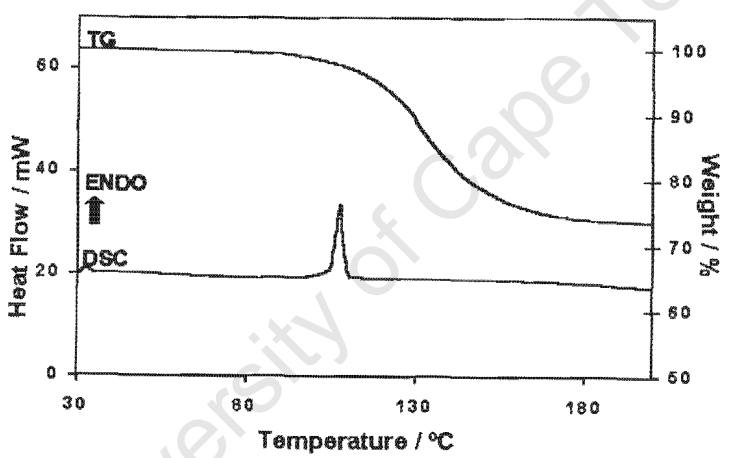

Figure 3.4.6. TG and DSC curves for **T7DMF**.

University of Cape Town

Hot stage Microscopy

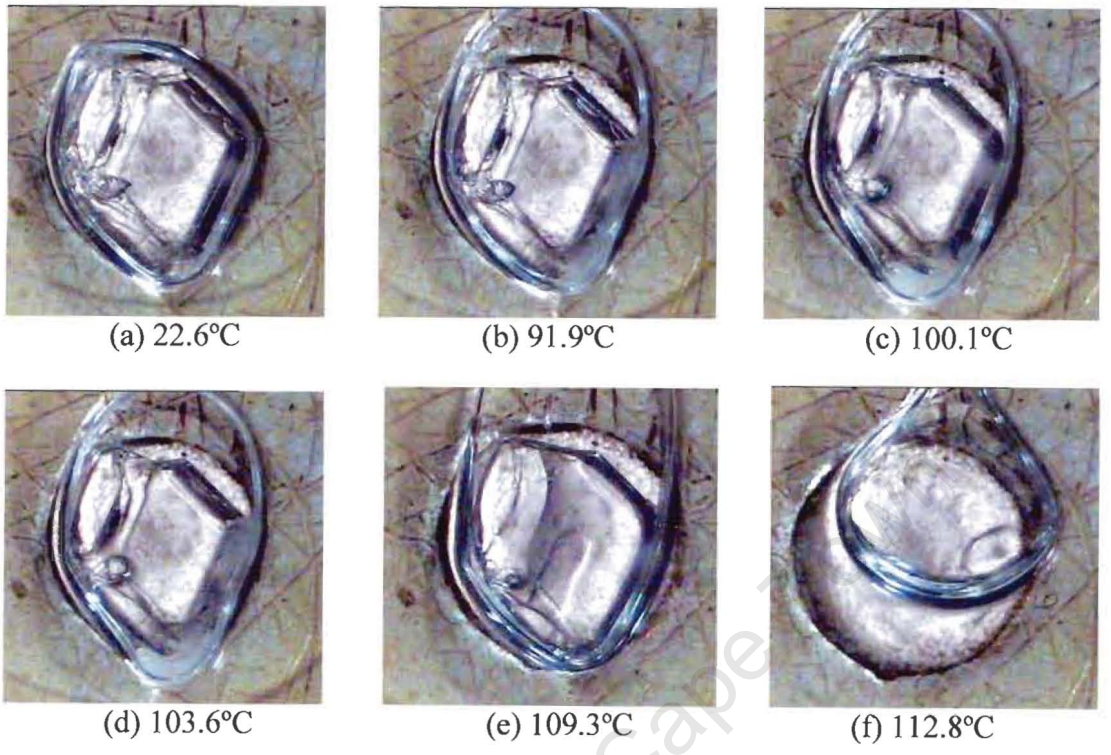

(a) 22.6°C (b) 91.9°C (c) 100.1°C

(d) 103.6°C (e) 109.3°C (f) 112.8°C

Figure 3.4.7. Thermal decomposition of a crystal of **T7DMF** illustrating that the host melts in the hot guest. Crystal at (a) room temperature, (b) melt starting at 91.9°C, (c), (d) and (e) melt at various stages of completion and (f) total melt has occurred by 112.8°C.

University of Cape Town

Kinetics of decomposition

Isothermal Thermogravimetry

A series of isothermal runs were carried out on crushed crystals of **T7DMF** over a temperature range 130-170°C at intervals of 10°C. The resulting α - time curves were deceleratory. After fitting the data to all the relevant deceleratory kinetic models the best fit curve was obtained with the three-dimensional diffusion controlled model, D3: $[1-(1-\alpha)^{1/3}]^2 = kt$ over the α range 0-0.96. The resultant Arrhenius plot is shown in Figure 3.4.8. An activation energy of 49(5) $kJmol^{-1}$ was obtained.

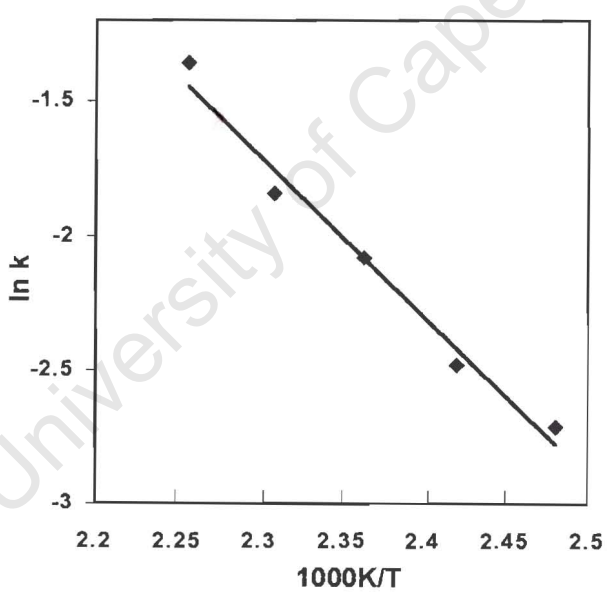

Figure 3.4.8. Plot of ln k versus 1/T for **T7DMF**.

University of Cape Town

T7DMSO

$C_{30}H_{22}O_2 \cdot 2C_3H_7NO$
Guest : dimethyl sulfoxide
Space Group : Pbca

a = 11.373(2)Å	α = 90°
b = 15.961(3)Å	β = 90°
c = 16.142(3)Å	γ = 90°

Volume = 2944(1)Å^3
Z = 4

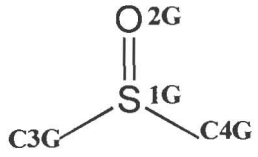

Crystal Structure and Refinement

A host:guest ratio of 1:2 was established by TG and this was confirmed by the crystal structure. The centrosymmetric space group Pbca was assigned as for the **T7DMF** structure. This was vindicated by the successful solution of the crystal structure in this space group. Once again, the host was situated on a centre of inversion (Wyckoff position a) with the guest molecules in general positions.

All the non-hydrogen atoms of the host and the guest were obtained by direct methods. All the non-hydrogen atoms of the host and the guest were refined anisotropically. The hydroxyl hydrogens were located in the difference electron density maps, and were refined isotropically. The hydroxyl hydrogens were then placed in geometrically calculated positions based on the O—H distance as a function of the O•••O distance[1]. All the non-hydrogen atoms of the guest refined with acceptable temperature factors: U_{eq}(S1G) = 0.05Å^2, U_{eq}(O2G) = 0.05Å^2, U_{eq}(C3G) = 0.13Å^2 and U_{eq}(C4G) = 0.08Å^2. The average U_{eq} value for the host atoms was 0.03Å^2. All the bond lengths and angles of the host molecule were consistent with known values[2]. At the end of the refinement the following bond lengths were obtained for the guest molecule: S1G—O2G = 1.487(4)Å,

University of Cape Town

S1G—C3G = 1.790(9)Å and S1G—C4G = 1.754(8)Å. The bond angles for the guest were (O2G—S1G—C3G = 104.8(4)°, O2G—S1G—C4G = 108.8(4)° and C4G—S1G—C3G = 94.2(5)°.

Crystal Packing

The host molecules adopt the trans conformation. Each unit cell contains four host molecules and eight guest molecules. Hydrogen bonding occurs between the hydroxyl groups of the host molecules and the oxygen and sulphur atoms of the guest. When viewed down [010] the host molecules pack in a zig-zag pattern with the bulky phenyl groups acting as spacers between the layers of host molecules. The guest molecules alternate between the phenyl groups of the host and lie in channels parallel to [100]. The channels vary in size from approximately 4.6Å × 5.3Å to 6.1Å × 5.0Å. This type of inclusion compound is referred to as tubulate.

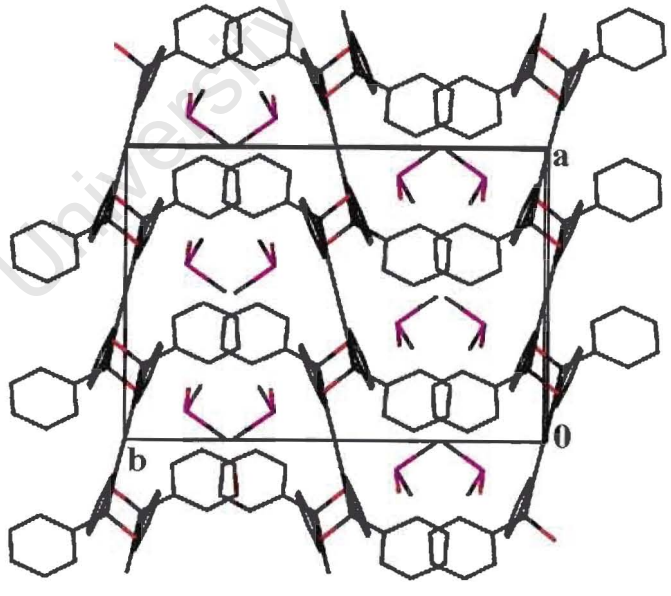

Figure 3.4.9. Packing diagram of **T7DMSO** down [001].

University of Cape Town

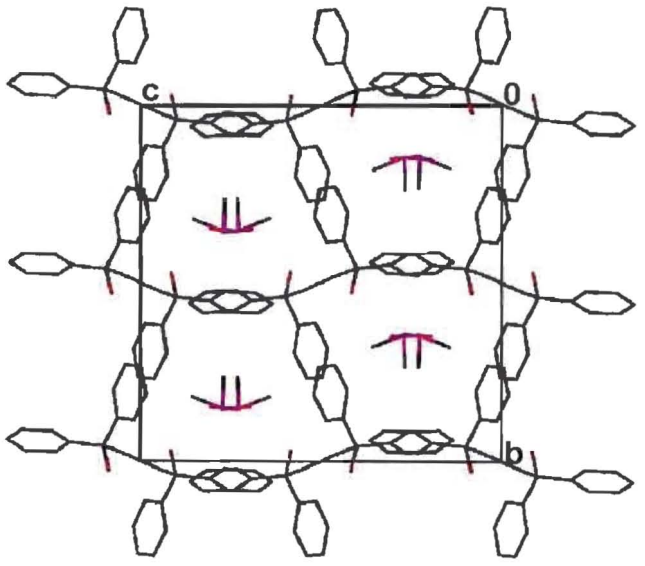

Figure 3.4.10. Crystal packing of **T7DMSO** down [100].

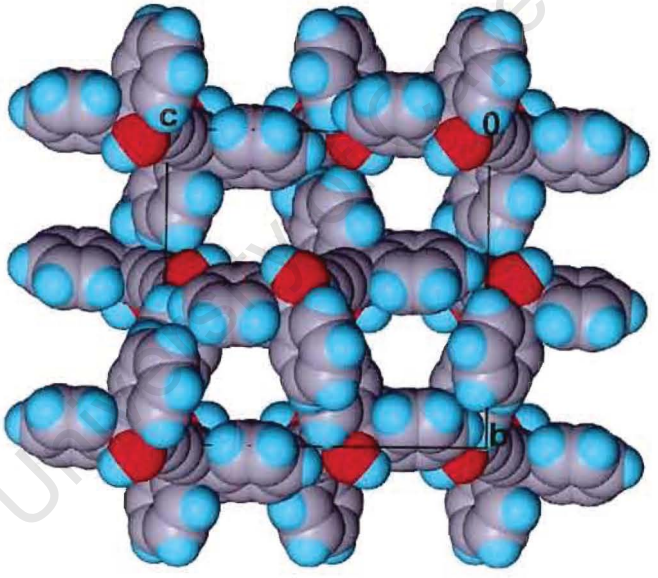

Figure 3.4.11. Packing diagram viewed down [100] with the atoms represented with van der Waals radii. Guests were omitted to show the channels occupied by them.

University of Cape Town

(a) (b)

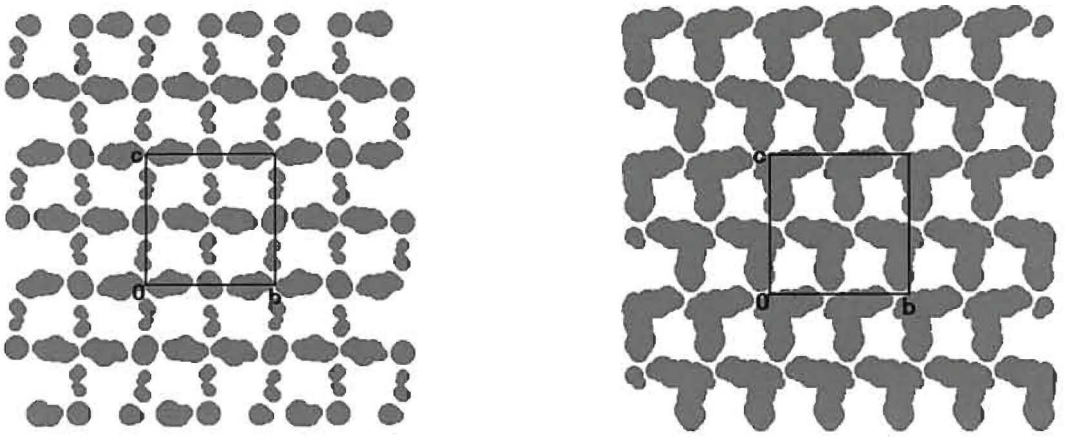

Figure 3.4.12. SECTION plot of **T7DMSO** viewed down [100] sectioned at (a) x = ½ and (b) x = ¾.

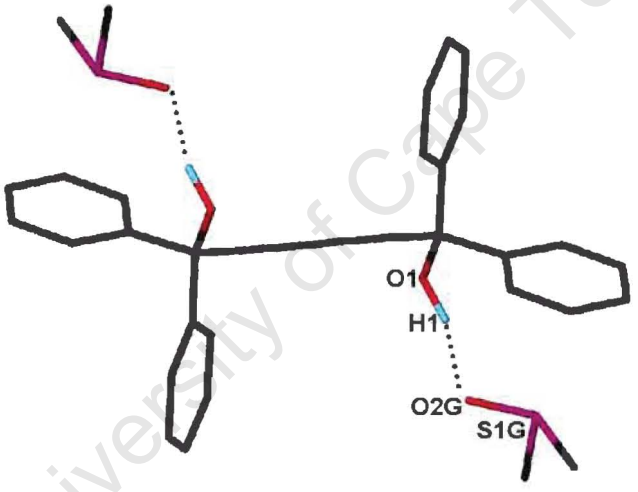

Figure 3.4.13. Hydrogen bonding in **T7DMSO**.

University of Cape Town

Table 3.4.3. Hydrogen bonding details of **T7DMSO.**

Donor (D)	Acceptor (A)	D—H / Å	D•••A / Å	D—H•••A / °
O1	O2G[a]	0.98(1)	2.676(1)	161(2)

a : x+½, y, -z+½

Thermal Analysis

The DSC curve shows a single endotherm (T_{on} = 171.8°C) which is associated with the dissolution of the host in the released guest and includes desolvation.

The TG shows a single mass loss step (expected mass loss: 27.4%, observed mass loss: 28.0%).

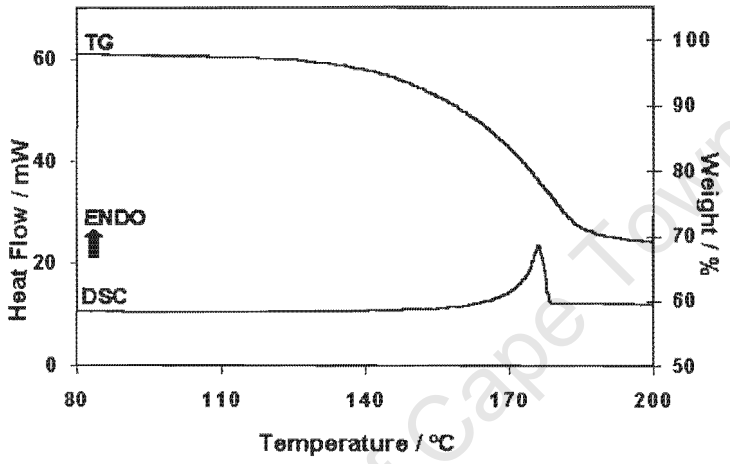

Figure 3.4.14. TG and DSC curves for **T7DMSO**.

Kinetics

Isothermal and non-isothermal methods were used to determine the kinetics of desolvation.

Isothermal thermogravimetry

Samples of **T7DMSO** obtained by crushing crystals of the bulk material were subjected to a succession of isothermal runs over a temperature range of 140-160°C at intervals of 2-3°C. The resulting α - time curves best fitted the deceleratory first order kinetic model, F1: $-\ln(1-\alpha) = kt$ over the α range 0-0.95. The resultant Arrhenius plot, Figure 3.4.15, revealed an activation energy of 106(2) $kJmol^{-1}$.

University of Cape Town

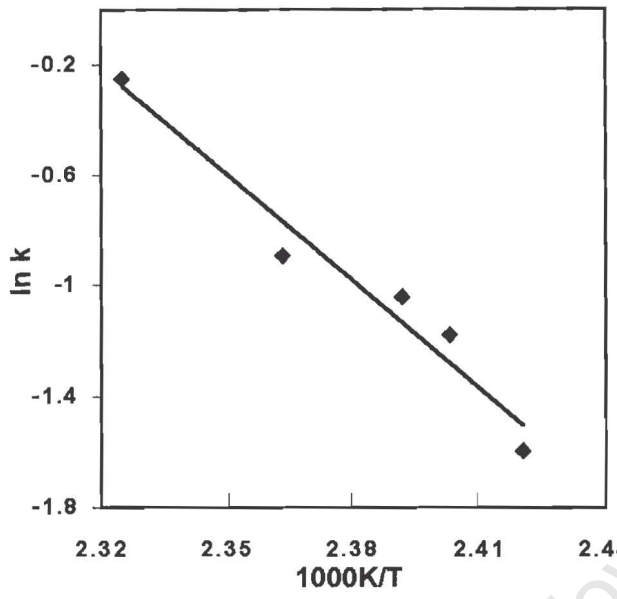

Figure 3.4.15. Plot of ln k vs 1/T for **T7DMSO**.

Non-isothermal kinetics

A series of TG runs over a temperature range of 80-200°C were performed at heating rates 1, 2, 5, and 10°Cmin^{-1}. The TG curves were analysed at different stages of decomposition ranging from 7.5% to 20% and converted into plots of -log β vs 1/T. The activation energy was calculated in the range 89(10) kJmol^{-1} to 109(9) kJmol^{-1}.

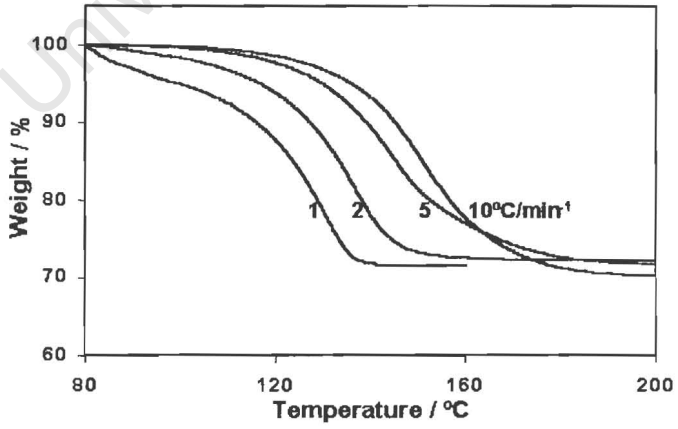

Figure 3.4.16. TG curves indicating the desolvation of **T7DMSO** over the temperature range 80 to 200°C at heating rates 1, 2, 5 and 10°C min^{-1}.

University of Cape Town

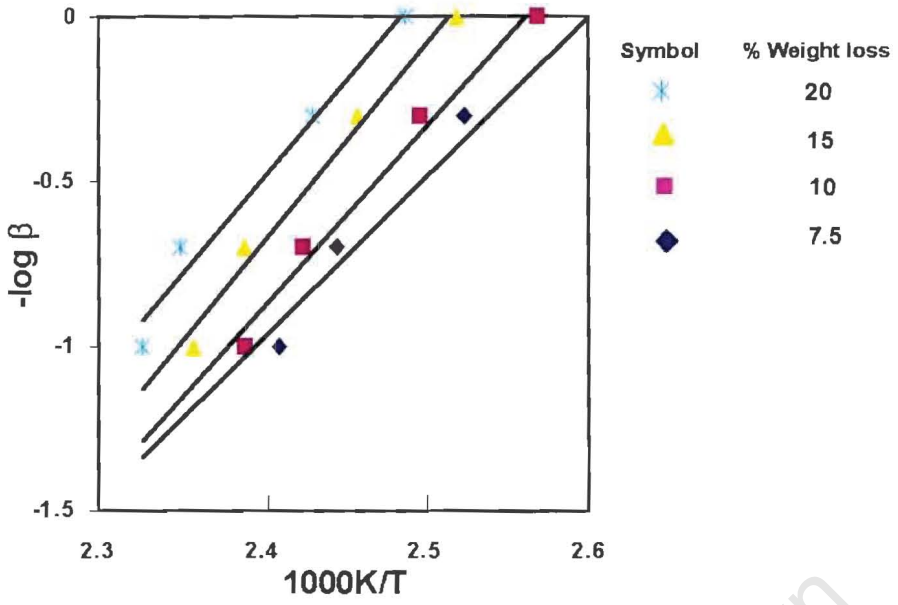

Figure 3.4.17. Plot of –log β vs 1/T for **T7DMSO**.

Competition Experiments

Two point competition experiments were carried out on the dimethylformamide and dimethyl sulfoxide system. The resultant plot is shown below in Figure 3.4.18.

The results clearly show that **TOD7** preferentially includes DMSO when the mole fraction of DMSO exceeds 0.2.

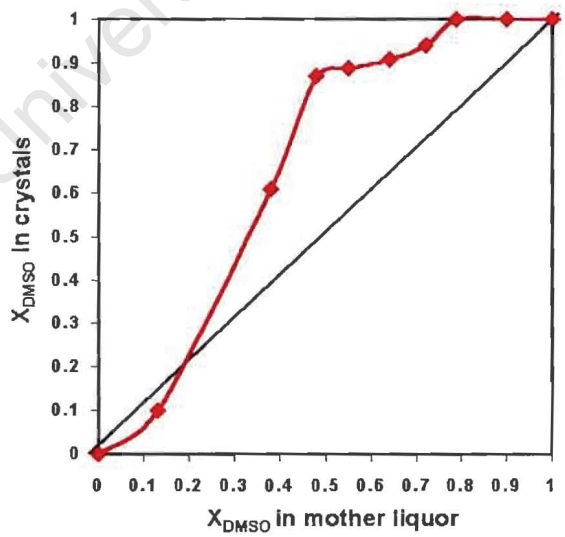

Figure 3.4.18. Results of the competition experiments between **TOD7** and guests DMF and DMSO.

University of Cape Town

Exchange Reactions

Exchange reactions between DMF and DMSO were performed as described in Chapter 2. Crystals of **T7DMF** were crushed and exposed to the vapour of DMSO in a closed vessel as illustrated in Figure 3.4.19. The overall exchange reaction can be described by the following equation:

$$\mathbf{TOD7{\bullet}2DMF}_{(s)} + 2DMSO_{(g)} \rightarrow \mathbf{TOD7{\bullet}DMSO}_{(s)} + 2DMF\uparrow$$

The DSC traces for the complexes are different and thus the reaction was monitored by DSC over a period of approximately 4 days. The results can be seen in Figure 3.4.20. The reaction is complete after 88 hrs and 30 minutes when only **T7DMSO** is present.

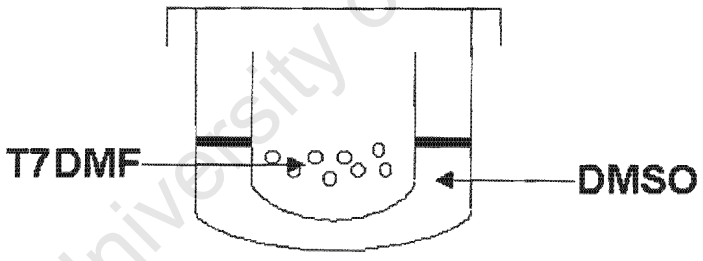

Figure 3.4.19. Schematic representation of the exchange experiment.

University of Cape Town

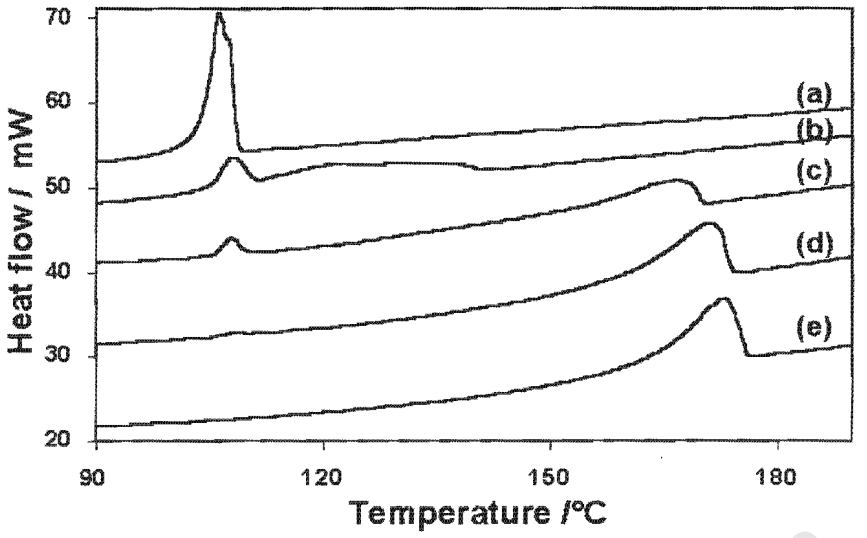

Figure 3.4.20. DSC results of the exchange reaction represented by:

TOD7•2DMF$_{(s)}$ + 2DMSO$_{(g)}$ → **TOD7•DMSO**$_{(s)}$ + 2DMF↑, after (a) 0 min, (b) 22 hrs, (c) 40 hrs, (d) 65 hrs, (e) 88 hrs 30 min.

Potential Energy Calculations

The program HEENY was used to calculate lattice energies. Once again, as described in Chapter 3.2, the results can be normalised by dividing the lattice energy by the molecular weights of the respective complexes. The results are tabulated below.

University of Cape Town

Table 3.4.4. Summary of lattice energy results.

Compound	Lattice Energy(LE) / kJmol^{-1}	LE / M_W (kJg^{-1})
T7DMF	-281.0	-0.501
T7DMSO	-399.5	-0.700

Discussion

Both **T7DMF** and **T7DMSO** crystallize in the space group Pbca with similar unit cell parameters and fractional co-ordinates. Their host frameworks are nearly isostructural; subtle variations occur due to the difference in the geometry and chemical composition of the guest molecules. When viewing the structures down [100] a difference in the degree of overlap of phenyl groups is observed.

In both structures hydrogen bonding occurs between the host and the guest molecules. In **T7DMF** and in **T7DMSO** the hydroxyl groups of the host are hydrogen bonded to the oxygen of the guest. In each case every host molecule is hydrogen bonded to two guest molecules.

Table 3.4.5. Summary of thermal analysis data for the above two structures.

Inclusion compound		**T7DMF**	**T7DMSO**
H : G ratio		1 : 2	1: 2
TG results	Calc. % mass loss	26.1	27.4
	Exp. % mass loss	26.2	28.0
DSC results	T_{on} (°C) :	105.0	171.8
Normal boiling points, T_b (°C)		153.0	189.0
T_{on}/T_b		0.686	0.909

The activation energy for the desolvation reaction of **T7DMF** (49(5) $kJmol^{-1}$) is considerably lower than that of **T7DMSO** (106(2) $kJmol^{-1}$). As described in Chapter 3.1, T_{on}/T_b is a good indicator of the stability of a compound. The higher value of 0.909 obtained for **T7DMSO** signifies its greater stability. The competition experiments favour the inclusion of DMSO. Lattice energy calculations also favour **T7DMSO** as the more stable structure.

University of Cape Town

The following guest exchange reaction was studied:

$$\textbf{TOD7•2DMF}_{(s)} + 2DMSO_{(g)} \rightarrow \textbf{TOD7•DMSO}_{(s)} + 2DMF\uparrow$$

The near isotructurality of the host frameworks of **T7DMF** and **T7DMSO**, the location of the guests in channels and the more negative lattice energy of **T7DMSO** rendered the guest exchange reaction successful.

University of Cape Town

References

1. I. Olovsson and P. Jönsson, *The Hydrogen Bond* – Structure and Spectroscopy, P.Schuster, G. Zundel and C. Sardefy (eds.), North-Holland Publishing Company, USA, 1975.

2. International Tables For Crystallography, Vol. C, (ed.) A.J.C. Wilson, Kluwer Academic Publishers, Dordrecht, pp.691, 1992.

University of Cape Town

CHAPTER 3.5 INCLUSION OF ANILINE AND NITROANILINES

Inclusion compounds were formed between the host, **TOD7**, and the guests aniline, o-nitroaniline (o-na) and m-nitroaniline (m-na). All attempts to form an inclusion compound between **TOD7** and p-nitroaniline (p-na) failed and on each occasion they crystallised as separate compounds. Crystal structures for **T7ANI**, **T7ONA** and **T7MNA** have been solved and these will be discussed. Unlike aniline, the isomers of nitroaniline are solids at room temperature and the crystals of **T7ONA** and **T7MNA** were grown from a 2:1(vol/vol) mixture of diethyl ether: n-hexane. Solid state reactions between the solid guests and the host have been studied.

University of Cape Town

Table 3.5.1 Crystal data, experimental and refinement parameters

	T7ANI	**T7ONA**	**T7MNA**
Compound	$C_{30}H_{22}O_2 \cdot 2C_6H_7N$	$C_{30}H_{22}O_2 \cdot 2C_6H_6N_2O_2$	$C_{30}H_{22}O_2 \cdot 2C_6H_6N_2O_2 \cdot C_{1.5}H_3$
M_w , $gmol^{-1}$	600.73	690.73	711.75
Temperature / K	173(2)	170(2)	298(2)
Crystal system	triclinic	triclinic	triclinic
Space group	$P\bar{1}$	$P\bar{1}$	$P\bar{1}$
a, Å	5.853(1)	8.373(2)	8.314(2)
b, Å	12.201(2)	10.433(2)	10.689(2)
c, Å	12.583(1)	11.397(2)	12.579(3)
α, °	67.220(2)	112.13(3)	101.04(3)
β, °	88.615(3)	105.17(3)	108.50(3)
γ, °	81.568(4)	96.84(3)	91.08(3)
V, $Å^3$	819.0(2)	863.3(3)	1036.7(4)
Z	1	1	1
Absorption coefficient, mm^{-1}	0.074	0.090	0.077
F(000)	318	362	371
Crystal size, mm	0.23 × 0.20 × 0.15	0.35 × 0.40 × 0.35	0.45 × 0.45 × 0.37
Index ranges	h: -7, 6; k: -15, 14; l: ±15	h: ±10; k: -8, 13; l: -14, 13	h: -10, 8; k: -13, 8; l: -14, 13
Reflections collected /unique	5693 / 3498	4035 / 2959	4993 / 3885
Data/ restraints/ Parameters	3498 / 2 / 212	2959 / 2 / 248	3885 / 2 / 240
Goodness-of-fit	0.907	1.048	1.035
ρ_{calc}, $g \cdot cm^{-3}$	1.218	1.329	1.135
Final R indices [$I > 2\sigma(I)$]	$R_1 = 0.0459, wR_2 = 0.1156$	$R_1 = 0.0459, wR_2 = 0.1101$	$R_1 = 0.0838, wR_2 = 0.2339$
R indices (all data)	$R_1 = 0.0698, wR_2 = 0.1327$	$R_1 = 0.0585, wR_2 = 0.1191$	$R_1 = 0.1240, wR_2 = 0.2687$
Largest difference peak and hole, $eÅ^{-3}$	0.413 and –0.288	0.270 and -0.196	0.457 and -0.328

University of Cape Town

T7ANI

$C_{30}H_{22}O_2 \cdot 2C_6H_7N$		
Guest : aniline		
Space Group : $P\bar{1}$		
a = 5.853(1)Å	α = 67.220(2)°	
b = 12.201(2)Å	β = 88.615(3)°	
c = 12.583(1)Å	γ = 81.568(4)°	
Volume = 819.0(2)Å^3		
Z = 1		

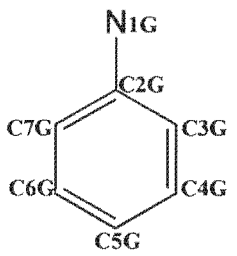

Crystal Structure and Refinement

Preliminary oscillation and Weissenberg photography indicated that **T7ANI** belonged to the triclinic system. A host: guest ratio of 1:2 was established by TG and confirmed by the crystal structure. The centrosymmetric space group $P\bar{1}$ was assigned. The host was located on a centre of inversion at Wyckoff position c, with the guest atoms in general positions. All the non-hydrogen atoms of the host and the guest were obtained by direct methods and refined anisotropically. The hydroxyl hydrogen was located in the difference electron density maps, refined isotropically and then placed in geometrically calculated positions[1]. The amine hydrogens of the guest were also found in the difference electron density maps and allowed to refine isotropically. All bond lengths and angles fall within the accepted ranges [2] and will be discussed further in Chapter 5.

Crystal Packing

Once again the acetylenic spacers of the host lie in layers parallel to [100] with the bulky phenyl groups creating voids which are occupied by guest molecules. The guests lie in channels parallel to [100]. The size of the channels varies in size from 5.2Å × 9.2Å to 5.2Å × 14.4Å.

University of Cape Town

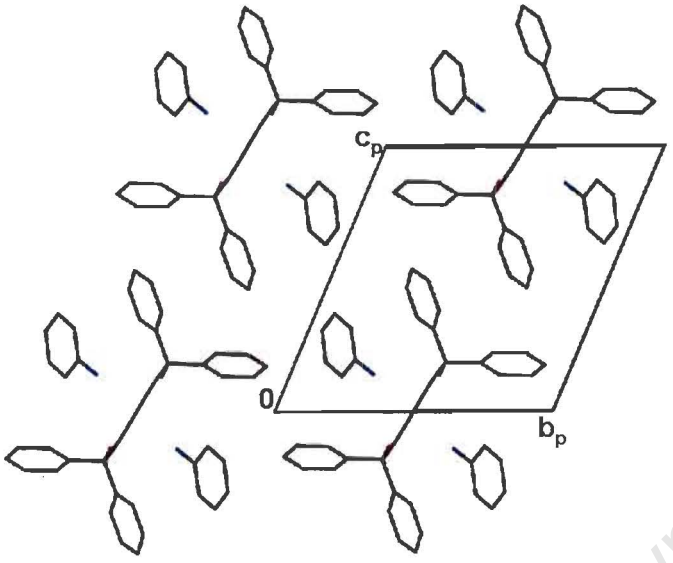

Figure 3.5.1.Crystal packing of **T7ANI** down [100].

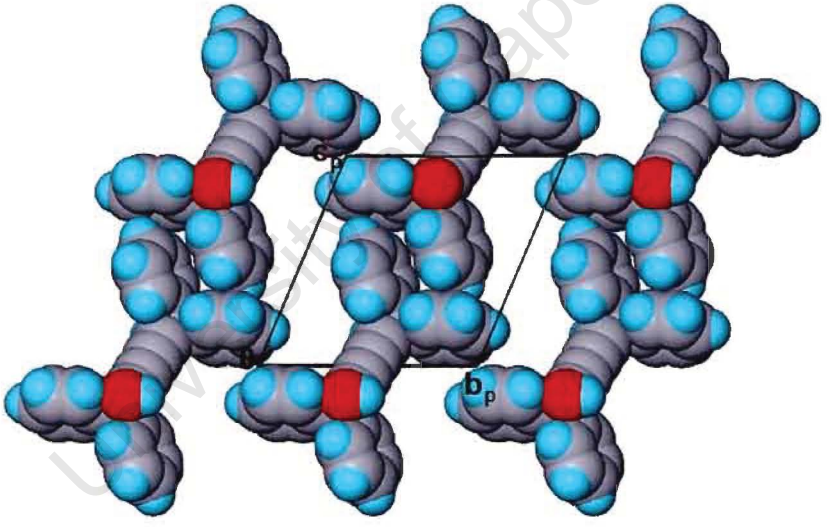

Figure 3.5.2. Space-filling diagram of **T7ANI** down [100] with guests omitted.

Hydrogen bonding occurs between the hydroxyl groups of the host and the nitrogen of the guest. Each host is hydrogen bonded to two guest molecules. This is illustrated in Figure 3.5.3. The resultant geometry of bonds around N1G is pyramidal.

University of Cape Town

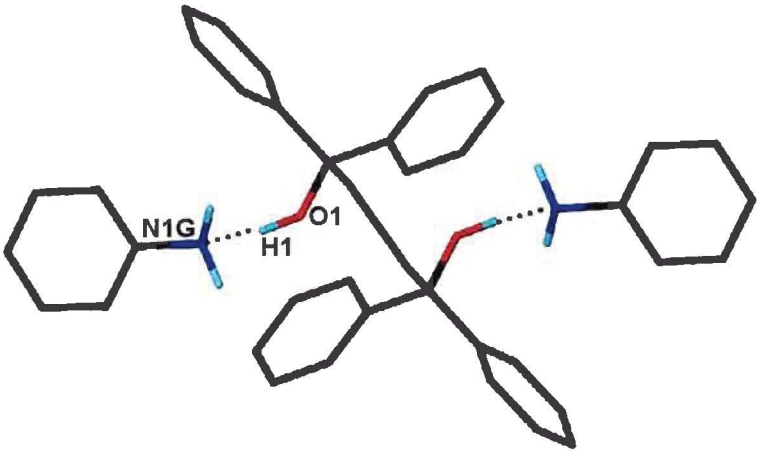

Figure 3.5.3. Hydrogen bonding in **T7ANI**.

Table 3.5.2. Hydrogen bonding details of **T7ANI**.

Donor (D)	Acceptor (A)	D–H / Å	D· · A / Å	D-H· · A / °
O1	N1G[a]	0.97(1)	2.889(2)	162(2)

a: -x+1, -y+1, -z

Thermal Analysis

The DSC shows a single endotherm (T_{on} = 88.8°C) which corresponds to the desolvation of the complex and the melt of the host in the released guest. The TG shows a mass loss of 30.8% (calculated:31.0%) which is consistent with the host to guest ratio of 1:2.

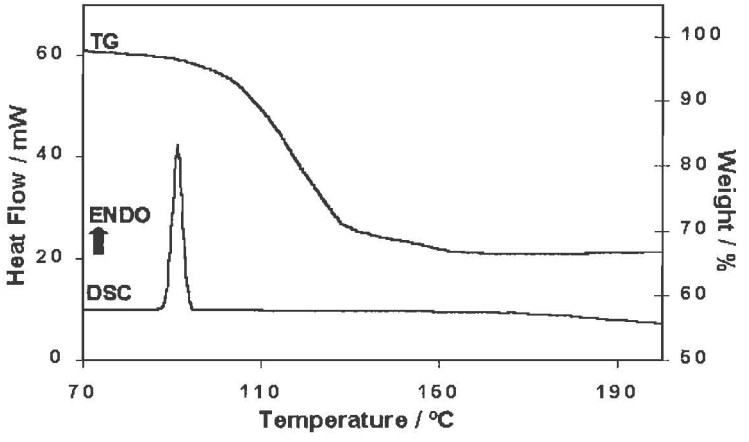

Figure 3.5.4. TG and DSC curves for **T7ANI**.

University of Cape Town

T7ONA

$C_{30}H_{22}O_2 \cdot 2C_6H_6N_2O_2$
Guest : o-nitroaniline
Space Group : $P\bar{1}$
a = 8.373(2) Å α = 112.13(3)°
b =10.433(2)Å β = 105.17(3)°
c = 11.397(2)Å γ = 96.84(3)°
Volume = 863.3(3)Å^3
Z = 1

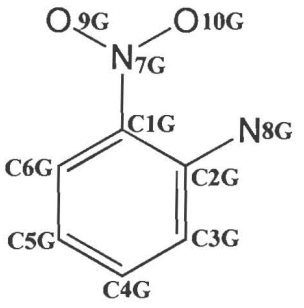

Crystal Structure and Refinement

The triclinic space group $P\bar{1}$ was assigned. A host:guest ratio of 1:2 was established by microanalysis (exptl: %C 72.4, %H 4.8, %N 8.0; calc: %C 73.0, %H 5.0, %N 8.1) and this was confirmed by the crystal structure. Again, the host was located on a centre of inversion (Wyckoff position f), with the guest atoms in general positions. All the non-hydrogen atoms were refined with anisotropic temperature factors. All the hydrogens were found in the electron density maps. The amine hydrogens of the guest were left to refine isotropically. The hydroxyl hydrogen of the host was refined isotropically and secured with bond length restraints[1]. Typical bond lengths and angles were obtained for both the host and the guest[2].

University of Cape Town

Crystal Packing

The host molecules pack in a zigzag pattern when viewed along [100]. The guest molecules are situated in channels parallel to [100]. The channels vary in size from 3.8Å × 7.2Å at the narrowest sections to 7.6Å × 8.0Å at the widest sections.

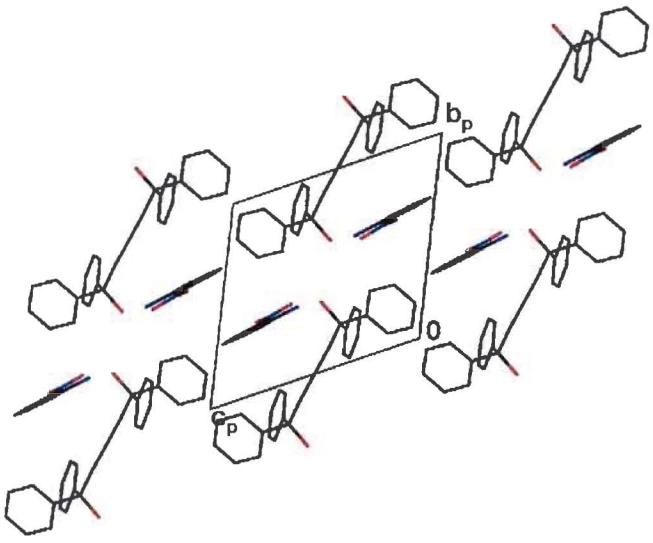

Figure 3.5.5. Crystal packing of **T7ONA** down [100].

A three-centre hydrogen bond exists between the host and the guest molecules. This is illustrated in Figure 3.5.6. Intramolecular hydrogen bonding occurs between the amino hydrogen atom and the nitro group of the guest. Intermolecular hydrogen bonding occurs between the hydroxyl hydrogen atoms of the host and the nitro group of the guest.

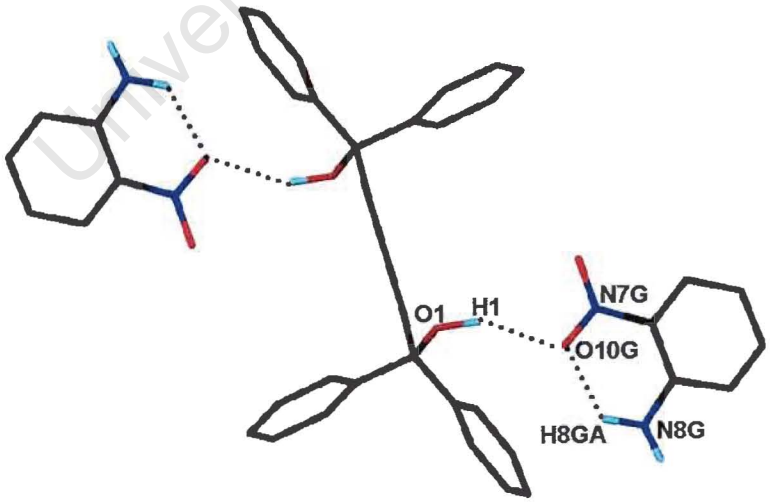

Figure 3.5.6. Hydrogen bonding in **T7ONA**.

University of Cape Town

Also, π—π interactions were observed between guest molecules. In Figure 3.5.7 the two guest molecules are labelled as rings I and J. The distance between the ring centroids (Cg(I) for ring I and Cg(J) for ring J) of the two guest molecules is 3.753Å. The perpendicular distance of Cg(I) onto ring J or alternately, the perpendicular distance of Cg(J) onto ring I is 3.363Å. These distances agree with known values for this type of interaction[3].

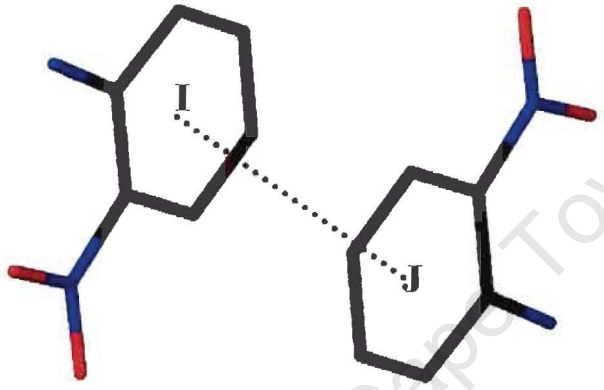

Figure 3.5.7. π—π interactions between two guest molecules.

University of Cape Town

Table 3.5.3. Hydrogen bonding details of **T7ONA**.

Donor (D)	**Acceptor (A)**	**D—H / Å**	**D•••A / Å**	**D—H•••A / °**
O1	O10G	0.97(2)	2.991(1)	154(4)
N8G	O10G	0.920(1)	2.642(1)	128(5)

Thermal Analysis

No mass loss was observed in the TG. Decomposition started after approximately 130°C.

The DSC curve shows one endotherm (T_{on}= 103.9°C) which corresponds to the melt of the complex. This was confirmed by hot stage microscopy.

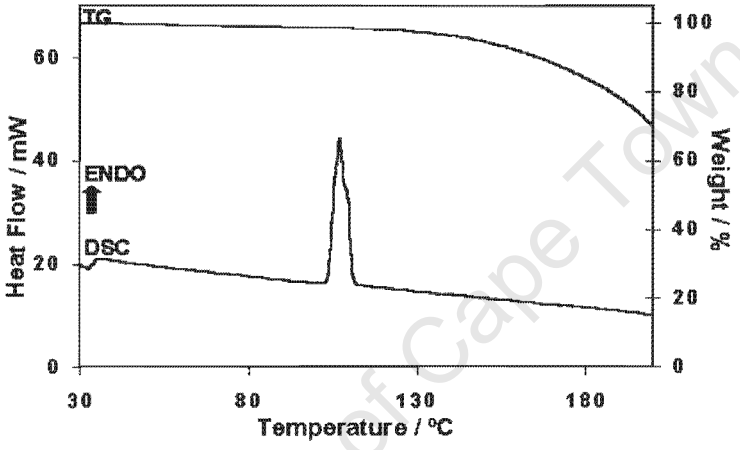

Figure 3.5.8. TG and DSC curves for **T7ONA**.

University of Cape Town

Hot stage Microscopy

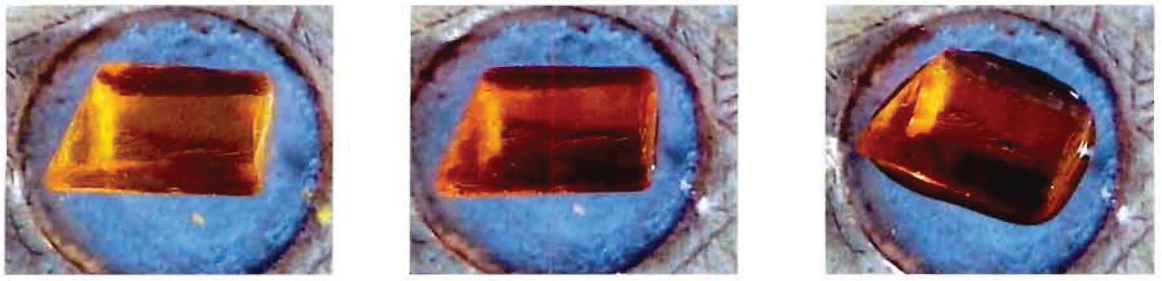

(a) 24.5°C (b) 111.4°C (c) 112.8°C

(d) 114.0°C (e) 116.0°C (f) 117.7°C

Figure 3.5.9. Thermal decay of a crystal of **T7ONA** at (a) room temperature , (c) melt is visible at 112.8°C, (d), (e) different stages of the melt at 114.0°C and 116.0°C and (f) total melt complete at 117.7°C.

University of Cape Town

T7MNA

$C_{30}H_{22}O_2 \cdot 2C_6H_6N_2O_2 \cdot C_{1.5}H_3$
Guest : m-nitroaniline
Space Group : $P\bar{1}$
a = 8.314(2)Å α = 101.04(3)°
b =10.689(2)Å β = 108.50(3)°
c = 12.579(2)Å γ = 91.08(3)°
Volume = 1036.7(4)Å^3
Z = 1

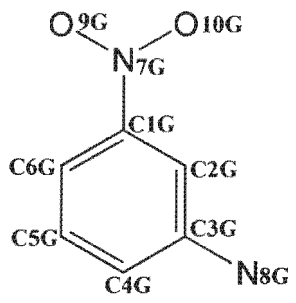

Crystal Structure and Refinement

The structure was solved in the centrosymmetric triclinic space group $P\bar{1}$. As was observed in the previous structure the host was located on a centre of symmetry, with the guest, m-na (referred to as guest A) in general positions. All the non-hydrogen atoms of the host and the guest were obtained by direct methods and refined anisotropically. The hydroxyl hydrogen was not located in the difference electron density maps, but a torsion angle to match the maximum electron density in the difference map was chosen. Thereafter the O—H distance was restrained to 0.97Å and the hydrogen was left to refine isotropically[1]. The amine hydrogens of m-na were not located in the electron density maps but were fixed in position with N—H distances of 0.86Å. Four residual peaks of electron density ranging from 0.81-0.86eÅ^{-3} remained after the refinement. The distances between the peaks are illustrated in Figure 3.5.10. The TG indicated that there was solvent present (a mass loss of 3.0% was observed at the start of the TG run). As the crystals were grown from a mixture of diethyl ether and n-hexane, one or both of these solvents could be present in the crystal in various percentages. The crystals could not be regrown and thus no further analysis could be done. There were no significant differences in the electron densities of the peaks and no distinction could be made between a carbon atom and an oxygen atom. The four

University of Cape Town

residual peaks were inserted as carbon atoms (later referred to as guest B). The mass loss of 3.0% in the TG was used to calculate the site occupancy factor for each of the carbon atoms of guest B. If it is assumed that one molecule of n-hexane is present in one mole of complex ie. the molecular formula for the complex is $C_{30}H_{22}O_2 \bullet 2C_6H_6N_2O_2 \bullet C_6H_{14}$, then the percentage mass loss expected in the TG would be 12.46%. Since a mass loss of 3.0% was observed in the TG, only one quarter of an n-hexane molecule is present in one mole of complex. Thus the carbon atoms of guest B were inserted with the following site occupancy factors of C5: ⅛, C6: ¼, C7: ¼ and C8: ⅛. Both C5 and C8 are situated on centres of symmetry with C5 at Wyckoff position g and C8 at Wyckoff position h. The disorder in guest B results in it appearing as a polymeric chain as is illustrated in Figure 3.5.11. These four carbon atoms; C5, C6, C7, C8 were treated isotropically. The following U_{eq} values were obtained after the final refinement: $U_{eq}(C5) = 0.15Å^2$, $U_{eq}(C6) = 0.20Å^2$, $U_{eq}(C7) = 0.18Å^2$, $U_{eq}(C8) = 0.17\ Å^2$. The average U_{eq} value for the carbon atoms of guest A was 0.06 $Å^2$. All the hydrogen atoms of guest B were omitted from the final model. The bond lengths and angles for both the host and guest A are in acceptable ranges[2] while those obtained for guest B are distorted due to the disorder.

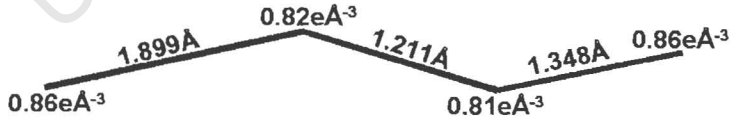

Figure 3.5.10. Electron density and bond distances in guest B.

University of Cape Town

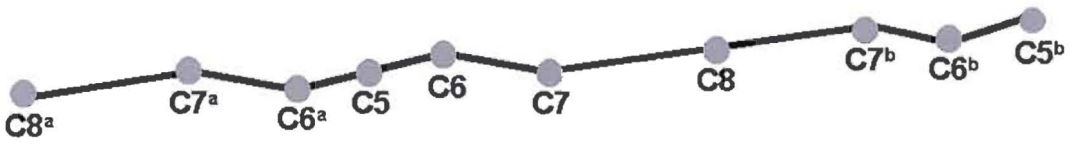

a: -x, 1-y, 1-z

b: -x-1, 1-y, 1-z

Figure 3.5.11. Disorder in guest B resulting in a polymeric chain.

Crystal Packing

The host molecules pack in a zigzag pattern when viewed along [100]. The guest molecules are situated in channels parallel to [100].

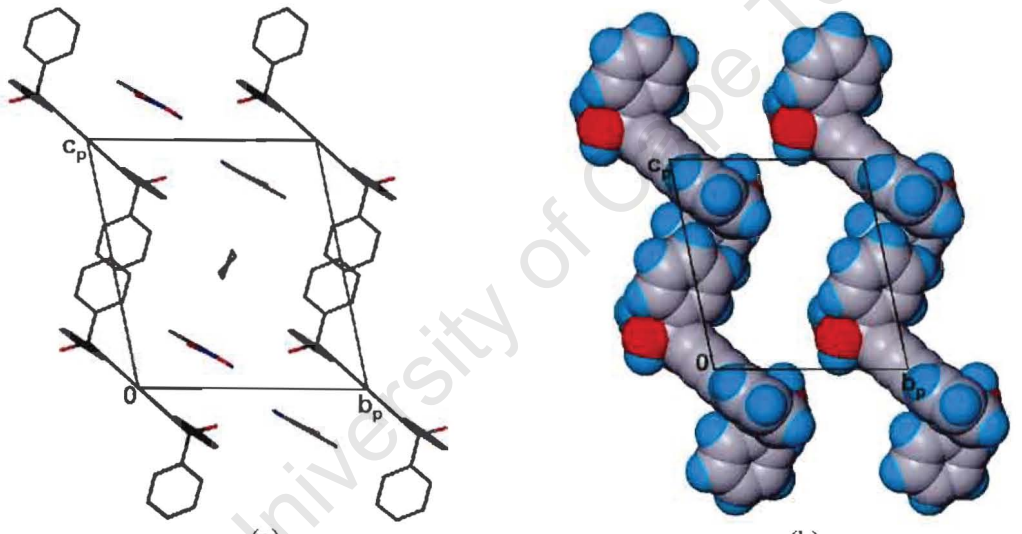

(a) (b)

Figure 3.5.12. (a) Packing diagram of **T7MNA** down [100] and (b) host molecules depicted with van der Waals radii with guest molecules omitted to illustrate the channels parallel to [100].

University of Cape Town

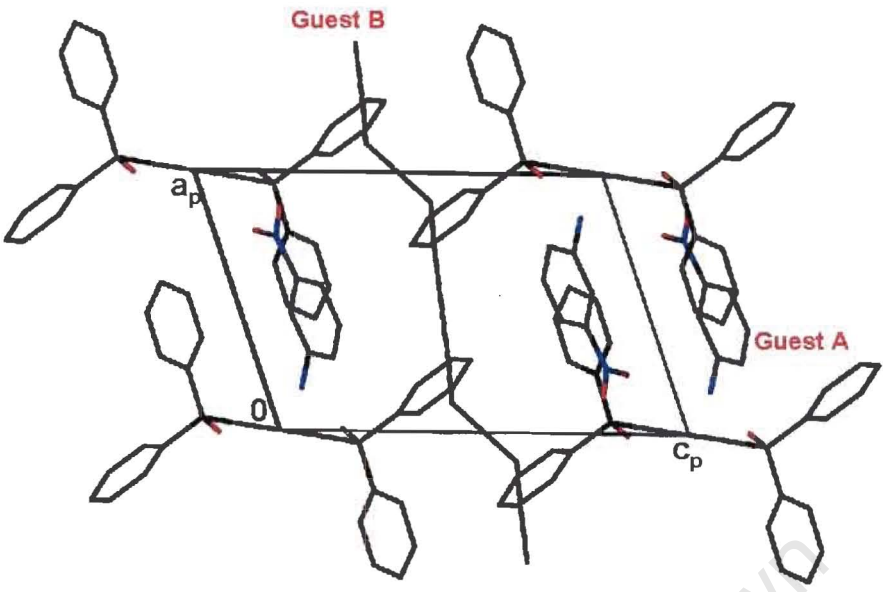

Figure 3.5.13. Packing diagram of **T7MNA** viewed down [010] indicating the guests A and B.

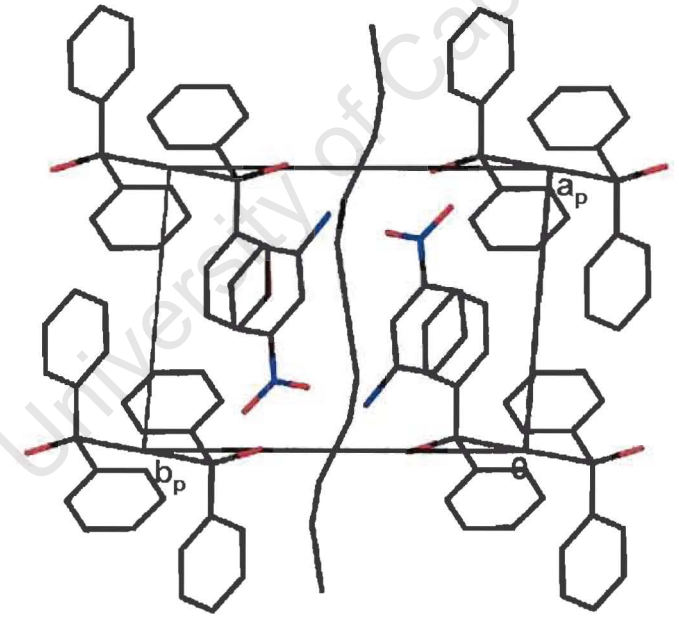

Figure 3.5.14. Crystal packing diagram of **T7MNA** viewed down [001].

University of Cape Town

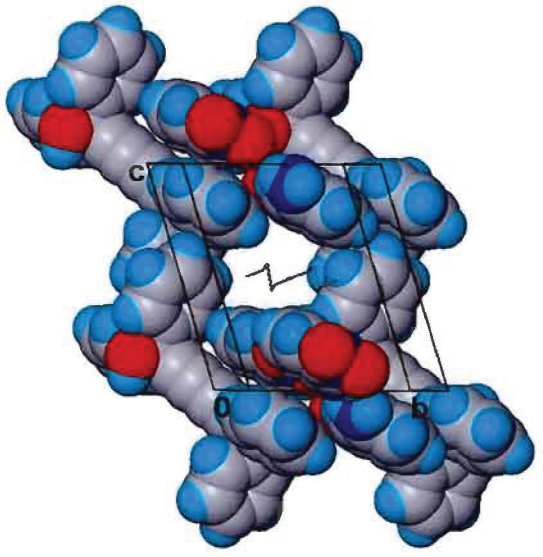

Figure 3.5.15. Packing diagram of **T7MNA**. The atoms of the host and guest A are shown in van der Waals radii and guest B is shown in stick form.

Hydrogen bonding occurs between the hydroxyl hydrogen atoms of the host and the amine hydrogen atoms of the m-na guest. Weak hydrogen bonding also occurs between the amine hydrogen atoms of m-na and the nitro group of adjacent m-na molecules. The twisted chains formed as a result of hydrogen bonding can be seen in Figure 3.5.16.

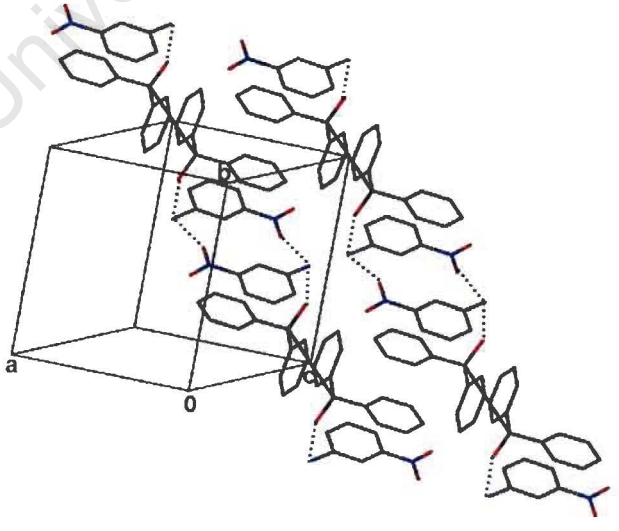

Figure 3.5.16. Diagram illustrating the hydrogen bonding in **T7MNA**. Only partial packing of the unit cell is shown and guest B has been omitted for clarity.

University of Cape Town

Table 3.5.4. Hydrogen bonding details of **T7MNA**.

Donor (D)	Acceptor (A)	D—H / Å	D•••A / Å	D—H•••A / °
O1*	N8G	0.97(1)	2.924(1)	171(3)
N8G*	O10G[c]	0.86	3.352(1)	168(2)
N8G*	O10G[d]	0.86	3.340(2)	157(2)

*: hydrogens on O1 and N8G were not found in the electron density maps but were fixed in position as described earlier.

c: x-1, y, z

d: -x+1, -y+1, -z+2

Thermal Analysis

The TG shows a mass loss of 3.0%. This mass loss corresponds to the loss of solvent (a host: n-hexane ratio of 1: ¼). The crystals of **T7MNA** were grown from a mixture of diethyl ether and petroleum ether. Unfortunately further analysis on **T7MNA** could not be carried out due to the limited amount of crystals present. All further attempts at regrowing the complex were unsuccessful. Decomposition occurs after approximately 130° C.

The DSC curve shows two endotherms which is consistent with the loss of solvent (T_{on} = 62.5° C) followed by the melt of the complex (T_{on} = 96.9° C).

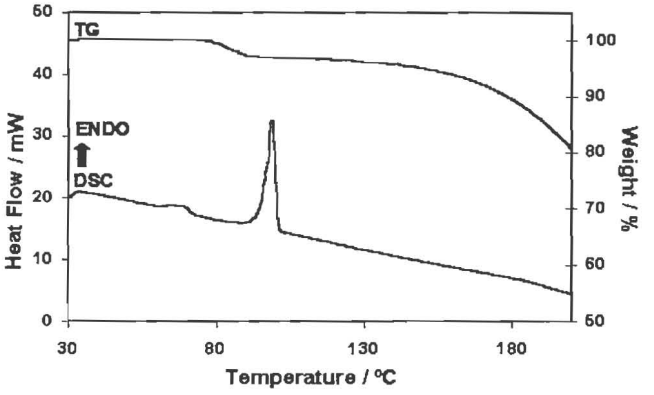

Figure 3.5.17. TG and DSC of **T7MNA**.

University of Cape Town

Solid state Experiments

Solid state experiments were performed as described in Chapter 2. Stoichiometric quantities of the host and the guest (ie. host: guest ratios of 1:2) were ground for 20 minutes at room temperature and at elevated temperatures. The elevated temperature experiments were carried out by grinding on a brass block heated on a hotplate and the temperature monitored with a thermometer. The XRD traces of the reaction products were compared with the XRD traces of the physical mixtures as well as with the calculated pattern obtained using the program LAZY PULVERIX.

TOD7 + o-na

Grinding experiments for **TOD7** and o-na were successful at 55°C. The powder XRD traces of the ground sample and the physical mixture are different. However the XRD traces of the ground sample and the calculated pattern for **T7ONA** also differ. Thus complexation had occurred but a different polymorph to the one obtained by growing crystals from solution had been formed. Also the XRD trace of the ground sample contains certain peaks from the XRD trace of the physical mixture which implies that the reaction did not go to completion. The results are illustrated in Figure 3.5.18.

University of Cape Town

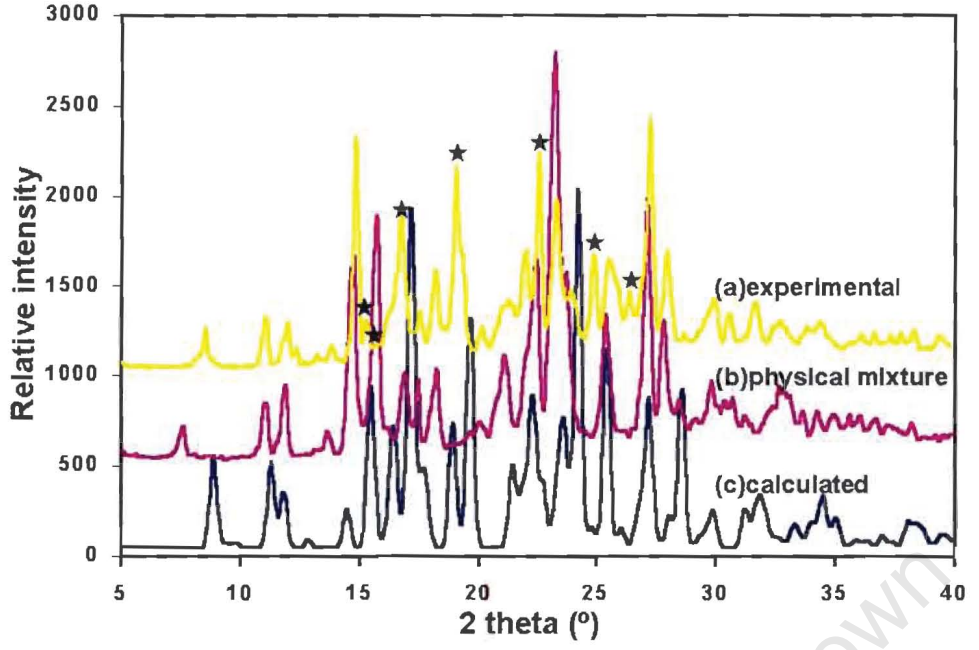

Figure 3.5.18. XRD powder patterns of (a) experimental co-ground product of **TOD7** and o-na (b) 1:2 physical mixture of **TOD7** and o-na and (c) calculated pattern of **T7ONA** using the program LAZY PULVERIX. The stars indicate the points at which (a) and (b) differ, either where a new peak is present or absent.

University of Cape Town

TOD7 + m-na

Grinding experiments succeeded at 77°C. Comparisons between the XRD traces of the ground sample and the physical mixture show that they are different. This result could not be compared to the calculated powder pattern of **T7MNA** as solvent is present in the crystal structure of **T7MNA**. Again it appears as if the reaction did not go to completion as the XRD trace of the ground sample contains some peaks of the XRD trace of the physical mixture.

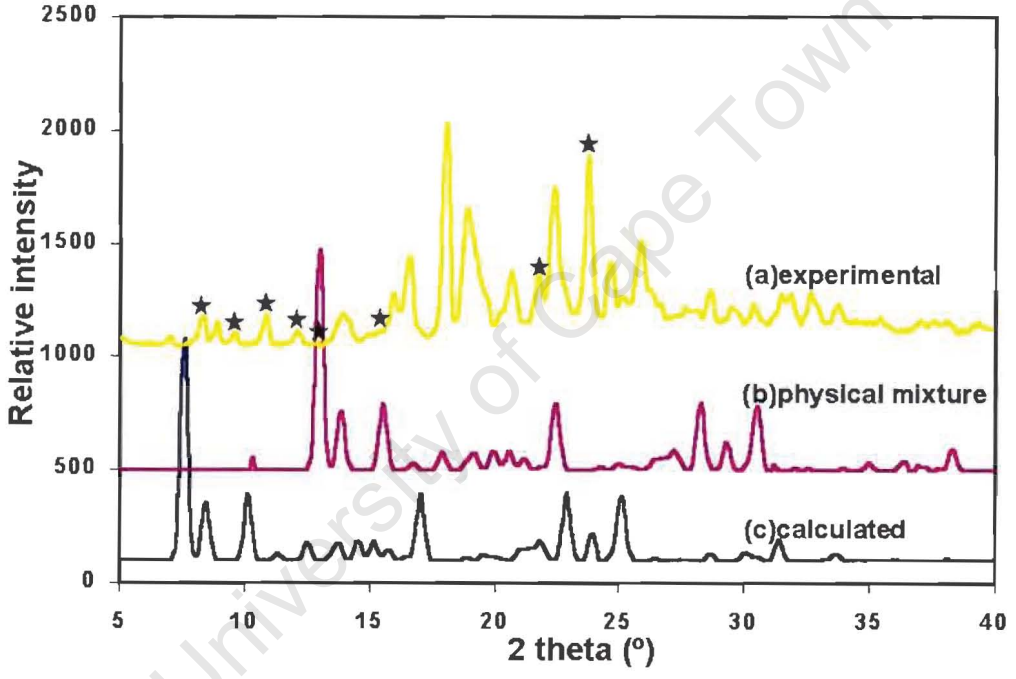

University of Cape Town

Figure 3.5.19. XRD powder patterns of (a) experimental co-ground product of **TOD7** and m-na (b) 1:2 physical mixture of **TOD7** and m-na and (c) calculated pattern of **T7MNA** using the program LAZY PULVERIX. Again, the stars indicate the points at which (a) and (b) differ.

TOD7 + p-na

Grinding experiments for **TOD7** and p-na proved unsuccessful. Co-grinding was attempted at temperatures as high as 97°C. The resultant XRD trace was similar to that of the physical mixture.

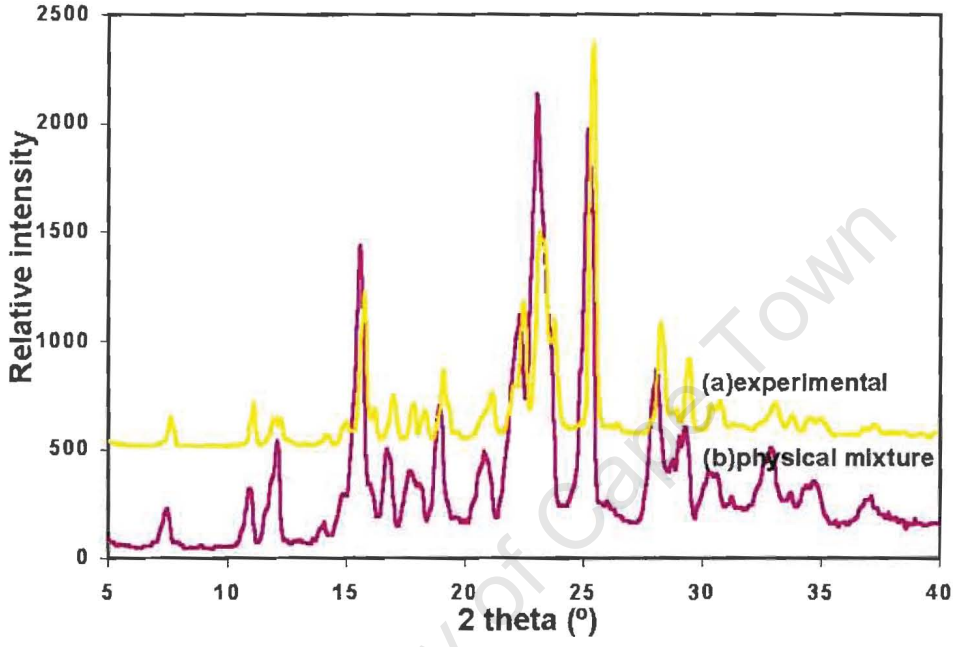

Figure 3.5.20. XRD powder patterns of (a) experimental co-ground product of **TOD7** and p-na and (b) 1:2 physical mixture of **TOD7** and p-na.

University of Cape Town

Discussion

T7ANI, T7ONA and **T7MNA** were successfully solved in the triclinic space group $P\bar{1}$. Hydrogen bonding in **T7ANI** occurs between the host and the amine hydrogens of the guest molecules. In the case of **T7ONA** the crystal structure is stabilised by hydrogen bonding between the host and the guest, intramolecular bonding within each guest molecule and π—π interactions between adjacent guest molecules. **T7MNA** is stabilised by hydrogen bonding between the host and guest, and between neighbouring guest molecules. Complexation between host, **TOD7**, and p-na proved unsuccessful and both crystallised separately. As the nitro and the amine groups of the guest move successively from the 1,2-positions in o-na to the 1,3-postions in m-na and finally to the 1,4-positions in p-na the stabilising three-centre hydrogen bond breaks down. It is this three-centre bond which appears to be the most important factor in determining the stability of each of these complexes. The greater stability of **T7ONA** is also reflected in the thermal analysis results. **T7ONA** has a higher melting point, $T_{on} = 103.9°C$, than **T7MNA** ($T_{on} = 96.9°C$).

Solid state reactions between **TOD7** and the guests, o-na and m-na resulted in complexes that were different from those obtained by crystallisation from solution. **TOD7** and o-na complexed at 55°C whereas **TOD7** and m-na complexed at a higher temperature of 77°C.

University of Cape Town

References

1. I. Olovsson and P. Jönsson, *The Hydrogen Bond* – Structure and Spectroscopy, P.Schuster, G. Zundel and C. Sardefy (eds.), North-Holland Publishing Company, USA, 1975.

2. International Tables For Crystallography, Vol. C, (ed.) A.J.C. Wilson, Kluwer Academic Publishers, Dordrecht, pp.691, 1992.

3. G.R. Desiraju and T. Steiner, *The Weak Hydrogen Bond in Structural Chemistry and Biology*, IUCr monographs on crystallography, Vol.9, Oxford University Press, 1999.

University of Cape Town

CHAPTER 3.6 INCLUSION OF BIPYRIDINES

The inclusion compounds formed between the host **TOD7**, and the solid guests 2,2'-bipyridine and 4,4'-bipyridine have been elucidated and their thermal characteristics established by TG and DSC. Both crystals were grown by slow evaporation at room temperature using stoichiometric amounts of the host and guest dissolved in ethanol as a solvent. **TOD7** is known for its ability to include many organic solvents but no structures with ethanol as a guest ~~was~~ were found on the CSD[1].

University of Cape Town

Table 3.6.1. Crystal data, experimental and refinement parameters.

	T72BIPY	**T74BIPY**
Compound	$C_{30}H_{22}O_2 \cdot 2C_{10}H_8N_2$	$C_{30}H_{22}O_2 \cdot ½C_{10}H_8N_2$
M_W, $gmol^{-1}$	726.84	492.57
Temperature/ K	173(2)	173(2)
Crystal system	monoclinic	triclinic
Space group	P $2_1/c$	$P\bar{1}$
a, Å	11.152(2)	9.960(2)
b, Å	7.943(2)	11.248(2)
c, Å	21.816(4)	13.429(3)
α, °	90	100.73(3)
β, °	102.47(3)	109.72(3)
γ, °	90	104.65(3)
V, $Å^3$	1886.8(7)	1308.0(5)
Z	2	2
Absorption coefficient, mm^{-1}	0.079	0.077
F(000)	764	518
Crystal size, mm	0.30 × 0.57 × 0.40	0.34 × 0.41 × 0.17
Index ranges	h: -13, 14; k: -9, 10; l: -26, 28	h: ±12, k: ±13; l: ±16
Reflections collected / unique	9940 / 4269	7576 / 4926
Data/ restraints/ Parameters	4269 / 2 / 254	4926/ 4 / 345
Goodness-of-fit	1.057	1.033
ρ_{calc}, $g \cdot cm^{-3}$	1.279	1.251
Final R indices [$I > 2\sigma(I)$]	$R_1 = 0.0437$, $wR_2 = 0.1071$	$R_1 = 0.0463$, $wR_2 = 0.1050$
R indices (all data)	$R_1 = 0.0646$, $wR_2 = 0.1174$	$R_1 = 0.0719$, $wR_2 = 0.1177$
Largest difference peak and hole, $eÅ^{-3}$	0.482 and -0.540	0.259 and -0.292

University of Cape Town

T72BIPY

$C_{30}H_{22}O_2 \cdot 2C_{10}H_8N_2$
Guest : 2-bipyridine
Space Group : $P2_1/c$
a = 11.152(2)Å $\alpha = 90°$
b = 7.943(2)Å $\beta = 102.47(3)°$
c = 21.816(4)Å $\gamma = 90°$
Volume = 1886.8(7)Å^3
Z = 2

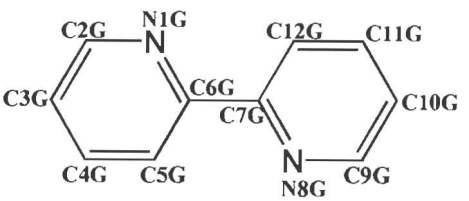

Crystal Structure and Refinement

T72BIPY was refined in the monoclinic space group $P2_1/c$. Due to symmetry the host was located on a centre of inversion at Wyckoff position c whereas the guests were found in general positions. All the non-hydrogen atoms of the host and guest were refined with anisotropic temperature factors. The hydroxyl hydrogens were located in the difference electron density maps, and were refined isotropically. The hydroxyl hydrogens were geometrically constrained a distance of 0.97Å from the parent oxygen atom[2]. The bond lengths and angles of the host and guest all compare with accepted values[3] and will be discussed later in Chapter 5. The dihedral angle between the phenyl groups of the guest refined to 3.8(1)°. The structure refined successfully with a final $R_1 = 0.0437$.

Crystal Packing

Each unit cell consists of two host and four guest molecules (Z=2). The host framework is stacked in zigzag layers perpendicular to [010]. The guest molecules are situated in channels parallel to [010] which vary in cross-sectional area from 8.2Å × 18.2Å to 6.7Å × 20.0Å. The packing of **T72BIPY** is illustrated in Figure 3.6.1.

University of Cape Town

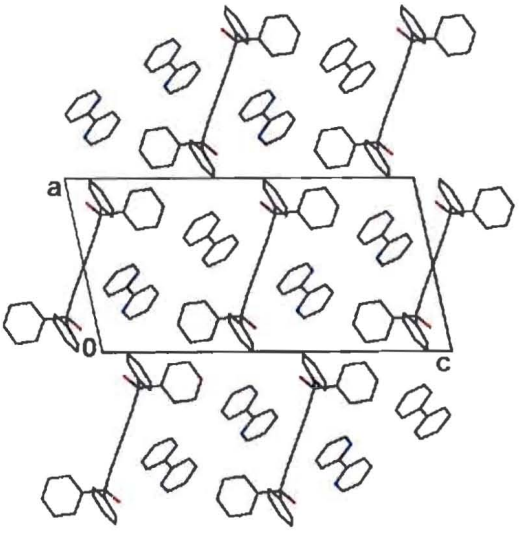

Figure 3.6.1. Crystal packing diagram of **T72BIPY** down [010].

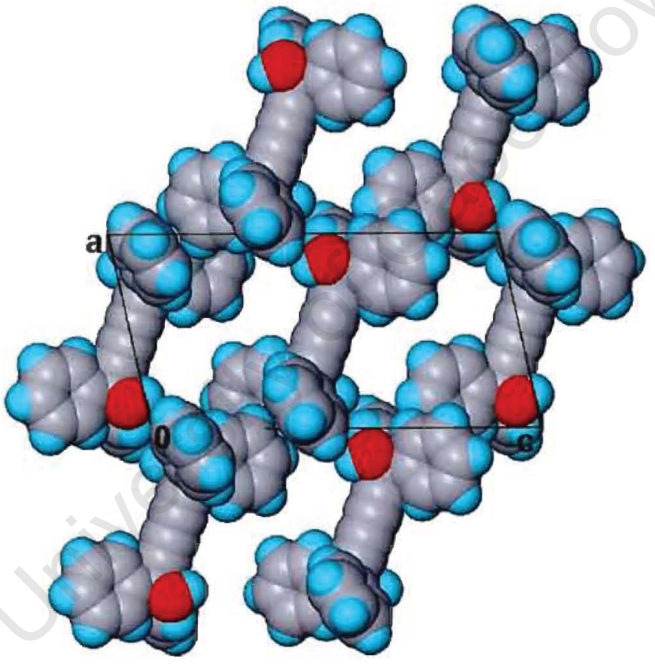

Figure 3.6.2. Space-filling diagram of **T72BIPY**, with the guest removed, viewed down [010].

(a) (b)

Figure 3.6.3. SECTION plot of **T72BIPY** viewed down [010], sectioned at (a) x = 0, (b) x = ½.

The crystal structure is stabilised by hydrogen bonding between the host hydroxyl groups and one of the nitrogen atoms of the guest. The other nitrogen atom of the guest is free and does not partake in any hydrogen bonding.

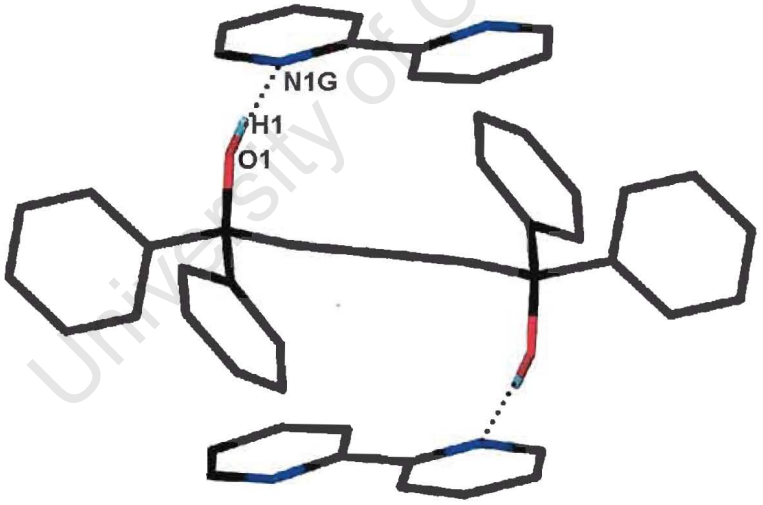

Figure 3.6.4. Hydrogen bonding in **T72BIPY**.

Table 3.6.2. Hydrogen bonding details of **T72BIPY.**

Donor (D)	**Acceptor (A)**	**D—H / Å**	**D•••A / Å**	**D—H•••A / °**
O1	N1G	0.97(1)	2.864(1)	176(2)

University of Cape Town

Thermal Analysis

The DSC curve shows one endotherm (T_{on} = 130.4˚C) which corresponds to the melt of the complex. The decomposition of the inclusion compound starts at approximately 157.0˚C and can be seen in the TG curve.

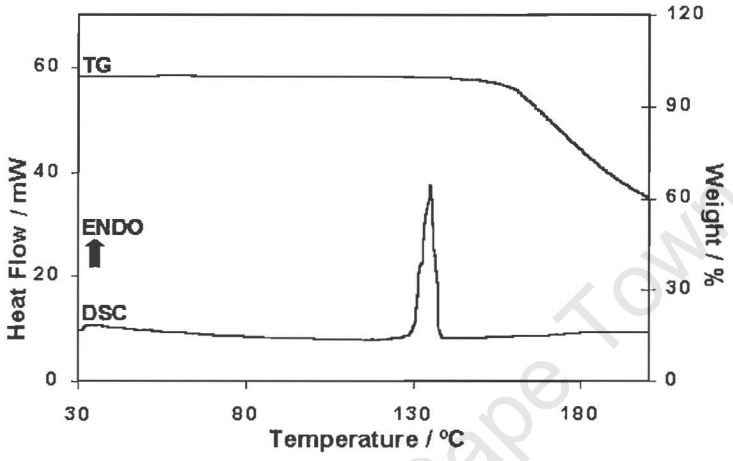

Figure 3.6.5. TG and DSC curves of **T72BIPY**.

University of Cape Town

T74BIPY

$C_{30}H_{22}O_2 \bullet \frac{1}{2}C_{10}H_8N_2$
Guest : 4-bipyridine
Space Group : $P\bar{1}$
a = 9.960(2)Å $\quad \alpha = 100.73(3)°$
b = 11.248(2)Å $\quad \beta = 109.72(3)°$
c = 13.429(3)Å $\quad \gamma = 104.65(3)°$
Volume = 1308.0(5) $Å^3$
Z = 2

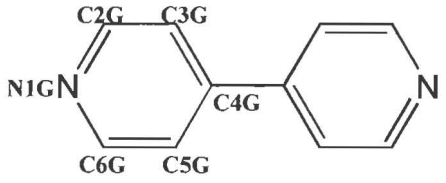

Crystal Structure and Refinement

It was established by oscillation and Weissenberg photography that **T74BIPY** belonged to the triclinic system. The centrosymmetric space group $P\bar{1}$ was assigned by symmetry considerations and on the mean $|E^2-1|$ statistics.

Once again direct methods were used to establish the positions of the host and the guest atoms. Unlike the previous structure, the host was located in general positions whereas the guest was situated on a centre of inversion (Wyckoff position a). The host adopts the gauche conformation. All the non-hydrogen atoms were refined anisotropically. All the hydrogen atoms of the host and the guest were located in the difference electron density maps. The hydroxyl hydrogens of the host were refined isotropically and placed in geometrically calculated positions based on the relationship between O•••O and O—H distances[2].

The bond lengths and angles of the host and guest were all in the expected ranges[3].

Crystal Packing

Each unit cell consists of two hosts and one guest molecule (Z=2). The host framework packs in wavy layers perpendicular to [010]. The guest molecules are situated in channels parallel to [100] which vary in size from approximately to 4.0Å × 6.7Å to 9.4Å × 5.4Å.

University of Cape Town

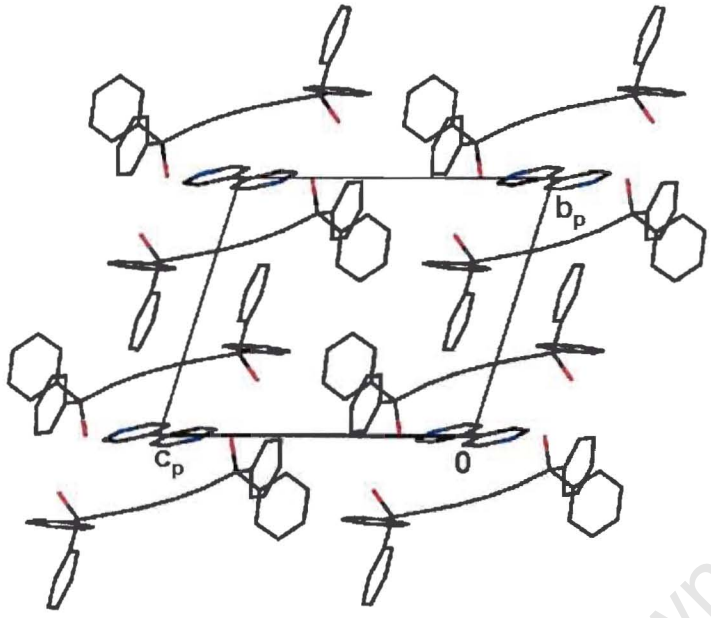

Figure 3.6.6. Crystal packing of **T74BIPY** down [100].

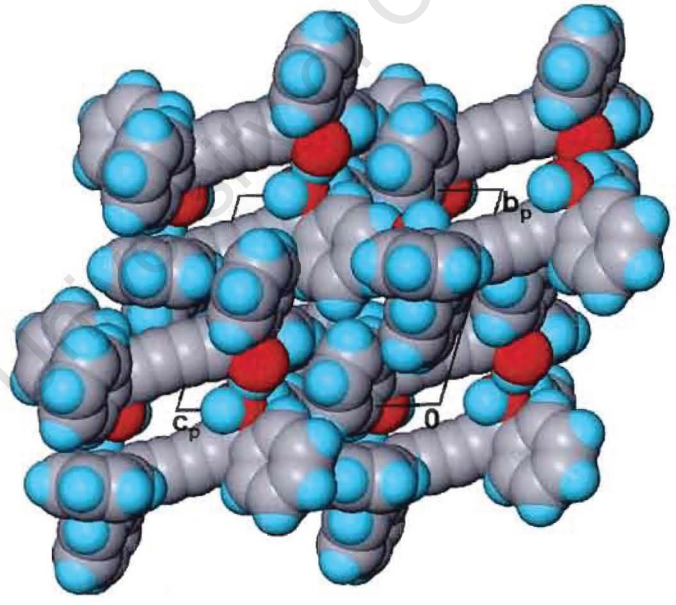

Figure 3.6.7. Space-filling diagram of **T74BIPY** down [100] with the guest removed to show the channels occupied by the guests.

University of Cape Town

Hydrogen bonding occurs between hydroxyl groups of adjacent host molecules to form dimeric units. These units are connected by hydrogen bonding between the host hydroxyl groups and the nitrogen atoms of the guest. This is illustrated in Figure 3.6.8.

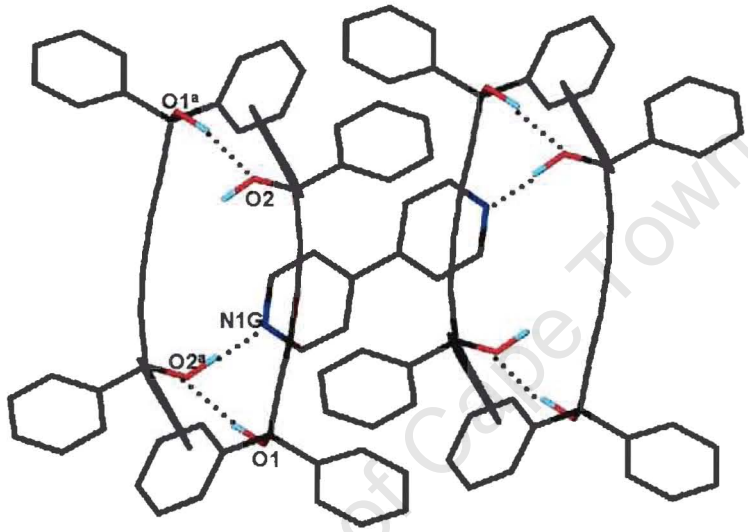

Figure 3.6.8. Hydrogen bonding in **T74BIPY**.

Table 3.6.3. Hydrogen bonding details of **T74BIPY**.

Donor (D)	**Acceptor (A)**	**D—H / Å**	**D•••A / Å**	**D—H•••A / °**
O1	O2[a]	0.97(1)	2.858(1)	165(2)
O2	N1G[a]	0.97(1)	2.651(2)	167(3)

a : -x+1, -y+2, -z

University of Cape Town

Thermal Analysis

The TG and DSC curves are illustrated in Figure 3.6.9. The DSC curve shows one endotherm (T_{on} = 201.2˚C) which corresponds to the melt of the complex. The decomposition of the inclusion compound is shown in the TG curve.

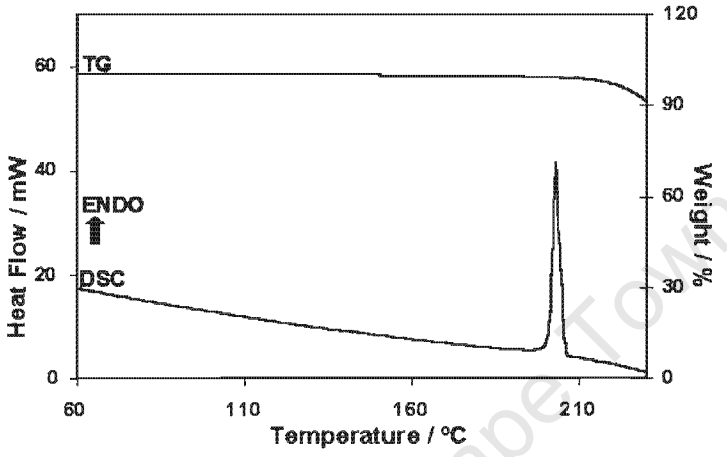

Figure 3.6.9. TG and DSC curves of **T72BIPY**.

University of Cape Town

Discussion

T72BIPY crystallizes in the monoclinic space group $P2_1/c$. The asymmetric unit consists of one half of a host molecule and one guest molecule. Due to symmetry the hydroxyl groups of the host are trans.

In contrast, **T74BIPY** crystallizes in the triclinic space group $P\bar{1}$ with one complete host molecule and one half of a guest molecule in the asymmetric unit. The hydroxyl groups of the host are gauche.

T72BIPY is stabilised by hydrogen bonding between the hydroxyl group of the host and one of the nitrogen atoms of the guest. The other nitrogen atom is not involved in hydrogen bonding. However, in **T74BIPY** a three-centre hydrogen bonding network exists between the hydroxyl groups of adjacent host molecules and the nitrogen atoms of the guest. In both structures the guests are accommodated in channels resulting from voids in the host framework.

The guests 2,2'-bipyridine and 4,4'-bipyridine are constitutional isomers. The two crystal structures **T72BIPY** and **T74BIPY** clearly illustrate the dramatic effect that the position of the nitrogen atoms of the guest plays in the crystal packing.

University of Cape Town

References

1. Cambridge Structural Database and Cambridge Structural Database System, Version 5.22(2001), Cambridge Crystallographic Data Centre, University Chemical Laboratory, Cambridge, England.

2. 1. I. Olovsson and P. Jönsson, *The Hydrogen Bond* – Structure and Spectroscopy, P.Schuster, G. Zundel and C. Sardefy (eds.), North-Holland Publishing Company, USA, 1975.

3. International Tables For Crystallography, Vol. C, (ed.) A.J.C. Wilson, Kluwer Academic Publishers, Dordrecht, pp.691, 1992.

University of Cape Town

CHAPTER 4

University of Cape Town

CHAPTER 4 CTV AND ITS INCLUSION COMPOUNDS

CTV

The inclusion behaviour of the host compound cyclotriveratrylene (2,3,7,8,12,13-hexamethoxy-5,10-dihydro-15*H*-tribenzo[a,d,g]cyclononene; **CTV**) was studied. Inclusion compounds were formed with the guests:

- carbon tetrachloride
- 1,1,1-trichloroethane + 1,1,1-trichloropropane
- 1,1,2-trichloroethane

The inclusion compounds are discussed in terms of thermal analysis, crystal structure and kinetics of desolvation.

The host numbering scheme is shown below:

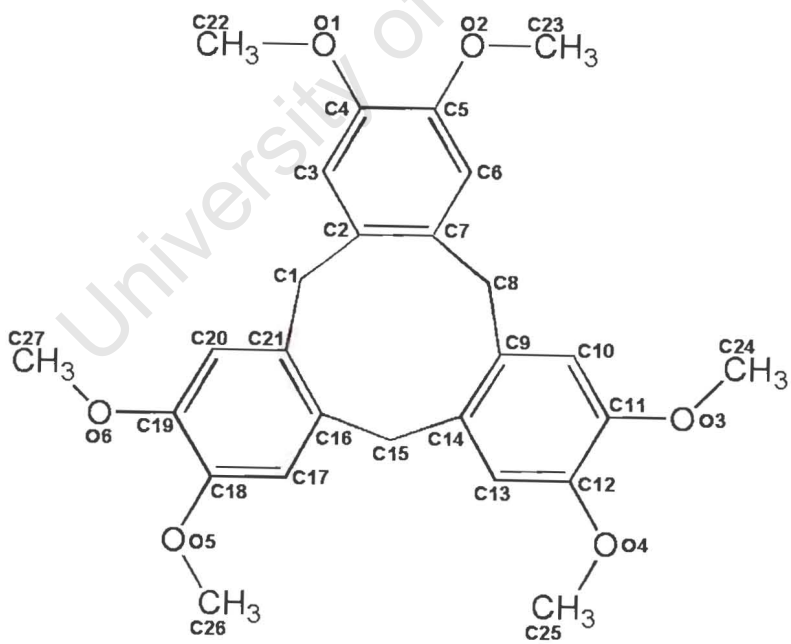

If there are two host molecules in the asymmetric unit, the first one is labelled as shown above and the second molecule is labelled with the suffix A.

University of Cape Town

CHAPTER 4.1 INCLUSION OF CHLORINATED GUESTS

In this chapter the inclusion compounds formed between the host **CTV** and the chlorinated guests carbon tetrachloride, 1,1,1-trichloroethane and 1,1,2-trichloroethane were studied. Crystals of **CTV** and the above-mentioned guests were grown with great difficulty. Experiments done at room temperature resulted in powders of host **CTV** precipitating from solution. All the crystals were grown by slow evaporation at elevated temperatures, typically at 55°C. The resultant crystals tended to be of poor quality and crumbled when taken out of the mother liquor. The structures of all three complexes were solved and the kinetics of desolvation determined. Due to the limited amount of **CTV** available, crystals of the complexes were grown and crushed for kinetic analysis as opposed to powders grown from stirred solutions. Guest exchange reactions were also performed.

University of Cape Town

Table 4.1.1. Crystal data, experimental and refinement parameters

	CTVCCL4	**CTV111**	**CTV112**
Compound	$C_{27}H_{30}O_6 \bullet CCl_4$	$C_{27}H_{30}O_6 \bullet C_2H_3Cl_3 \bullet C_3H_5Cl_3$	$C_{27}H_{30}O_6 \bullet 2C_2H_3Cl_3$
M_w, $gmol^{-1}$	604.32	731.32	717.30
Temperature / K	173(2)	173(2)	173(2)
Crystal system	orthorhombic	monoclinic	triclinic
Space group	Pnma	$P2_1/n$	$P\bar{1}$
a, Å	9.712(2)	20.429(4)	14.403(3)
b, Å	16.778(3)	12.335(3)	15.147(3)
c, Å	17.544(4)	14.220(3)	15.347(3)
α, °	90	90	98.94(3)
β, °	90	102.27(3)	91.56(3)
γ, °	90	90	92.31(3)
V, $Å^3$	2859(1)	3501(1)	3303(1)
Z	4	4	4
Absorption coefficient, mm^{-1}	0.454	0.532	0.562
F(000)	1256	1520	1488
Crystal size, mm	0.47 × 0.09 × 0.05	0.55 × 0.35 × 0.07	0.39 × 0.50 × 0.40
Index ranges	h:-11,8;k:-16,20;l:-17,21	h: -24,25; k -14, 11; l: -17,15	h: -11,18; k: -18,19; l:-13,17
Reflections collected/unique	10629 / 2539	13437 / 6326	13479 / 11444
Data/ restraints/ Parameters	2539 / 0 / 181	6326 / 0 / 405	11444 / 0 / 787
Goodness-of-fit	1.044	1.061	1.242
ρ_{calc}, $g \cdot cm^{-3}$	1.404	1.387	1.443
Final R indices [$I > 2\sigma(I)$]	$R_1 = 0.0447$, $wR_2 = 0.0850$	$R_1 = 0.0773$, $wR_2 = 0.2169$	$R_1 = 0.1241$, $wR_2 = 0.3410$
R indices (all data)	$R_1 = 0.0937$, $wR_2 = 0.1028$	$R_1 = 0.1207$, $wR_2 = 0.2500$	$R_1 = 0.1961$, $wR_2 = 0.3831$
Largest difference peak and hole, $eÅ^{-3}$	0.269 and -0.441	0.721 and -0.977	1.669 and -0.741

University of Cape Town

CTVCCL4

$C_{27}H_{30}O_6 \bullet CCl_4$
Guest : carbon tetrachloride
Space Group : Pnma
a = 9.712(2)Å $\alpha = 90°$
b = 16.778(3)Å $\beta = 90°$
c = 17.544(4)Å $\gamma = 90°$
Volume = 2859(1)Å^3
Z = 4

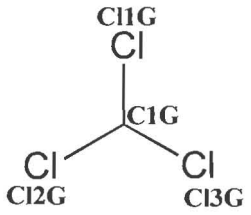

Crystal Structure and Refinement

A host to guest ratio of 1: 1 was established by TG and this was confirmed by the crystal structure. The following reflection conditions were observed:

0kl : k + l = 2n (0k0: k=2n , 00l: l=2n)

hk0 : h = 2n (h00: h=2n)

h0l : none

The orthorhombic space group Pnma was assigned based on the above reflection conditions and the mean $|E^2 - 1|$ statistics. All the non-hydrogen atoms of the host and the guest were obtained by direct methods and treated anisotropically. Each unit cell consists of four host molecules and four guest molecules. Both the host and guest molecules are situated on mirrors at Wyckoff position c. The following atoms were placed with a site occupancy factor of 0.5: C1, C1G, Cl1G and Cl3G. All the hydrogen atoms were obtained in the electron density maps but were placed with bond length restraints. Bond lengths and angles for both the host and guest are in acceptable ranges[1]. The geometry of the carbon tetrachloride molecule refined with the following unique bond distances (C—Cl = 1.750(4)Å, 1.757(2)Å and 1.770(4)Å) and bond angles (Cl—C—Cl = 109.3(2)°, 109.7(2)°, 109.6(2)° and 109.5(2)°). The guest atoms refined with the following temperature factors: U_{eq}(C1G) = 0.03Å^2, average U_{eq}(carbon atoms) = 0.04Å^2. The structure refined with a final R_1 = 0.0447.

University of Cape Town

Crystal Packing

The bowl-shaped host molecules stack in columns parallel to [100] with each molecule in the cavity of the other. Alternating columns have the host cavity facing in opposite directions. No significant hydrogen bonds were found between the host and the guest molecules which implies that the structure is stabilised by van der Waals interactions. The guest molecules lie in channels parallel to [100]. The channels vary in size from approximately 3.7Å × 6.6Å to 7.5Å × 7.3Å.

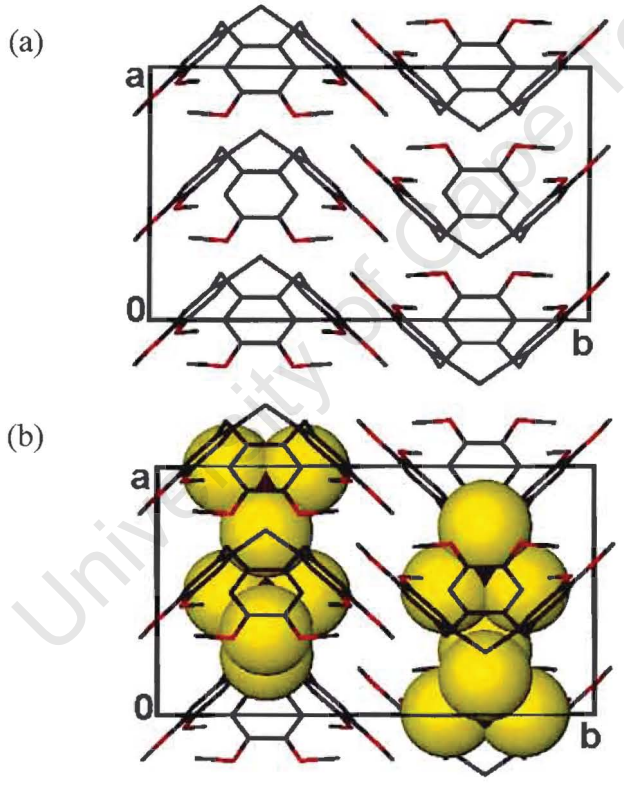

University of Cape Town

Figure 4.1.1. Packing diagram of **CTVCCL4** down [010] with the host represented in stick form and (a) guests omitted and (b) guests represented in van der Waals radii.

(a) (b)

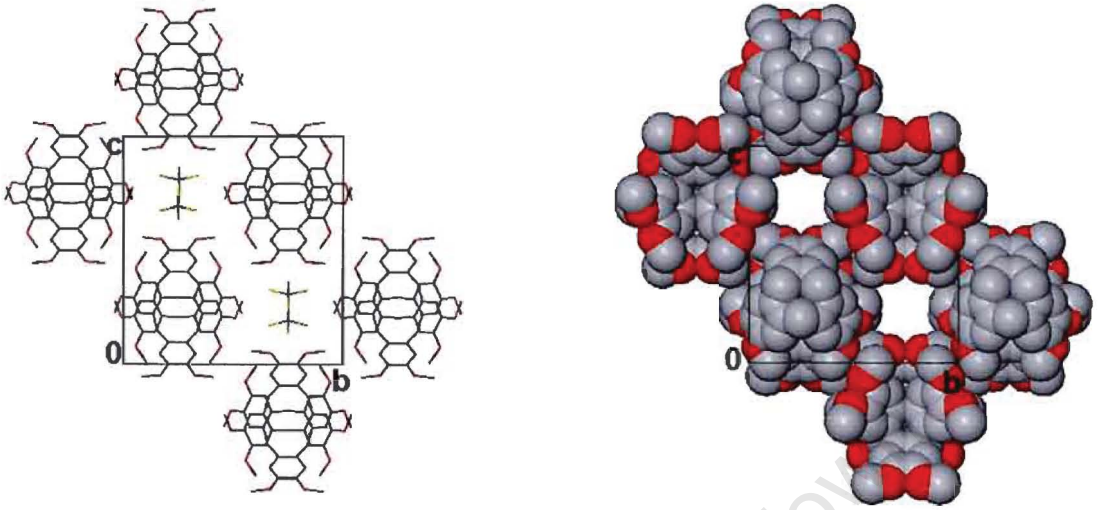

Figure 4.1.2. Packing diagrams of **CTVCCL4** down [100]. In Figure 4.1.2 (b) guests are omitted and the host atoms are depicted in van der Waals radii.

University of Cape Town

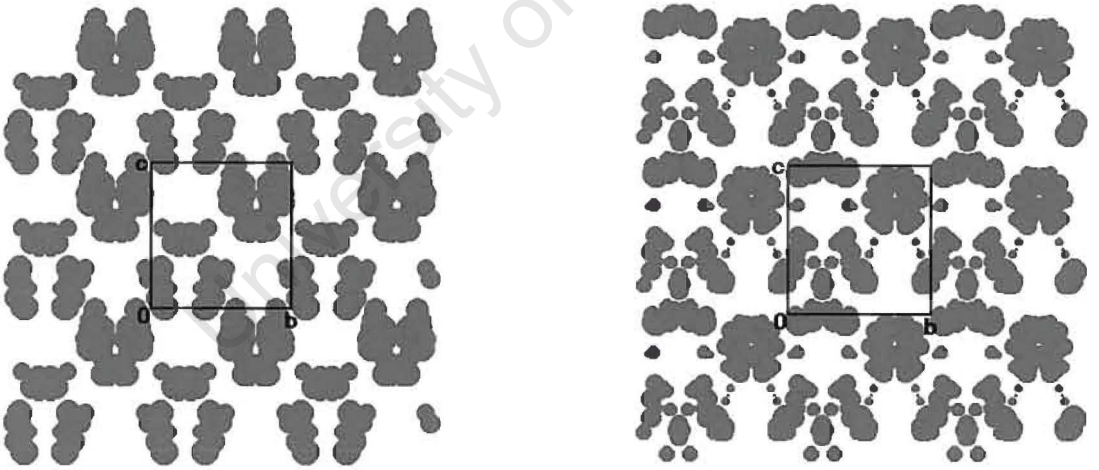

Figure 4.1.3. SECTION plots of **CTVCCL4** down [100] with the guests removed at (a) x = 0.45 and (b) x = 0.85.

Thermal Analysis

Two endotherms were observed in the DSC. Endotherm A (T_{on} = 75.2°C) corresponds with the loss of guest and endotherm B (T_{on} = 228.5°C) represents the host melt.

The TG showed a mass loss of 25.7% (calculated mass loss: 25.5%), which is consistent with the host:guest ratio of 1:1.

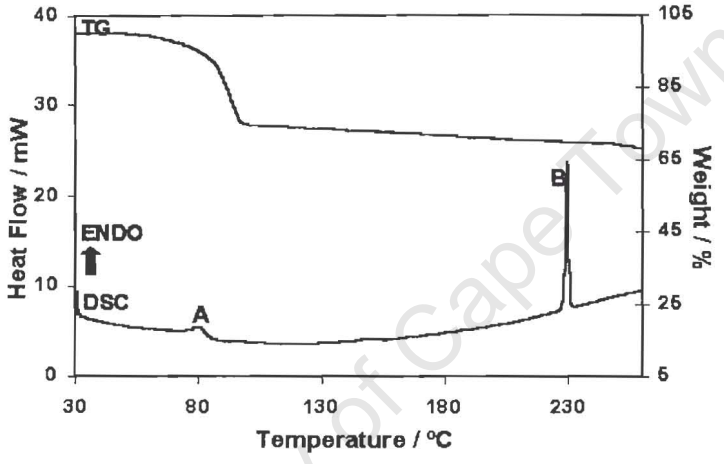

Figure 4.1.4. TG and DSC curves for **CTVCCL4**.

University of Cape Town

Kinetics of desolvation

Isothermal kinetics

Crystals of **CTVCCL4** were crushed and a series of isothermal TG runs performed over the temperature range 85-100°C. The resultant α vs time curves were deceleratory. The best results were obtained with the first order kinetic model

F1: $kt = -\ln(1-\alpha)$ over the α range 0-0.9. The plot of $-\ln k$ vs $1/T$ is illustrated in Figure 4.1.5. An activation energy of 171(11) $kJmol^{-1}$ was obtained for the desolvation reaction.

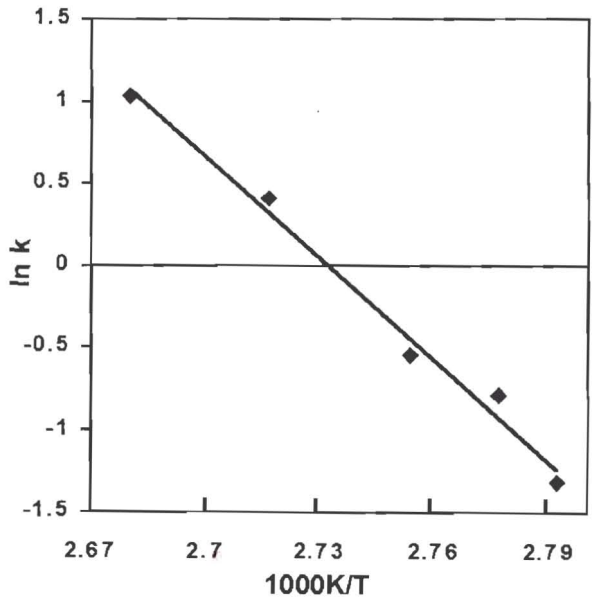

Figure 4.1.5. Plot of lnk vs 1/T for **CTVCCL4**.

University of Cape Town

CTV111

$C_{27}H_{30}O_6 \cdot C_2H_3Cl_3 \cdot C_3H_5Cl_3$
Guests : 1,1,1- trichloroethane + 1,1,1- trichloropropane
Space Group : $P2_1/c$
a = 20.429(4)Å $\alpha = 90°$
b = 12.335(3)Å $\beta = 102.27(3)°$
c = 14.220(3)Å $\gamma = 90°$
Volume = 3501(1)Å^3
Z = 4

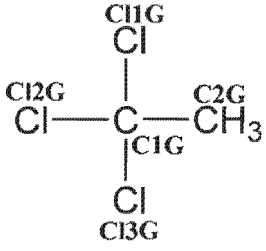

Guest A

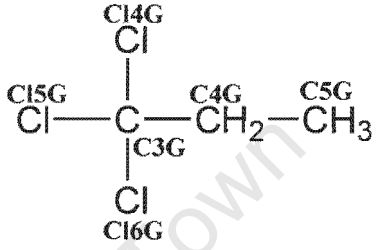

Guest B

Crystal structure and Refinement

CTV111 was unexpectedly grown from a solution of **CTV** and 1,1,1-trichloroethane, the latter subsequently found to be contaminated with trace amounts of 1,1,1-trichloropropane. This was confirmed by ^{1}H-NMR spectroscopy which showed two peaks at δ= 2.7 and 3.4ppm instead of one. Gas chromatography of the solvent 1,1,1-trichloroethane also showed two peaks that were very close to one another at retention times 1.88 and 2.03 minutes. These correspond to the two guests; 1,1,1-trichloroethane and 1,1,1- trichloropropane. The crystal could not be regrown using a a purer sample of 1,1,1-trichloroethane as it has been declared a restricted solvent under the Montreal protocol.

The structure of **CTV111** was solved in the monoclinic space group $P2_1/c$. All the host and the guest molecules were found in general positions (Z=4). Direct methods revealed the positions of all the non-hydrogen atoms except two carbon atoms of guest B. Upon subsequent refinement two peaks with electron densities of 2.47 eÅ^{-3}

University of Cape Town

and 2.56eÅ^{-3} were found in the region of guest B. The first peak was a distance of 1.526Å from guest B and the second peak was 1.404Å from the first peak. These were assigned as carbon atoms. All the non-hydrogen atoms were treated anisotropically. Hydrogen atoms were located in the electron density maps but were placed with the following C—H distances depending on the type of hydrogen: -OC<u>H</u>$_3$ and -C<u>H</u>$_3$ 0.96Å, aromatic hydrogens 0.93Å and C<u>H</u>$_2$ 0.97Å. Bond lengths and angles for the host fell within the expected ranges[1]. Guests A and B refined with C—Cl distances in the range of 1.714(8)Å — 1.787(6)Å and Cl—C—Cl angles in the range of 105.4(3)°—110.9(5)°. The guest atoms refined with temperature factors: U_{eq}(C1G) = 0.05Å^2, U_{eq}(C2G) = 0.06Å^2, U_{eq}(C3G) = 0.11Å^2 , U_{eq}(C4G) = 0.18Å^2 , U_{eq}(C5G) = 0.19Å^2 , U_{eq}(Cl1G) = 0.12Å^2 , U_{eq}(Cl2G) = 0.08Å^2 , U_{eq}(Cl3G) = 0.08Å^2 ,U_{eq}(Cl4G) = 0.12Å^2 , U_{eq}(Cl5G) = 0.13Å^2 and U_{eq}(Cl6G) = 0.19Å^2.

Crystal Packing

The crystal packing is illustrated in Figure 4.1.6. The host molecules are stacked in columns parallel to [001] with adjacent columns in an anti-parallel relationship. The host molecules are separated from each other by one molecule of guest A which is situated in the host cavity. The methyl groups of guest A point into the host cavity at an angle of 151.6° to its centroid. Thus when the packing diagram is viewed down [010] each column consists of alternating molecules of host and guest A. Guest B occupies channels of approximate size 5.5Å × 10.7Å, parallel to [010] created between every two of these columns. Again, no significant hydrogen bonding was observed in this structure which suggests that the structure is stabilised by van der Waals interactions.

University of Cape Town

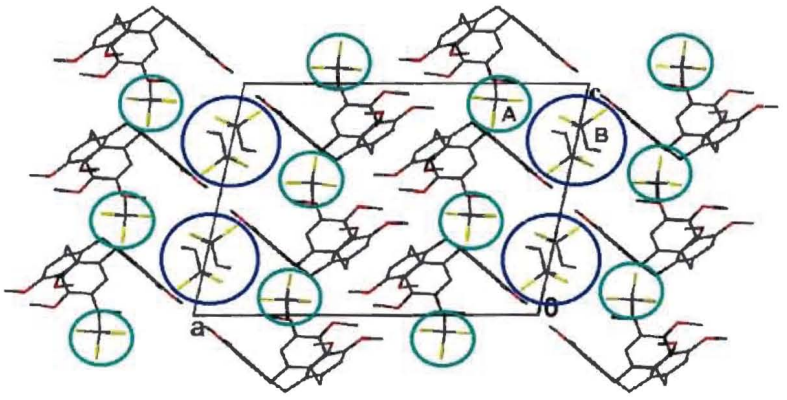

Figure 4.1.6. Crystal packing diagram of **CTV111** viewed down [010] indicating guests A and B.

University of Cape Town

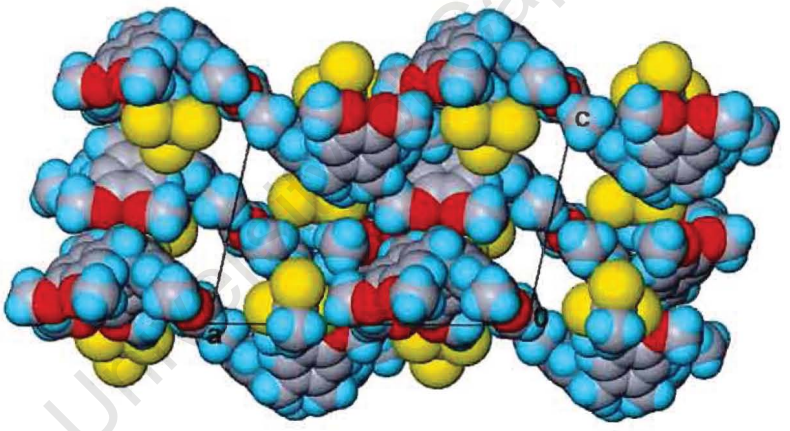

Figure 4.1.7. Space-filling diagram of **CTV111** down [010] with guest B removed.

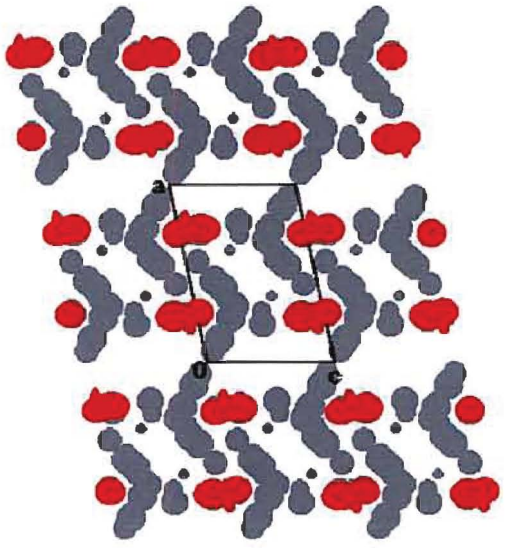

Figure 4.1.8. SECTION plot of **CTV111** at y =0 with guest B removed and Guest A shaded in red.

University of Cape Town

Thermal Analysis

As seen in the previous structure the loss of guest is reflected in endotherm A (T_{on} = 69.3˚C) and the melt of the host is described by endotherm B (T_{on} = 229.0˚C). Thus endotherm A corresponds to simultaneous loss of the guests.

The TG shows a single mass loss step (experimental mass loss: 35.4%; calculated mass loss: 37.4%) which is consistent with the host: guest ratio described above.

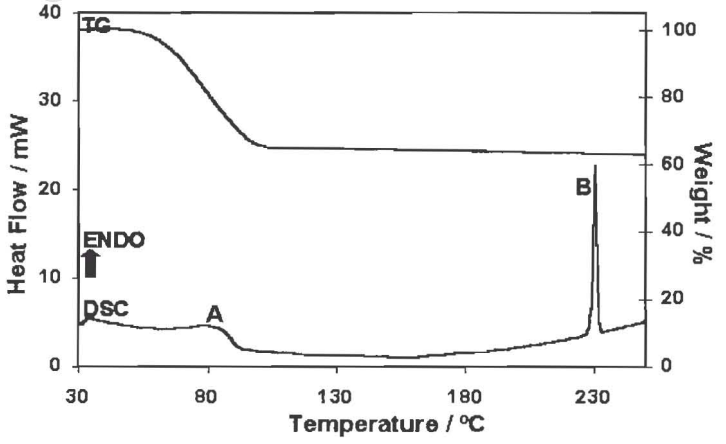

Figure 4.1.9. TG and DSC curves for **CTV111.**

Kinetics

The kinetics of desolvation of **CTV111** was studied using both isothermal and non-isothermal methods. As described above crystals of the complex were grown and crushed for analysis.

Isothermal Kinetics

A series of isothermal TG runs were carried out over the temperature range 60-80°C. The resultant TG curves were converted into α vs time curves. The data best fit the first order kinetic model F1: kt = -ln (1-α) over the α range 0-0.95. The resultant Arrhenius plot is shown in Figure 4.1.10. An activation energy of 113(1) $kJmol^{-1}$ was obtained.

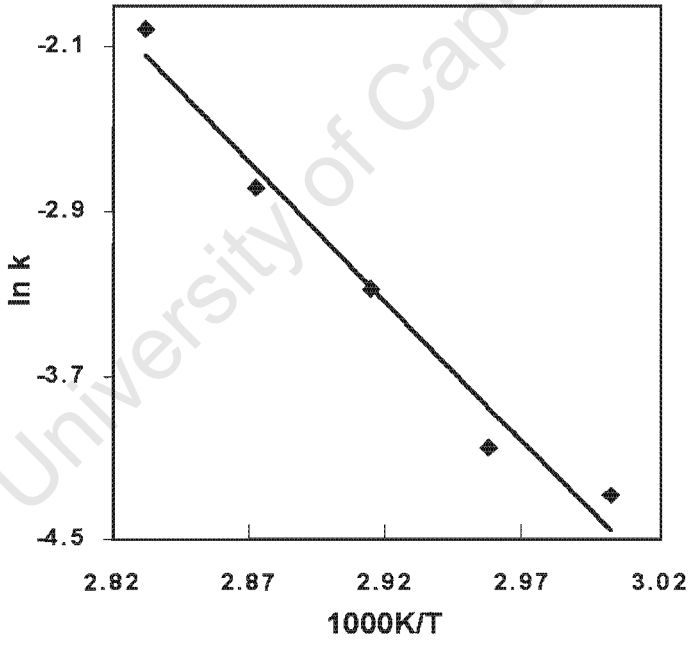

Figure 4.1.10. Plot of ln k vs 1/T for the desolvation of **CTV111.**

University of Cape Town

CTV112

$C_{27}H_{30}O_6 \cdot 2C_2H_3Cl_3$
Guest : 1,1,2- trichloroethane
Space Group : $P\bar{1}$
a = 14.403(3)Å $\alpha = 98.94(3)°$
b = 15.147(3)Å $\beta = 91.56(3)°$
c = 15.347(3)Å $\gamma = 92.31(3)°$
Volume = 3303(1)Å^3
Z = 4

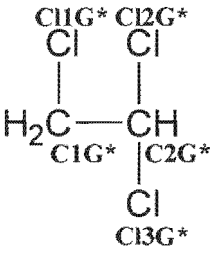

*: The other guests are labelled with suffixes **H**, **I** and **J**.

Crystal structure and Refinement

As was described earlier the crystals of **CTV112** grown were of low quality and all further attempts to grow better quality crystals failed. However, structure determination was carried out and the centrosymmetric space group $P\bar{1}$ was assigned based on the mean $|E^2 - 1|$ statistics. The asymmetric unit consists of two independent host molecules and four independent guest molecules. Each unit cell contains four host molecules and eight guest molecules. All the non-hydrogen atoms were obtained by direct methods and refined anisotropically. Hydrogen atoms were inserted as described in the previous structure. A residual electron density of 1.664eÅ^{-3} found near one of the guests and could not be modelled. Bond lengths and angles obtained for the host molecules were in the required ranges[1]. The U_{eq} values for the guest atoms were in the range of 0.06—0.16Å^2 for the carbon atoms and 0.06—0.12Å^2 for the chlorine atoms. Three of the guest atoms have a similar geometry and the fourth is distorted with two of the chlorine atoms in an eclipsed position when the molecule is viewed down the C—C bond. Both geometries are depicted in Figure 4.1.11. Table 4.1.2 indicates the bond lengths and angles obtained for the guest molecules after the final refinement. At the end of the refinement R_1= 0.1241.

University of Cape Town

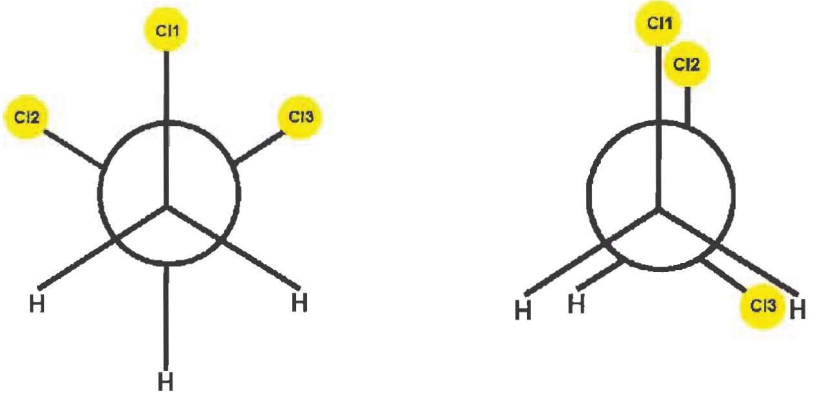

(a) (b)

Figure 4.1.11. Schematic diagram depicting the view down the C—C bond for guests labelled (a) **G, H ,I** and (b) **J**.

Table 4.1.2. Selected bond lengths and angles for guests **G, H, I** and **J**.

Guest	C—C	C—Cl	Cl—C—Cl
G	1.47(1)	1.73(1) 1.84(1)	108.1(5)
H	1.44(1)	1.75(1) 1.78(1)	109.7(5)
I	1.40(2)	1.74(1) 1.84(2)	110.2(7)
J	1.2(1)	1.73(1) 2.26(2)	100.8(8)

University of Cape Town

Crystal packing

Again the host molecules are arranged in columns, this time perpendicular to [001] with the host cavity of each alternate column pointing in the same direction. Guests **H** and **J** are situated in two separate host cavities while guests **G** and **I** lie in voids created by the host framework. The channels occupied by guests **G** and **I** are constricted and run parallel to [100]. The size of the channels varies from approximately 3.7Å × 4.9Å to 6.6Å × 5.6Å. As was observed for the previous structures, no significant hydrogen bonding was detected.

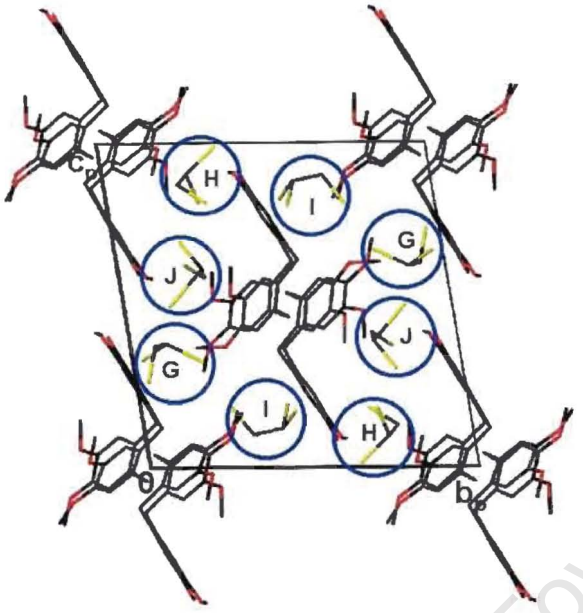

Figure 4.1.11. Crystal packing diagram of **CTV112** down [100] indicating the guests **G**, **H, I** and **J**.

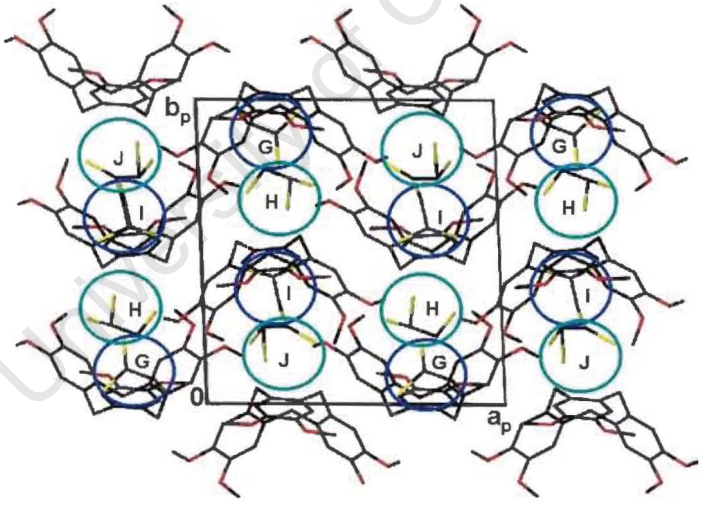

Figure 4.1.12. Packing diagram of **CTV112** down [001] with the guests G and I encircled in blue and H and J in green.

University of Cape Town

Thermal Analysis

Once again two endotherms were observed in the DSC. Endotherm A (T_{on} = 100.5°C) was attributed to the loss of all guests and endotherm B (T_{on} = 228.7°C) to the host melt.

The host:guest ratio of 1:2 was confirmed by TG. A single step of mass loss 37.4% (calculated: 37.2%) was observed in the TG.

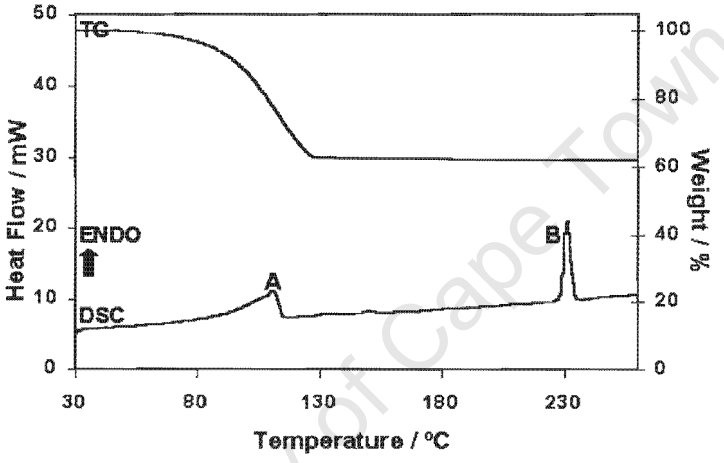

Figure 4.1.13. TG and DSC curves for **CTV112**.

University of Cape Town

Kinetics of desolvation

Once again due to the limited amount of host available all experiments were performed on crushed crystals of **CTV112**. Both isothermal and non-isothermal methods were used to determine the kinetics of desolvation of **CTV112**. For each of these methods samples were taken from the same batch to ensure that the results are comparable and consistent.

Isothermal kinetics

A series of isothermal TG runs were performed at numerous temperatures over the range 70-90°C. Various kinetic models were fitted to the resultant α vs time curves in order to obtain the best fit. The diffusion controlled model **R3** : $kt = 1 - (1-\alpha)^{1/3}$ gave the best fit over the α range: 0- 0.95. The Arrhenius plot is illustrated in Figure 4.1.14. An activation energy of 84(7) $kJmol^{-1}$ was obtained.

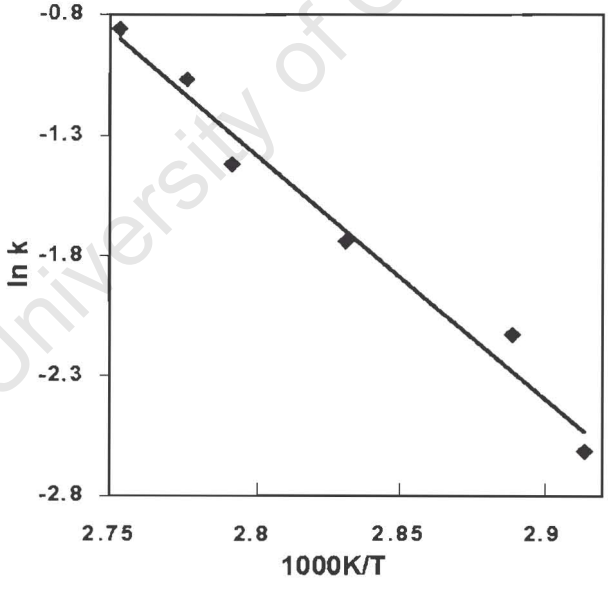

Figure 4.1.14. Arrhenius plot of **CTV112**.

Non-isothermal kinetics

A series of TG runs over a temperature range of 30-130°C were performed at heating rates 1, 2, 5, 10 and 20°Cmin^{-1}. These TG curves were analysed at different stages of

University of Cape Town

decomposition ranging from 5% to 30% and reduced to plots of -log β vs 1/T. The activation energy was calculated in the range 73(3) kJmol^{-1} to 80(5) kJmol^{-1}.

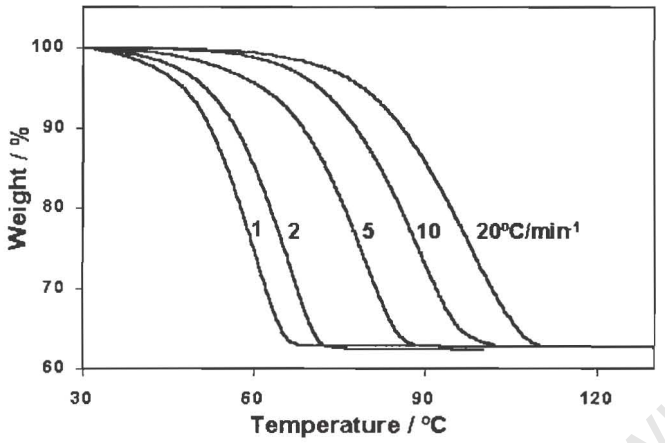

Figure 4.1.15. TG curves indicating the desolvation of **CTV112** over the temperature range 30 to 130°C at heating rates 1, 2, 5,10 and 20°C min^{-1}.

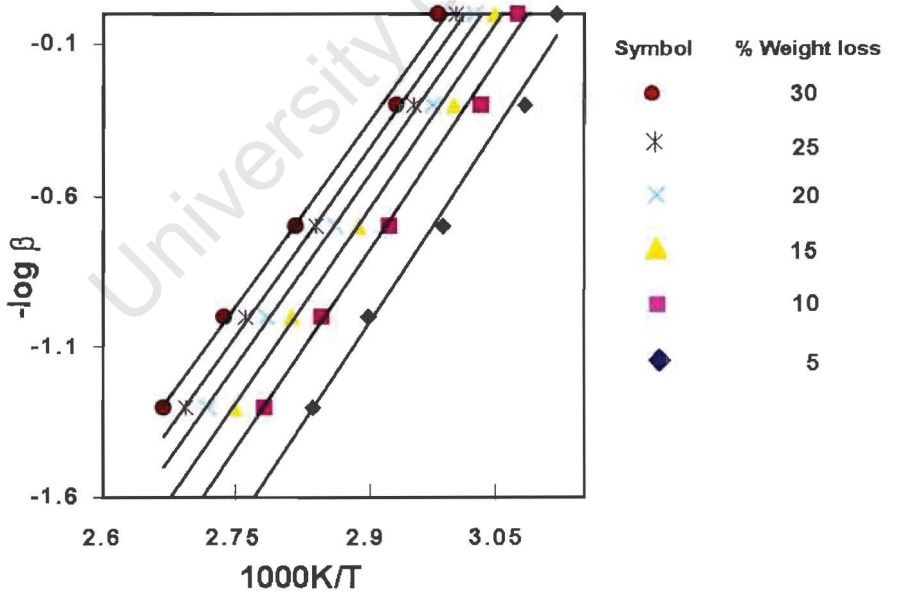

Figure 4.1.16. Plot of –log β vs 1/T for **CTV112**.

University of Cape Town

Guest Exchange Reactions

Guest exchange reactions were performed as described earlier in Chapter 3.4. Crystals of **CTVCCL4** were grown and exposed to the vapours of 1,1,1-trichloroethane. In this case the reaction was monitored using TG due to the significant differences in weight percentages between **CTVCCL4** and **CTV111**. The exchange reaction proceeded very quickly and was complete after 2 hours. The results are shown in Figure 4.1.17.

The reaction can be described by the following equation:

$$\mathbf{CTV{\bullet}CCl_{4(s)}} + C_2H_3Cl_3{\bullet}C_3H_5Cl_{3\,(g)} \rightarrow \mathbf{CTV{\bullet}}C_2H_3Cl_3{\bullet}C_3H_5Cl_{3\,(s)} + CCl_4\uparrow$$

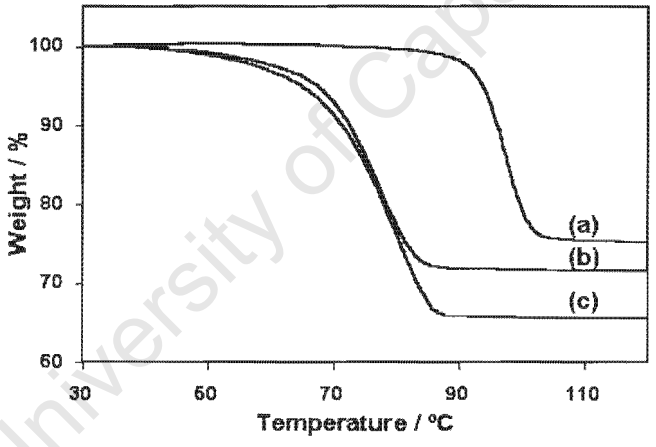

Figure 4.1.17. TG curves for the exchange reaction at time = (a) 0 min, (b) 65 minutes and (c) 120 minutes.

University of Cape Town

Discussion

The three structures were successfully solved in different crystal systems. **CTVCCL4** solved in the orthorhombic space group Pnma. The asymmetric unit comprised one half of a host molecule and one half of a guest molecule. The guest molecules lie in channels parallel to [100].

CTV111 crystallized in the monoclinic space group $P2_1/n$, with one host molecule and two guest molecules in the asymmetric unit. Each host molecule contains one guest molecule with its methyl group directed towards the host cavity. The other guests are situated in channels parallel to [010].

The crystal structure of **CTV112** was solved in the triclinic space group $P\bar{1}$ with two independent host molecules and four independent guest molecules in the asymmetric unit. Once again each host molecule contains one guest molecule in its cavity with the other guests in channels parallel to [100].

University of Cape Town

In all three structures the host molecules pack in columns with the host cavities aligned in opposite directions in adjacent columns. In **CTVCCL4** these columns are parallel to [100], in **CTV111** they are parallel to [001] and in **CTV112** the columns are parallel to [010]. The presence or absence of guest molecules in the host cavity particularly affect the length of the cell dimension along these columns. Similar packing motifs and observations were reported by J.W. Steed et al.[2] for inclusion compounds of **CTV** and certain organic guests including chloroform.

In **CTVCCL4** the host molecules stack with each molecule in the cavity of the previous one, resulting in the length of the crystallographic a axis of 9.712(2)Å. The guests are situated in channels along [100] created between the columns. In **CTV111** each host molecule contains one guest molecule with its methyl group directed towards the cavity (half of the guest molecules present lie in the host cavity) thus increasing the size of the crystallographic c axis to 14.220(3)Å. The other guests occupy channels parallel to [010] produced by voids between the columns. Similarly, in **CTV112** each host molecule contains one guest molecule resulting in the b axis length of 15.147(3)Å.

The thermal analysis data are summarised in Table 4.1.3.

Inclusion compound			**CTVCCL4**	**CTV111**	**CTV112**
H : G ratio			1 : 1	1: 1:1	1 : 2
TG results	Calc. % mass loss		25.5	37.4	37.2
	Exp. % mass loss		25.7	35.4	37.4
DSC results	T_{on} (° C) :	A*	75.2	69.3	100.5
		B*	228.5	229.0	228.7
Normal boiling points T_b (° C)			76.7	74.1	113.5
T_{on} / T_b			0.980	0.935	0.885
E_a (isothermal kinetics)			171(11)	113(1)	84(7)

*: A and B refer to the endotherms illustrated in previous DSC diagrams.

In all three complexes guest release is followed by the melt of the host. There is good correlation between the ratio T_{on} / T_b and the activation energies obtained for the desolvation reactions.

Guest exchange reactions were also successful between **CTVCCL4** and the guest 1,1,1-trichloroethane. Good agreement was obtained between the two methods used to obtain the activation energy for desolvation of **CTV112**. Isothermal methods revealed an activation energy of 84(7) $kJmol^{-1}$ and non-isothermal methods gave a range of 73(3) $kJmol^{-1}$ to 80(5) $kJmol^{-1}$.

University of Cape Town

References

1. International Tables for crystallography, Vol. C, (ed.) A.J.C. Wilson, Kluwer Academic Publishers, Dordrecht, pp.691, 1992.

2. J.W. Steed, H. Zhang and J.L. Atwood, *Supramolecular Chem.*, 7, 37-45, 1996.

University of Cape Town

CHAPTER 5

University of Cape Town

CHAPTER 5 HOST CONFORMATIONS

TOD7

The host compound **TOD7,** Figure 5.1**,** adopts one of two conformations depending on the relative dispositions of the hydroxyl groups, namely trans or gauche. In this thesis, of the 18 inclusion compounds formed with **TOD7,** 6 (33.3%) of these have the host adopting the gauche conformation and 12 (66.7%) of these have the host adopting the trans conformation.

This trend is also seen in the CSD[1] and in a recent thesis completed by D. Vujovic[2]. In the CSD[1], of the 34 structures with **TOD7** as the host molecule, 26 (76%) favours the trans conformation, 2 (6%) have no 3D co-ordinates and the remaining 6 (18%) favour the gauche conformation. In the diagrams below, selected bond lengths and torsion angles are tabulated for all the structures in this study involving **TOD7** as the host compound. Even though the numbering scheme of the host compound is arbitrary, direct comparisons can be made between the torsion angles for each of the different structures. eg. τ_1 of the host molecule A can be compared to τ_1 of the host molecule B. This can be done as the smallest torsion angles have been chosen. The torsion angles τ_1 and τ_2 define the orientation of the phenyl groups relative to the acetylenic spacer and τ_3 indicate the relative orientations of the hydroxyl groups. In all the structures where the host was located on a centre of inversion, $\tau_3 = 180°$, which indicates the trans conformation. The gauche conformation is characterised by $|\tau_3| < 90°$. The dihedral angle is defined as the angle between the least squares planes of the two phenyl rings on the same carbon atom. As was observed by Vujovic[2], the dihedral angles for all the structures are in the range 72° - 90° thus indicating that the phenyl ring planes are nearly orthogonal.

University of Cape Town

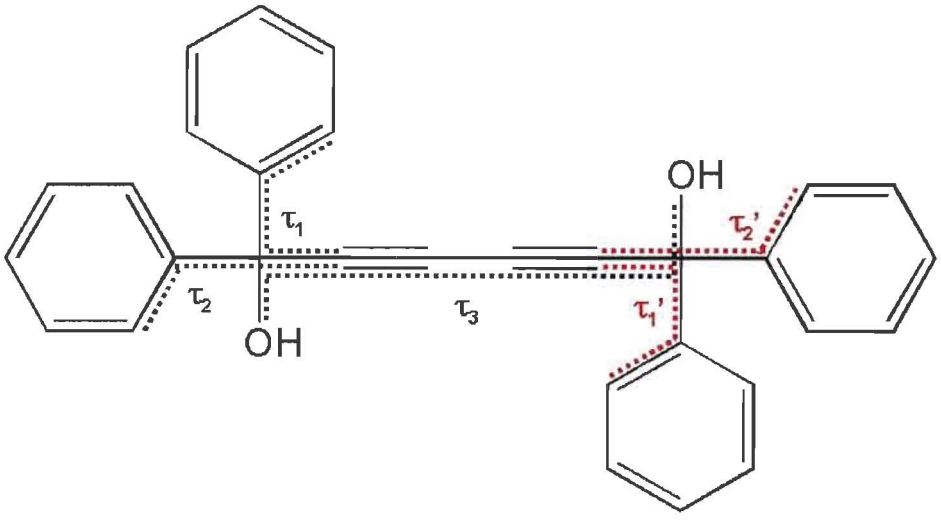

Figure 5.1 Diagram indicating the torsion angles τ_1, τ_2 and τ_3 defined for **TOD7**.

Table 5.1. Torsion angles for **TOD7**.

Complex	Guest	τ_1 / °, τ_1' / °	τ_2 / °, τ_2' / °,	τ_3 / °	Dihedral angle/°
T7CCL4[a]	carbon tetrachloride	-7.2(4), 20.5(5)	55.5(5), -84.5(4)	-57.7(3)	87.6(2) 85.7(2)
T7CHCL3[a]	chloroform	-8.4(3), 21.7(4)	53.5(4), -87.5(3)	-56.1(2)	83.0(1) 83.2(1)
T7CH2CL2[b]	dichloromethane molecule 1	-9.0(3), 27.0(4)	48.6(3), 82.6(3)	-54.3(2)	80.0(1) 80.7(1)
	molecule 2	-2.9(3), 15.1(3)	-52.6(3), 88.9(3)	57.2(2)	85.1(1) 90.0(1)
T7CH3CN	acetonitrile	18.4(2)	64.1(2)	180	82.73(7)
T7PYR	pyridine	15.8(4)	62.2(3)	180	84.58(9)
T72PIC	2-picoline	-19.4(4)	60.4(3)	180	80.03(9)
T73PIC	3-picoline	-12.3(3)	48.0(3)	180	81.64(9)
T74PIC	4-picoline	-27.3(2)	49.2(2)	180	79.54(6)
T7DMF	dimethylformamide	16.8(3)	67.8(2)	180	82.19(9)
T7DMSO	dimethylsulphoxide	18.0(7)	68.4(5)	180	80.5(2)
T7BENZ[b]	benzene molecule 1	14.3(4), -26.4(4),	-40.0(4), -87.2(4),	60.8(3)	72.5(2) 82.7(2)
	molecule 2	-0.3(5), 11.2(5)	48.7(4), -76.0(4)	-62.8(3)	82.7(2) 87.7(2)
T7TOL[b]	toluene molecule 1	-15.8(2), 15.8(2)	-78.1(2), -41.4(2)	61.5(1)	72.02(6) 85.59(7)
	molecule 2	-2.2(2), 10.5(2)	50.3(2), -71.6(2)	-63.3(1)	81.72(6) 84.97(6)
T7MESI	mesitylene	3.0(2)	-70.3(2)	180	86.05(7)
T72BIPY	2-bipyridine	-13.6(2)	55.3(2)	180	81.52(6)
T74BIPY[a]	4-bipyridine	-15.9(2), 26.0(2)	-54.2(2), -44.7(2)	46.7(1)	75.64(7) 73.00(7)
T7ANI	aniline	14.5(2)	-61.6(2)	180	79.33(5)
T7ONA	o-nitroaniline	-6.4(2)	64.5(2)	180	88.28(6)
T7MNA	m-nitroaniline and n-hexane	7.9(3)	-50.5(3)	180	79.4(1)

a: the asymmetric unit consists of one whole host molecule
b: the asymmetric unit consists of two whole host molecules

University of Cape Town

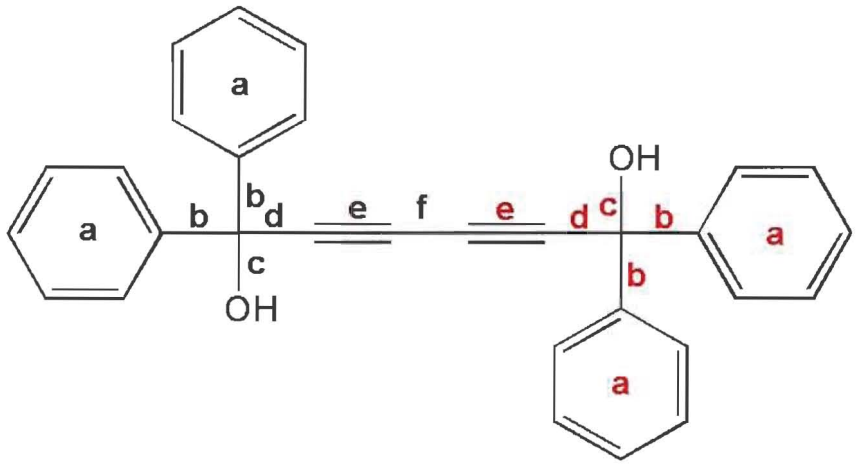

Figure 5.2 Diagram indicating the bond lengths a, b, c, d, e and f defined for **TOD7**.

Table 5.2 Ranges of bond lengths observed for **TOD7**.

Complex	a=C_{ar}≅C_{ar}(Å)	b=C_{ar}—Csp^3(Å)	c=Csp^3—O(Å)	d= Csp^3—Csp(Å)	e=Csp≡Csp(Å)	f=Csp—Csp(Å)
T7CCL4	1.318(6) 1.401(6)	1.522(5) 1.535(5)	1.434(4) 1.440(4)	1.473(5) 1.485(5)	1.187(5) 1.190(5)	1.379(6)
T7CHCL3	1.320(5) 1.393(4)	1.526(4) 1.542(4)	1.431(3) 1.433(3)	1.478(4) 1.483(4)	1.197(4) 1.202(4)	1.374(4)
T7CH2CL2	1.364(4) 1.392(4)	1.530(3) 1.540(3)	1.432(3) 1.434(3)	1.474(3) 1.485(3)	1.198(3) 1.202(3)	1.376(3) 1.380(3)
T7CH3CN	1.365(3) 1.385(3)	1.525(2) 1.536(2)	1.433(2)	1.481(2)	1.198(2)	1.370(3)
T7PYR	1.360(5) 1.388(5)	1.535(4) 1.539(4)	1.425(3)	1.478(4)	1.200(3)	1.383(5)
T72PIC	1.362(5) 1.394(4)	1.539(4)	1.420(3)	1.486(4)	1.198(4)	1.377(6)
T73PIC	1.346(5) 1.389(4)	1.535(3) 1.542(3)	1.421(3)	1.492(3)	1.200(3)	1.372(5)
T74PIC	1.353(4) 1.395(3)	1.538(2) 1.539(2)	1.412(2)	1.478(2)	1.189(2)	1.378(3)
T7DMF	1.352(4) 1.389(3)	1.527(3) 1.537(3)	1.423(2)	1.484(3)	1.193(3)	1.379(4)
T7DMSO	1.358(8) 1.398(6)	1.538(6) 1.541(6)	1.426(5)	1.489(6)	1.197(7)	1.384(9)
T7BENZ	1.355(8) 1.413(7)	1.530(4) 1.544(4)	1.435(3) 1.441(3)	1.470(4) 1.479(4)	1.197(5) 1.208(5)	1.365(5) 1.373(5)
T7TOL	1.364(3) 1.399(3)	1.528(2) 1.539(2)	1.432(2) 1.434(2)	1.476(2) 1.483(2)	1.193(2) 1.201(2)	1.382(2) 1.383(2)
T7MESI	1.353(3) 1.401(3)	1.522(2) 1.535(2)	1.435(2)	1.480(2)	1.200(2)	1.382(3)
T72BIPY	1.355(2) 1.394(2)	1.531(2) 1.535(2)	1.426(1)	1.484(2)	1.195(2)	1.384(3)
T74BIPY	1.361(3) 1.392(2)	1.530(2) 1.539(2)	1.428(2) 1.444(2)	1.482(2) 1.484(2)	1.198(2) 1.198(2)	1.381(2)
T7ANI	1.370(3) 1.391(2)	1.528(2)	1.430(2)	1.484(2)	1.197(2)	1.376(3)
T7ONA	1.376(3) 1.396(2)	1.529(2)	1.438(2)	1.482(2)	1.195(2)	1.384(3)
T7MNA	1.355(5) 1.389(4)	1.538(3)	1.423(3)	1.476(4)	1.202(3)	1.364(5)
Typical values[3]	1.375-1.391 (0.013)	1.517-1.539 (0.016)	1.432-1.449 (0.012)	1.464-1.481 (0.012)	1.187-1.197 (0.010)	1.374-1.384 (0.012)

University of Cape Town

The bond lengths **a**, **b**, **c**, **d**, **e** and **f** are defined in Figure 5.2. **a** represents the aromatic bond lengths; the smallest and the largest values are reported for each structure eg. in **T7CCL4** the values for **a** vary from 1.318(6) to 1.401(6)Å. The typical bond length of a paraffinic[3] C—C bond is 1.514(3)Å. Significantly lower values were obtained for **f**, presumably due to the delocalization of electron density in the acetylenic group.

Outliers were obtained for the structures **T7CCL4** and **T7CHCL3** with respect to the aromatic bond length **a**, with the bond lengths shorter than expected. This was due to the poor refinement of certain of the aromatic rings.

The typical values against which the bond lengths and torsion angles were compared, were obtained from the "*International Tables for crystallography, Vol. C*"[4]. These values were in turn compiled from X-ray diffraction results from the September 1985 version of the CSD.

University of Cape Town

CTV

In all the structures involving **CTV** on the CSD[1] (43 in total) the host adopts the bowl-shaped or crown conformation. The crown conformation was adopted in all three structures completed in this study.

The host is defined by the torsion angles τ_1, τ_2 and τ_3 and the bond lengths **a**, **b**, **c**, **d** and **e** as depicted in Figures 5.4 and 5.5. τ_1 indicates the torsion angle between the methoxy group and the phenyl ring to which it is attached. In the structure **CTVCCL4**, the host is situated on a mirror plane. Three unique values were obtained for τ_1, only the smallest and the largest absolute values are quoted. In the structures **CTV111** and **CTV112** six unique torsion angles were obtained for τ_1. Once again the smallest and the largest absolute values have been tabulated. The large range in τ_1,

from 0° to 86.3° is an indicator of the flexibility of the methoxy groups. Similar analyses were performed for τ_2 and τ_3.

The torsion angles τ_2 and τ_3 define the conformation of the cyclononane ring. τ_2 describes the relationship between two methylene carbon atoms and τ_3 indicates the torsion angle between two aromatic carbon atoms shared by the cyclononane ring. Slight deviations from the crown conformation can be seen in the torsion angle τ_2, which falls in the range 0° to 8°.

As was done for **TOD7** the bond length **b** represents all the aromatic bond lengths for a molecule. The extreme values are quoted. Similar analyses were performed for the other bond lengths **a**, **c** and **d**.

A significant difference in bond length within the aromatic rings is observed with alternating short and long bond lengths. This is a common characteristic of o-dimethoxybenzene derivatives. This is believed to be due to the resonance form[5] depicted in Figure 5.3 and also incomplete delocalization of π electrons.

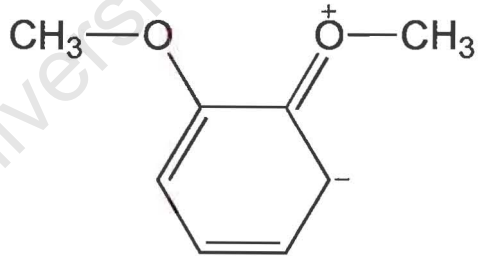

Figure 5.3. Resonance ~~from~~ form of an o-dimethoxybenzene ring.

University of Cape Town

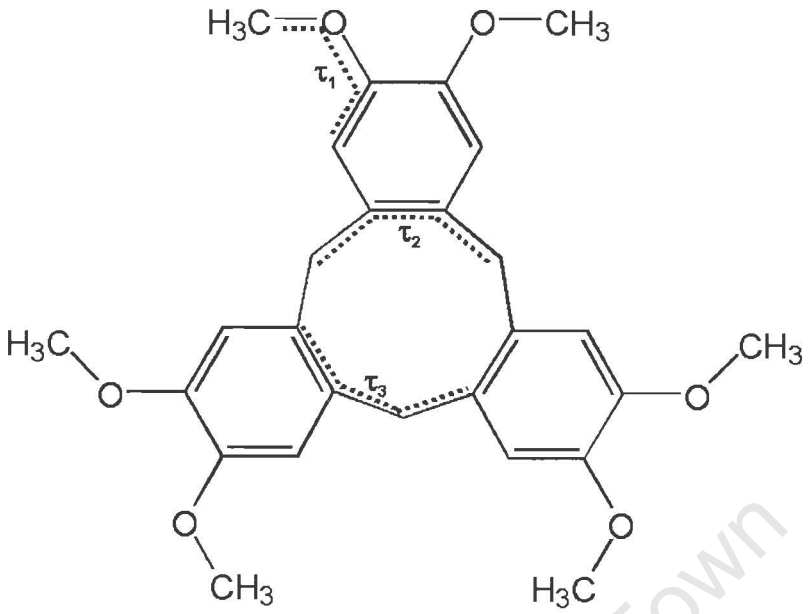

Figure 5.4. Torsion angles τ_1, τ_2 and τ_3 as defined for **CTV**.

Table 5.3. Ranges of torsion angles observed for **CTV**.

Complex	Guest	τ_1 / °	τ_2 / °	τ_3 / °
CTVCCL4	carbontetrachloride	-8.5(4) 16.3(4)	-0.0(1) 8.0(4)	-89.9(3) -103.1(3)
CTV111	1,1,1-trichloroethane + 1,1,1-trichloropropane	-0.0(6) 15.2(6)	-0.6(5) 1.9(5)	-94.0(4) -96.6(4)
CTV112	1,1,2-trichloroethane molecule 1 molecule 2	-2(1) 16(1) 0(1) 86(1)	-2(1) 4(1) 0(1) 4(1)	-91.2(9) -99.2(8) -92.9(9) -98.2(8)

University of Cape Town

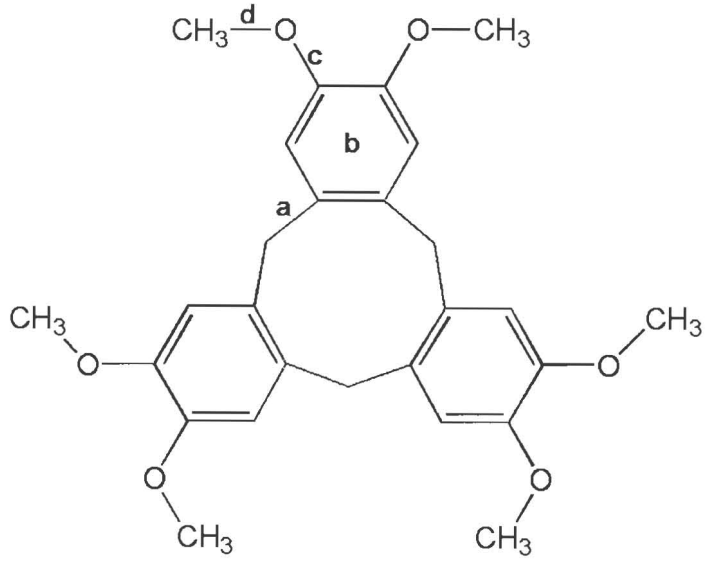

Figure 5.5. Bond lengths a, b, c and d defined for **CTV**.

Table 5.4. Ranges of bond lengths observed for **CTV**.

Complex		a=C_{ar}—Csp^3(Å)	b=C_{ar}≅C_{ar}(Å)	c=C_{ar}—O(Å)	d=Csp^3—O(Å)
CTVCCL4		1.512(4) 1.518(3)	1.373(4) 1.409(4)	1.374(3) 1.377(3)	1.423(4) 1.429(3)
CTV111		1.510(5) 1.523(5)	1.369(6) 1.411(5)	1.366(5) 1.379(4)	1.408(5) 1.435(6)
CTV112	molecule 1	1.51(1) 1.54(1)	1.37(1) 1.42(1)	1.353(8) 1.382(8)	1.402(9) 1.437(9)
	molecule 2	1.50(1) 1.54(1)	1.36(1) 1.42(1)	1.362(9) 1.38(1)	1.41(1) 1.428(9)
Typical values[3]		1.505-1.516 (0.009)	1.375-1.391 (0.013)	1.363-1.377 (0.011)	1.405-1.426 (0.016)

Asymmetry parameters were also calculated for **CTV**[6]. These measure the degree to which a ring deviates from ideal symmetry. For each of the structures, asymmetry parameters were calculated for the 9-membered ring of **CTV**. Deviations from mirror symmetry and three-fold symmetry were determined. The calculation uses related torsion angles such that a value of zero is obtained when that symmetry element is present.

University of Cape Town

The following equations define: (i) mirror plane symmetry and (ii) two-fold symmetry.

$$\text{(i)} \quad \Delta C_s = \left[\frac{\sum_{i=1}^{m} (\phi_i + \phi_i')^2}{m} \right]^{1/2} \quad \text{and} \quad \text{(ii)} \quad \Delta C_2 = \left[\frac{\sum_{i=1}^{m} (\phi_i - \phi_i')^2}{m} \right]^{1/2}$$

where m is the number of individual comparisons and ϕ_i and ϕ_i' are the symmetry related torsion angles.

Equation (ii) was modified to calculate three-fold symmetry:

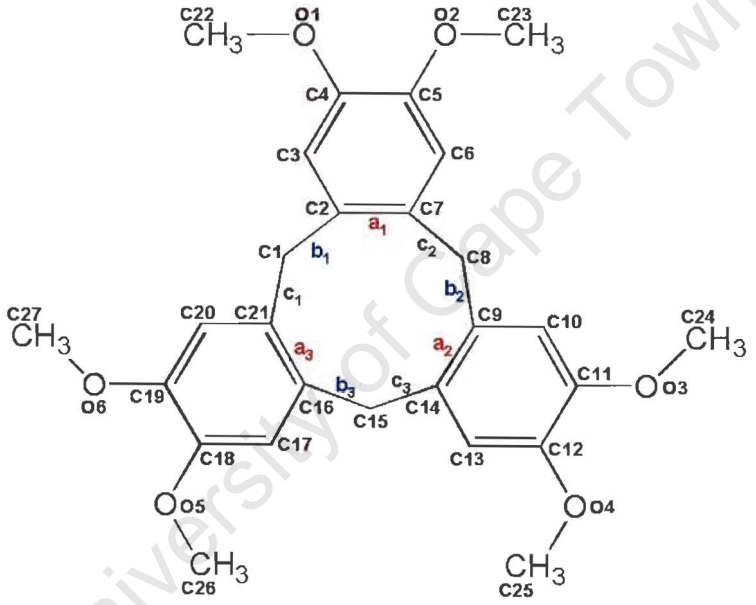

Figure 5.6. **CTV** indicating torsion angles such that torsion angle

$$a_1 = C1\text{—}C2\text{—}C7\text{—}C8.$$

The three-fold asymmetry parameter was calculated using the equation:

$$\Delta C_3 = \left[\frac{(a_1 - a_2)^2 + (a_2 - a_3)^2 + (a_1 - a_3)^2 + (b_1 - b_2)^2 + (b_2 - b_3)^2 + (b_1 - b_3)^2 + (c_1 - c_2)^2 + (c_2 - c_3)^2 + (c_1 - c_3)^2}{9} \right]^{1/2}$$

University of Cape Town

The host numbering schemes for **CTV111** and **CTV112** are similar. This same numbering scheme is followed as indicated in Chapter 4 and is indicated again in Figure 5.7. The second host molecule in the asymmetric unit of **CTV112** is labelled with the suffix A. The host in **CTVCCL4** is situated on a mirror plane and thus a slightly different numbering scheme was adopted viz. the symmetry related atom of C8 is labelled as C8' etc.

An example is shown in the case of **CTV111**:

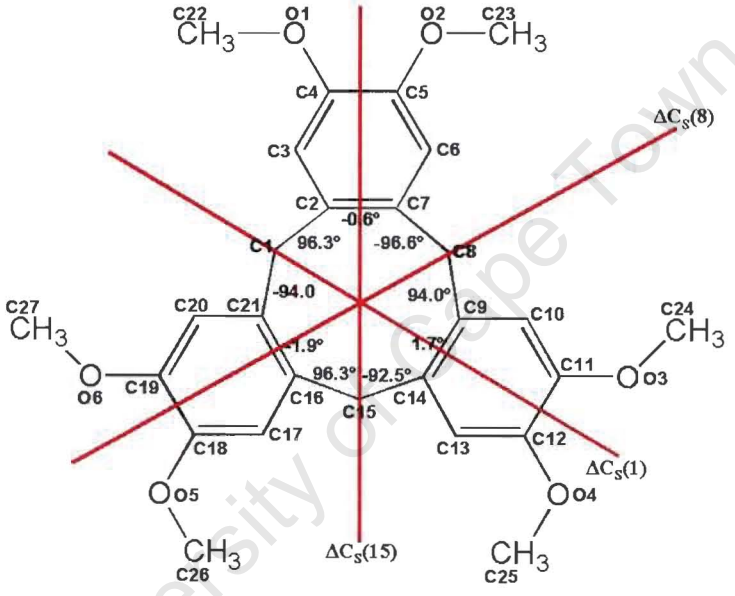

Figure 5.7. Torsion angles and mirror planes shown for the host in **CTV111**.

The mirror plane asymmetry parameters $\Delta C_s(1)$, $\Delta C_s(8)$ and $\Delta C_s(15)$ were calculated for each mirror plane. The number in brackets represents the number of the atom intersected by the mirror plane.

Table 5.5. Asymmetry parameters for **CTV**.

Structure		$\Delta C_s(1)$/ $\Delta C_s(1A)$	$\Delta C_s(8)$/ $\Delta C_s(8A)$	$\Delta C_s(15)$/ $\Delta C_s(15A)$/ $\Delta C_s(8')$	ΔC_3
CTVCCL4		0	9.9	9.9	10.4
CTV111		1.5	1.9	0.6	1.7
CTV112	molecule 1	4.0	1.6	5.8	5.5
	molecule 2	4.5	3.4	3.2	2.2

University of Cape Town

For the structure **CTVCCL4**, $\Delta C_s(1)=0$ due to symmetry. There are large deviations from mirror plane symmetry with respect to the other mirror planes with $\Delta C_s(8)$ and $\Delta C_s(8')$ both equal to 9.9. For the structure **CTV111**, the host deviates only slightly from mirror plane symmetry along all directions, with the best value obtained for $\Delta C_s(15)$ at 0.6. In molecule one of **CTV112** the lowest value and hence the smallest deviation from mirror plane symmetry is obtained for $\Delta C_s(8)$. In the second molecule of **CTV112** the values are consistent along all directions and range from 3.4 to 4.5.

The host molecule in **CTV111** is the one whose rotational symmetry approximates three-fold most closely (ΔC_3 =1.7) while the host molecule in **CTVCCL4** shows the greatest deviation from three-fold symmetry.

University of Cape Town

References

1. Cambridge Structural Database and Cambridge Structural Database System, Version 5.22(2001), Cambridge Crystallographic Data Centre, University Chemical Laboratory, Cambridge, England.
2. D. Vujovic, PhD thesis, University of Cape Town, South Africa, December 2001.
3. CRC Handbook of Chemistry and Physics, 55th Edition, (ed.) R.C. Weast, CRC Press, Ohio, 1974-1975.
4. International Tables for crystallography, Vol. C, (ed.) A.J.C. Wilson, Kluwer Academic Publishers, Dordrecht, pp.691, 1992.
5. G. I. Birnbaum, D.D. Klug, J.A. Ripmeester and J.S. Tse, *Can.J. Chem.*, 63, 3258-3262, 1985.
6. Atlas of Steroid Structure, Vol.1, (ed.) W.L. Duax and D.A. Norton, A Division of Plenum Publishing Corporation, New York, pp. 18, 1975.

University of Cape Town

CHAPTER 6

University of Cape Town

CHAPTER 6 SUMMARY AND CONCLUSION

The inclusion ability of the hosts **TOD7** and **CTV** was studied. The selectivity of these hosts for certain organic guests was investigated and the results rationalised using one or more of the following: thermal analysis, kinetics of decomposition, competition experiments or exchange reactions.

Brief overview of inclusion compounds formed with **TOD7**.

	Guest	H:G ratio	Code name	Space group	Host conformation	Voids occupied by guests
A	carbon tetrachloride	1: ½	**T7CCL4**	C2/c	gauche	cages
	chloroform	1: ½	**T7CHCL3**	C2/c	gauche	cages
	dichloromethane	1: ½	**T7CH2CL2**	$P2_1/n$	gauche	cages
	benzene	1: 1	**T7BENZ**	$P\bar{1}$	gauche	cages
	toluene	1: ¾	**T7TOL**	$P\bar{1}$	gauche	cages
B	mesitylene	1: 1	**T7MESI**	C2/c	trans	channels
C	acetonitrile	1: 2	**T7CH3CN**	$P2_1/n$	trans	channels
	pyridine	1: 2	**T7PYR**	$P2_1/c$	trans	channels
	2-picoline	1: 2	**T72PIC**	$P\bar{1}$	trans	channels
	3-picoline	1: 2	**T73PIC**	$P2_1/c$	trans	cages
	4-picoline	1: 2	**T74PIC**	$P2_1/c$	trans	channels
	N,N-dimethylformamide	1:2	**T7DMF**	Pbca	trans	channels
	dimethyl sulfoxide	1:2	**T7DMSO**	Pbca	trans	channels
	aniline	1: 2	**T7ANI**	$P\bar{1}$	trans	channels
	o-nitroaniline	1: 2	**T7ONA**	$P\bar{1}$	trans	channels
	m-nitroaniline + n-hexane	1: 2: ¼	**T7MNA**	$P\bar{1}$	trans	channels
	2,2-bipyridine	1: 2	**T72BIPY**	$P2_1/c$	gauche	channels
	4,4-bipyridine	1: ½	**T74BIPY**	$P\bar{1}$	trans	channels

University of Cape Town

As can be seen in the above table the inclusion compounds have been divided into groups depending on similarities in their structures.

In the case of **TOD7** and the chlorinated guests ie. carbon tetrachloride, chloroform and dichloromethane, all the structures exhibit similar packing motifs. Hydrogen bonding occurs between hydroxyl groups of adjacent host molecules, which form four-centre hydrogen bond networks. The chlorinated guests occupy cages created by the host structure. Similar hydrogen bonding networks were observed between **TOD7**

and the aromatic guests, benzene and toluene. However in these structures, the host framework creates channels that are occupied by the guests. In all these structures the host adopts the gauche conformation. Carbon tetrachloride is non-polar and the guests chloroform, dichloromethane, benzene and toluene are relatively weakly polar guests. This trend of non-polar and weakly polar guests causing **TOD7** to adopt the gauche conformation is a common feature that was observed in this study and by searches done on the CSD[1]. The thermal analysis results, most notably the T_{on}/T_b ratio, indicate that **T7CH2CL2** has greater stability compared to **T7CCL4**, **T7CHCL3** and **T7CH3CN**. Weak C—H•••π interactions between the host and the guest contribute to the enhanced stability of **T7CH2CL2.** The importance of C—H•••π interactions has been re-iterated recently by H. Suezawa et al[2].

Mesitylene is also a non-polar guest but the packing in **T7MESI** differs from those in Group A. The host adopts the trans conformation due to symmetry considerations and the guest is situated in channels. In **T7MESI** O—H•••π hydrogen bonding occurs between the hydroxyl group of the host and the phenyl group of the guest.

Group C contains all guests that have a nitrogen or an oxygen atom available for hydrogen bonding to the host hydroxyl group. In all these structures except **T72BIPY** the host is situated on a centre of symmetry and consequently the host adopts the trans configuration.

In the series involving pyridine and the picolines, the T_{on}/T_b ratio and the normalised lattice energy favour **T7PYR** as the most stable compound with **T72PIC** as the least stable compound.. The competition experiments are concentration dependent. This

University of Cape Town

suggests that kinetic effects play a role in determining the outcome. All of these structures are stabilised by hydrogen bonding between the hydroxyl groups of the host and the nitrogen atom of the guest such that each host molecule is hydrogen bonded to two guest molecules. In all these structures except **T73PIC** the guests are situated in channels.

Both **T7DMF** and **T7DMSO** crystallize in the space group Pbca with their host frameworks nearly isostructural. The competition experiments, normalised lattice energy results and T_{on}/ T_b favour **T7DMSO** as the more stable compound. In both structures hydrogen bonding occurs between the hydroxyl groups of the host and the oxygen atom of the guest. The activation energy for desolvation of **T7DMSO** is approximately twice that of **T7DMF**. Guest exchange between dimethyl sulfoxide and N,N-dimethylformamide was successful.

As mentioned earlier, solid guests 2,2'-bipyridine and 4,4'-bipyridine are interesting in that when complexed with **TOD7**, both result in the host adopting different conformations. In **T72BIPY** the asymmetric unit consists of one half of a host molecule and one whole guest molecule. The host adopts the trans conformation. In **T74BIPY** the asymmetric unit contains one whole host molecule and one half of a guest molecule. The host adopts the gauche conformation.

Inclusion compounds were formed between **TOD7** and the guests, aniline and o- and m-nitroaniline. Inclusion was not successful between **TOD7** and p-nitroaniline. It is believed that the three-centre hydrogen bond present in **T7ONA** is responsible for its greater stability. The DSC results also indicate a higher melting point for **T7ONA**

University of Cape Town

than for **T7MNA**. An unexpected result was obtained when m-nitroaniline was crystallized with **TOD7** from a solution of diethyl ether and n-hexane. The resultant material was a mixed guest inclusion compound containing both m-nitroaniline and n-hexane. Solid state reactions between **TOD7** and the solid guests, o- and m-nitroaniline were successful. The resultant complex between **TOD7** and o-nitroaniline differed from that grown from solution.

Brief overview of inclusion compounds of **CTV** investigated in this study.

Guest	H:G ratio	Code name	Space group	Voids occupied by guests
carbon tetrachloride	1: 1	**CTVCCL4**	Pnma	channels
1, 1, 1-trichloroethane + 1, 1, 1-trichloropropane	1: 1: 1	**CTV111**	$P2_1/n$	In the host cavity + in channels
1, 1, 2-trichloroethane	1: 1	**CTV112**	$P\bar{1}$	In the host cavity + in channels

In all three complexes the host, **CTV,** adopts the crown conformation. Similar packing of the host framework occurs in all three structures with the host molecules stacked in columns, with one host molecule in the cavity of the previous one. This packing arrangement is a common feature of **CTV**[1]. Selected guests are situated in channels, as was observed in all three structures and other guests are situated in the host cavity. The ratio T_{on}/T_b and the activation energy is higher for **CTVCCL4** suggesting that **CTVCCL4** has greater stability. **CTV112** has the lowest activation energy and the lowest ratio of T_{on}/T_b implying that it has the lowest stability.

University of Cape Town

In this study the inclusion compounds formed between the two hosts **TOD7** and **CTV** and small organic guests were investigated. The two host compounds, **TOD7** and **CTV**, are structurally very different. **TOD7** is a rigid, bulky wheel and axle host that includes guests in voids created by the host framework. **CTV** is a bowl-shaped host capable of including guests in its cavity as well as in voids created by the host framework. However both of these hosts conform to the principles of directed host design as described by Weber[3]. The bulky phenyl groups of **TOD7** and the bowl shape of **CTV** prevent close packing, thus ensuring that both are successful as host compounds.

University of Cape Town

References

1. Cambridge Structural Database and Cambridge Structural Database System, Version 5.22(2001), Cambridge Crystallographic Data Centre, University Chemical Laboratory, Cambridge, England.
2. H.Suezewa et al., *J. Chem. Soc., Perkin Trans.*, 2, 2053, 2001.
3. E. Weber, J.L Atwood, J.E.D. Davies, D.D. MacNicol (Eds.), Inclusion Compounds, vol. 4, ch.5, Oxford University Press, Oxford, pp. 188-263, 1991.

University of Cape Town

APPENDICES

University of Cape Town

APPENDICES

Supplementary material for all the crystal structures presented in this thesis can be found on the attached CD.

For each structure the following files are included:

(a) **Structurename.res**: A SHELX file that can be viewed via the X-SEED interface. Allows one to view the molecule and the crystal packing.

(b) **Structurename_1.doc**: An MS-WORD97 file which contains the atomic coordinates, isotropic and anisotropic displacement parameters, bond lengths, bond angles and torsion angles.

(c) **Structurename_2.doc**: An MS-WORD97 file containing tables of observed and calculated structure factors.

The files for each structure have been arranged in folders as follows:

Folder name	Structure
Appendix3.1	**T7CCL4, T7CHCL3, T7CH2CL2, T7CH3CN**
Appendix3.2	**T7PYR, T72PIC, T73PIC, T74PIC**
Appendix3.3	**T7BENZ, T7TOL, T7MESI**
Appendix3.4	**T7DMF, T7DMSO**
Appendix3.5	**T7ANI, T7ONA, T7MNA**
Appendix3.6	**T72BIPY, T74BIPY**
Appendix4.1	**CTVCCL4, CTV111, CTV112**

University of Cape Town

Host (H)	Guest (G)	H:G ratio	Code name
CTV			
	carbon tetrachloride	1: 1	CTVCCL4
	1,1,1-trichloroethane / 1,1,1-trichloropropane	1: 1: 1	CTV111
	1,1,2-trichloroethane	1: 2	CTV112

University of Cape Town

CTV

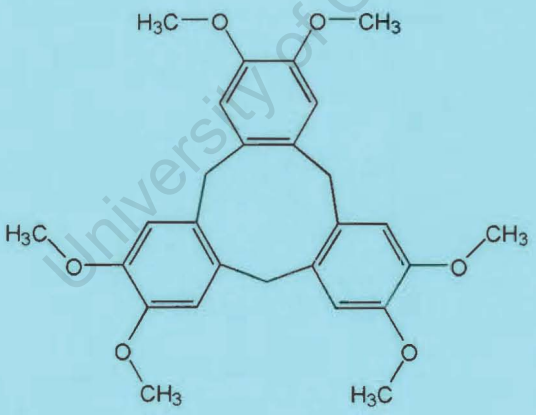

Host (H)	Guest (G)	H:G ratio	Code name
TOD7			
	carbon tetrachloride	1: ½	T7CCL4
	chloroform	1: ½	T7CHCL3
	dichloromethane	1: ½	T7CH2CL2
	acetonitrile	1: 2	T7CH3CN
	pyridine	1: 2	T7PYR
	2-picoline	1: 2	T72PIC
	3-picoline	1: 2	T73PIC
	4-picoline	1: 2	T74PIC
	benzene	1: 1	T7BENZ
	toluene	1: ¾	T7TOL
	mesitylene	1: 1	T7MESI
	N,N-dimethylformamide	1: 2	T7DMF
	dimethyl sulfoxide	1: 2	T7DMSO
	aniline	1: 2	T7ANI
	o-nitroaniline	1: 2	T7ONA
	m-nitroaniline / n-hexane	1: 2: ¼	T7MNA
	2,2'-bipyridine	1: 2	T72BIPY
	4,4'-bipyridine	1: ½	T74BIPY

University of Cape Town

TOD7